Chem Soc Rev

REVIEW ARTICLE

View Article Online
View Journal

Cite this: DOI: 10.1039/d5cs00583c

Advancements in polymer materials for high-energy-density lithium-ion batteries

Yuting Du,†[a] Shenzhen Deng,†[a] Yuanyuan Zhu,[a] Jianan Jiang,[a] Guangxu Yang,[a] Mingbo Wu[ab] and Zhongtao Li*[a]

Received 27th May 2025

DOI: 10.1039/d5cs00583c

rsc.li/chem-soc-rev

Polymers are anticipated to address the bottleneck challenges in high-energy-density batteries due to their inherent flexibility, tunable structures, and ease of functionalization. In this review, we first analyze the requirements for cathode, anode, and electrolyte materials in high-energy-density batteries, alongside the existing challenges within current material systems. We then summarize and discuss the current status and developmental trends of polymer materials in these domains. Furthermore, we elucidate the challenges faced by polymer materials in high-energy-density batteries, including issues related to stability, ion transport, processing, and system integration. Finally, we present an overview of the current landscape and regulatory considerations for polymer materials in high-energy-density lithium batteries, proposing future development directions in this field. The insights provided are expected to facilitate the application of polymer materials in lithium batteries and advance the development of high-energy-density lithium battery technologies.

1. Introduction

Driven by the global transition towards low-carbon and sustainable energy systems, high-energy-density lithium-ion batteries (LIBs) have emerged as the cornerstone of next-generation energy storage technologies,[1,2] serving as a pivotal driving force for advancing electric vehicles, smart grids, and portable electronic devices.[3–5] Since their commercialization in 1991,[6] LIBs have progressively supplanted traditional lead–acid and nickel-metal hydride batteries due to their superior energy densities, extended cycling lives, and reduced self-discharge rates.[7,8] Nevertheless, the expanding application frontiers have revealed critical limitations in conventional LIB architectures, particularly regarding energy density ceilings,[9,10] safety concerns,[11] and cost-effectiveness barriers.[12] This technological impasse underscores the imperative for developing high-specific-energy LIB systems, whose successful realization would have profound implications for both fundamental electrochemistry research and industrial energy storage applications.[13]

[a] State Key Laboratory of Heavy Oil Processing, College of Chemical Engineering, China University of Petroleum (East China), Qingdao 266580, P. R. China. E-mail: liztao@upc.edu.cn

[b] College of Chemical Engineering, Qingdao University of Science and Technology, Qingdao 266061, China

† These authors contributed equally to this paper.

Yuting Du

Yuting Du is currently a doctoral student at China University of Petroleum (East China). She obtained a master's degree in Materials and Chemical Engineering in 2023. Under the guidance of Professor Li Zhongtao from China University of Petroleum (East China), she focuses on the research field of functional polymer materials in energy storage devices.

Shenzhen Deng

Shenzhen Deng is currently an associate professor at China University of Petroleum (East China). He was awarded the Shandong Province "Taishan Scholar" Young Expert award. He received his PhD degree in inorganic chemistry from Nankai University in 2022 under the supervision of Prof. Zhiqiang Niu. His research interests focus on nanocarbon materials and advanced energy storage devices.

1.1. Definition and performance metrics of high-energy-density batteries

High-energy-density lithium-ion batteries (LIBs) refer to novel battery architectures that demonstrate substantial improvements in energy density, power density, and cycle longevity compared to conventional LIB systems. These advanced energy storage solutions achieve paradigm-shifting advancements through coordinated optimization of three critical components:[14] (1) cathode materials engineered with enhanced specific capacity, elevated voltage plateaus, exceptional structural stability, and minimized parasitic reactions;[15,16] (2) anode materials designed for high specific capacity, reduced charge-transfer resistance, and robust mechanical integrity;[17] (3) electrolyte systems optimized for superior ionic conductivity, expanded electrochemical stability windows, and improved interfacial compatibility.[18,19] This multifaceted approach enables synergistic enhancement of electrochemical performance metrics, positioning these next-generation LIBs as indispensable power sources to address burgeoning energy demands across transportation and grid-scale energy storage sectors.

The core performance metrics of high-energy-density LIBs are as follows (Fig. 1):

(1) Energy density: according to the US Department of Energy's goals, the energy density of lithium-ion batteries for electric vehicles needs to reach 500 Wh kg^{-1} by 2030.[20] The current mainstream lithium iron phosphate battery has an energy density of less than 200 Wh kg^{-1}, while ternary lithium-ion batteries have an energy density between 200 and 300 Wh kg^{-1}.[21] To achieve this goal, researchers are exploring new materials and battery structures such as lithium metal batteries and solid-state batteries.

(2) Cycle life: it is required that the capacity retention rate should be no less than 80% after at least 1000 charge and discharge cycles.

(3) Temperature adaptability: wide temperature performance (−60 °C to 80 °C) is the key to extreme environment applications. Some ionic liquid electrolyte technologies have achieved an operating range of −40 °C to 70 °C, which is of great significance for battery applications in different climate conditions.[22,23]

(4) Safety: it needs to pass tests such as nail penetration and thermal runaway inhibition. For example, high nickel ternary materials combined with flame retardant electrolytes can pass the nail penetration test,[24] and solid-state batteries become an

Yuanyuan Zhu

Yuanyuan Zhu is currently a doctoral student at China University of Petroleum (East China). He obtained a master's degree in Materials and Chemical Engineering in 2023. Under the guidance of Professor Li Zhongtao from China University of Petroleum (East China), he focuses on the research field of functional polymer materials in energy storage devices.

Jianan Jiang

Jianan Jiang is currently pursuing a master's degree in Chemical Engineering and Technology from China University of Petroleum (East China), under the supervision of Professor Li, focusing on research related to solid electrolytes in lithium-ion batteries.

Guangxu Yang

GuangXu Yang is currently a doctoral student at China University of Petroleum (East China). He obtained a master's degree in Materials and Chemical Engineering in the university of Jinan. Under the guidance of Professor Li Zhongtao from China University of Petroleum (East China), his research focuses on the preparation and characterization of high-nickel cathode materials for lithium-ion batteries.

Zhongtao Li

Zhongtao Li is a professor and doctoral supervisor at the College of Chemical Engineering, China University of Petroleum (East China). He was granted the Shandong Province "Outstanding Young Scientist" fund and recognized as a "Taishan Scholar" young expert. His current research focuses on the structural design and development of nanocomposite materials in the fields of new energy and catalysis.

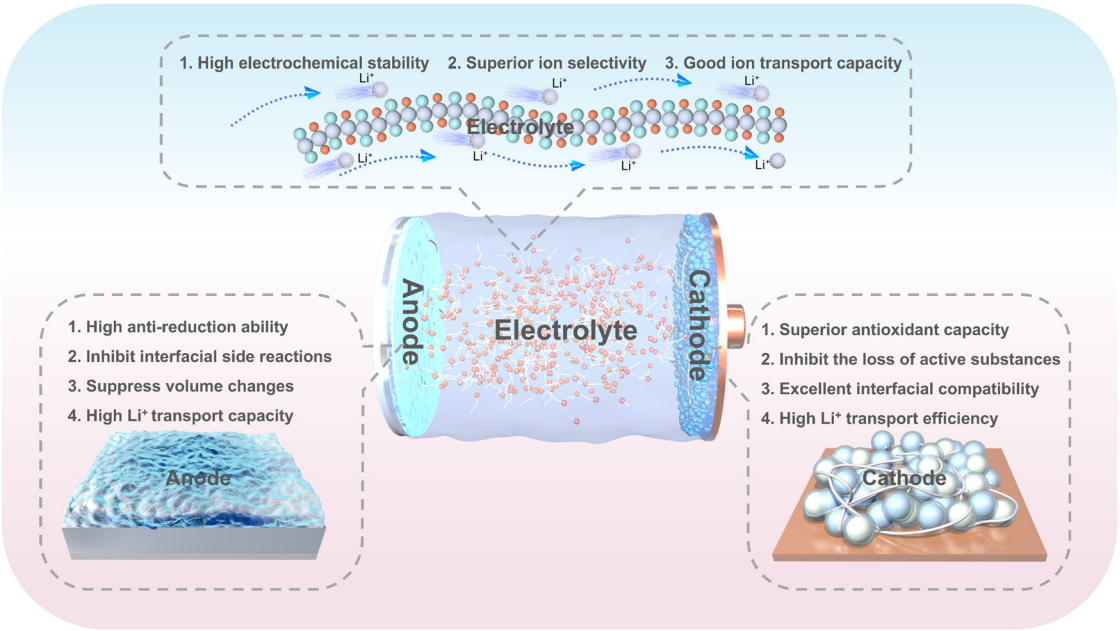

Fig. 1 The core performance metrics of high-energy-density LIBs.

important direction for safety upgrade due to the non-flammable nature of solid-state electrolytes.[25]

These metrics collectively define the technological boundaries of high-specific-energy batteries, demanding co-optimization of cathode/anode active materials, electrolyte formulations, and interfacial engineering strategies.

1.2. Limitations of current high-energy-density battery material systems

Despite significant advancements in material development, the industrial application of high-energy-density lithium-ion batteries faces critical technical barriers.[26] These challenges are systematically analyzed for electrode materials and electrolyte systems:

(1) Technical bottlenecks of high-capacity cathode material systems: during initial charge/discharge, lithium-rich manganese-based oxide cathodes release lattice oxygen irreversibly, triggering electrolyte decomposition and interfacial reactions.[27] This substantially reduces first-cycle coulombic efficiency and degrades long-term capacity retention.[28,29] Sulfur cathode systems, despite their high theoretical capacity of 1675 mAh g^{-1}, generate polysulfide intermediates (Li_2Sn, $4 \leq n \leq 8$) that dissolve in ether electrolytes. This dissolution causes shuttling, leading to irreversible active material loss and accelerated capacity decay.[30,31] These issues are key technical barriers to the practical application of high-energy-density lithium-ion batteries.

(2) Structural stability challenges in high-specific-capacity anodes: silicon-based anode materials undergo substantial volumetric expansion up to 300% during lithiation/delithiation processes, leading to particle pulverization, current collector delamination, and dynamic reconstruction of the solid electrolyte interphase (SEI), ultimately resulting in rapid capacity degradation.[32,33] Lithium metal anodes face dendritic growth due to heterogeneous lithium-ion deposition during cycling, where the tip effect of dendrites can penetrate separators, inducing electrolyte infiltration and posing risks of internal short circuits and thermal runaway.[34] Although nanostructural engineering[35] and interfacial modification techniques[36] partially mitigate volume fluctuations and dendritic growth, critical gaps persist in cycle longevity and areal capacity loading, failing to meet the technical specifications required for commercial applications.

(3) Inherent limitations of conventional liquid electrolytes: liquid electrolyte systems based on carbonate/ether solvents exhibit intrinsic safety risks due to their low flash points and high flammability,[37] which can trigger thermal runaway cascades under thermal abuse conditions. Furthermore, persistent interfacial reactions between highly reactive electrode materials (*e.g.*, lithium metal, sulfur cathodes) and liquid electrolytes lead to progressive degradation of electrode–electrolyte interfaces, accelerating capacity decay kinetics.[38,39] These limitations not only constrain further improvements in energy density, but also critically undermine operational reliability under extreme temperature ranges and high-rate operating conditions.

In summary, the development of high-energy-density lithium-ion batteries critically demands multidisciplinary collaborative innovation across material architecture design, interface regulation mechanisms, and system integration paradigms to achieve transformative progress toward practical implementation.

1.3. Utilization of polymers in battery technology

Polymeric materials demonstrate exceptional advantages in critical material systems for high-energy-density lithium secondary batteries due to their intrinsic flexibility, structural tunability, and surface functionability, providing innovative solutions to bottlenecks such as electrode/electrolyte interface

stability, volume expansion effects, and ion transport kinetics.[40–42] In conventional lithium-ion battery systems, polymeric materials have established multidimensional technical frameworks: in electrode engineering, they serve both as mechanically buffering binder matrices and topological regulators for constructing 3D conductive networks;[41,43] in electrolyte systems, polymer-based solid-state electrolytes and their derivative functional additives, combining ionic conduction with interfacial compatibility, significantly enhance electrochemical stability windows and thermodynamic safety.[40,44]

Polymeric materials serve three critical functions in lithium-ion battery systems:

(1) Cathode applications: primarily employed as binders polymeric components ensure robust adhesion between active materials and current collectors while facilitating electron transport.[45] Advanced strategies involve functional group incorporation and surface modifications to strengthen binder-active material interactions,[46,47] thereby improving capacity retention and interfacial stability.

(2) Anode applications: in lithium-ion battery anodes, polymeric materials play equally vital roles. Anode materials require high specific capacity, robust structural stability, and low charge-transfer impedance. Conventional anode binders like styrene–butadiene rubber (SBR) and sodium carboxymethyl cellulose (CMC) blends effectively mitigate volumetric fluctuations and electrode pulverization during cycling, thereby enhancing cyclic stability and operational safety.[33,48] Furthermore, nanostructural engineering and interfacial modifications of polymeric components significantly improve anode performance (nanofiller-incorporated polymer matrices reduce volume expansion rates while boosting electrochemical activity). In lithium metal anode research, polymeric advancements demonstrate breakthrough progress: engineered interfacial layers suppress dendritic growth by homogenizing lithium-ion (Li^+) flux density, thereby elevating safety metrics and cycle longevity.[41]

(3) Electrolyte innovations: electrolytes, as critical ion-transport components in lithium-ion batteries, fundamentally determine charge–discharge efficiency and safety metrics.[49] While conventional liquid electrolytes exhibit sufficient ionic conductivity, their intrinsic flammability and chemical instability pose significant safety risks.[37] This has driven the exploration of polymer electrolytes, where material innovations address these limitations through exceptional flexibility and mechanical robustness, effectively buffering electrode volume variations during cycling while enhancing operational safety. These advancements underscore the transformative potential of polymer electrolytes in advancing both electrochemical performance and operational safety in next-generation battery systems.

Capitalizing on their intrinsic flexibility, structural programmability, and surface modifiability, polymeric materials offer innovative design paradigms to address critical scientific challenges in high-energy-density systems, as shown in Fig. 2. This review systematically elucidates the key performance metrics required for cathode, anode, and electrolyte materials in high-energy-density batteries while rigorously analyzing the fundamental limitations of current material systems. We specifically

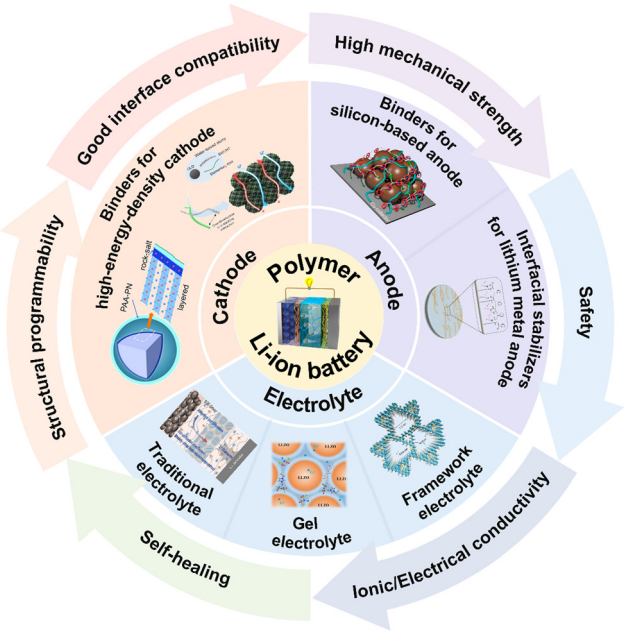

Fig. 2 Polymer materials for high-energy-density lithium-ion batteries.

focus on core scientific challenges facing polymer-based materials in practical high-energy-density applications, including electrochemical stability under high-voltage/active interfacial conditions, coupled relationships between multiscale ion-transport engineering and charge-transfer impedance minimization, scalability alignment between processability optimization and manufacturing compatibility, and system integration challenges. Finally, by establishing a multidimensional "Structure–Performance–Process" evaluation framework, we propose future development directions for polymer-based materials targeting practical high-energy-density lithium metal batteries. Through constructing a theoretical framework linking material architectures to functional outcomes, this work provides cross-scale research strategies to surpass existing energy density limits of lithium secondary batteries, driving the transformative transition of next-generation high-energy-density technologies from fundamental research to industrial deployment.

2. Polymers in high-energy-density cathodes

Cathode materials, serving as the energy density-determining components in lithium-ion batteries, have consistently maintained their position as a central research focus for performance optimization. While conventional layered oxides (*e.g.*, $LiCoO_2$)[50,51] and polyanionic compounds (*e.g.*, $LiFePO_4$)[52] have achieved commercial viability, their theoretical capacities and voltage plateaus increasingly approach fundamental physical limits. Recent advancements in high-nickel ternary materials (*e.g.*, $LiNi_xCo_yMn_{1-x-y}O_2$(NCM))[53] and Li-rich Mn-based oxides (LRMO),[54] which exhibit high specific capacities exceeding 250 mAh g^{-1}, have garnered significant attention. However,

their practical performance remains constrained by structural degradation during high-voltage cycling, including lattice oxygen evolution and transition metal dissolution.[55] In this context, polymeric materials have demonstrated unique regulatory capabilities in cathode systems through multifunctional design strategies. Functional modifications of polymeric binders significantly enhance structural stability, while composite architectures integrating conductive polymers with carbon-based additives establish three-dimensional bicontinuous electron/ion transport networks, thereby improving charge transfer kinetics in high-loading cathodes. Additionally, self-healing polymers utilizing dynamic hydrogen bonding or disulfide bond exchange mechanisms effectively address mechanical stress accumulation during fast-charging processes. This section will methodically examine the applications and challenges of polymeric materials in high-energy-density cathodes, with a primary focus on binder engineering advancements.[56,57]

2.1. The failure mechanism and design criteria for polymer binders in cathodes of high-energy-density batteries

The growing demand for high-energy-density lithium-ion batteries has positioned the development of cathode materials with combined high capacity and structural stability as a critical challenge.[58,59] As the main provider of battery capacity and the bearer of high voltage environments, cathode materials usually face serious failure problems. Taking NMC cathode materials as an example, their poor cycling stability at high voltage is mainly due to the interaction between the electrolyte and highly reactive delithiated cathode surfaces, which leads to battery capacity decay and performance degradation.[60] In addition, the cathode material undergoes structural changes during the charging and discharging process, such as the dissolution of transition metal ions, oxygen precipitation, and particle cracking, which further exacerbate the battery failure process.[61] Studies have shown that the failure of cathode materials involves not only chemical and physical changes in the materials themselves, but also interfacial reactions with the electrolyte, such as the formation and decomposition of CEI films, which consume the active material and reduce the conductivity of the battery.[62] In addition, the cathode material will show obvious cracks and fatigue mechanisms during long-term high rate cycling, leading to electrolyte penetration into the particles, which will trigger further side reactions, thus accelerating the failure of the battery.[60]

As key functional components in LIB cathode systems, binders play a decisive role in maintaining electrode structural integrity, optimizing interfacial stability, and enhancing electrochemical performance.[63] While traditional polyvinylidene fluoride (PVDF)-based binders[64] have achieved commercial success due to their electrochemical stability, interfacial adhesion strength, and electrolyte wettability.[65] In contrast, novel functionalized polymer binders demonstrate multidimensional performance regulation capabilities through molecular architecture design and interface engineering strategies.[66] To meet the structure-function synergy requirements for high-specific-energy cathode systems, polymer binders must adhere to the following design principles (Fig. 3):

(1) Optimization of electrode–electrolyte interfacial compatibility:[67] during high-voltage cycling, interfacial side reactions induced by disproportionation dissolution of transition metal (TM, *e.g.*, Mn, Ni) ions and lattice oxygen evolution lead to non-uniform growth of the cathode–electrolyte interphase (CEI) layer and a sharp surge in interfacial impedance. Functional polymer binders address these challenges by constructing ordered interfacial passivation layers that synergistically integrate steric hindrance effects and chemical chelation mechanisms, effectively suppressing TM ion dissolution and decelerating electrolyte decomposition kinetics.[68] This capability significantly enhances the long-term cycling stability of high-voltage battery systems.

(2) Suppression of cathode structural stress evolution:[69] repeated charge–discharge cycles induce microcracking and interlayer slippage through cathode lattice stress reconstruction, leading to mechanical failure, particularly exacerbated under high-voltage or fast-charging conditions. Polymer binders with robust intermolecular interactions address these challenges *via* stress dissipation mechanisms, effectively buffering electrode volumetric expansion ($>8\%$) while preserving structural continuity of 3D conductive frameworks.[70,71]

(3) Construction of multiscale charge transport networks:[72] limited ion/electron multiscale transport in high-areal-capacity cathodes primarily stems from high interfacial impedance of the CEI layer and point-contact conduction modes between active particles.[73] Conjugated polymer binders incorporating polar functional groups (*e.g.*, –COOH, $-SO_3H$) establish hierarchical ion/electron conduction pathways by reducing Li^+ diffusion activation energy and optimizing electron tunneling effects, thereby synergistically minimizing bulk and interfacial charge-transfer resistances to enhance overall electrochemical performance.[74]

(4) Enhancement of thermodynamic stability:[75] oxygen release from high-nickel ternary materials (*e.g.*, $LiNi_{0.8}Co_{0.1}Mn_{0.1}O_2$ (NCM811)) under thermal abuse (>150 °C) triggers electrolyte chain oxidation reactions, posing thermal runaway risks.[74,76] Thermally stable polymer matrices (decomposition temperature >300 °C) featuring radical scavenging capabilities (*e.g.*, hindered phenol moieties) and oxygen vacancy anchoring effects mitigate this by *in situ* quenching reactive oxygen species ($O^{2-\bullet}$, $O^{-\bullet}$) and stabilizing surface oxygen coordination environments, achieving over 50 °C improvement in oxygen release onset temperature during thermal shock conditions.[77,78]

2.2. Function and research progress for polymer binders in cathodes of high-energy-density batteries

2.2.1. Good electrochemical compatibility. The evolution of high-energy-density lithium-ion batteries toward high-voltage and high-nickel configurations intensifies critical challenges in cathode structural stability and interfacial compatibility. Under high-voltage operation (>4.5 V *vs.* Li/Li^+), exacerbated transition metal (TM) ion dissolution and lattice oxygen evolution trigger cascading degradation:[79] structural collapse of cathode active

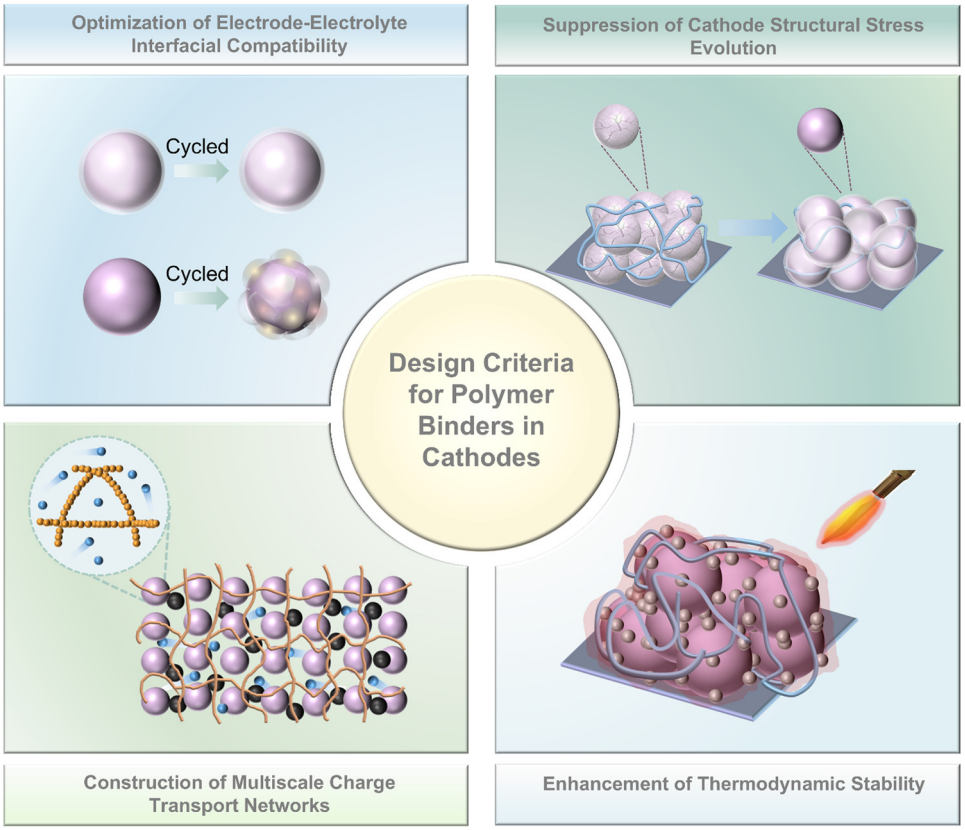

Fig. 3 Design criteria for polymer binders in cathodes of high-energy-density batteries.

materials, continuous electrolyte decomposition, and passivation failure of lithium metal anodes, ultimately leading to capacity decay and safety risks. While conventional polyvinylidene fluoride (PVDF) binders exhibit robust mechanical adhesion, their chemical inertness and lack of functional groups render them ineffective in mitigating these interfacial side reactions. Consequently, developing advanced polymer binders with integrated structural stabilization and interfacial regulation capabilities has emerged as a pivotal strategy to enhance electrochemical compatibility.

In high-energy-density lithium-ion systems, TM dissolution arises irreversibly from multiple factors: redox activity of TM ions, acidic component-induced cathode–electrolyte interfacial reactions, and thermal accumulation during cycling. Although industrially adopted PVDF binders demonstrate superior mechanical adhesion in cathodes, their nonpolar molecular architecture and absence of functional groups limit chemical anchoring of TM ions, failing to construct protective interfacial layers against metal ion dissolution. TM dissolution triggers multi-mechanism electrochemical degradation: (1) structural corrosion of cathode active materials directly reduces specific capacity; (2) dissolved TM ions migrate and electrodeposit on anode surfaces, forming electron-insulating passivation layers that severely degrade Li^+ transport kinetics and cause irreversible capacity loss; (3) TM leaching disrupts layered oxide lattice integrity, exacerbating cationic disorder and Li/Ni mixing, thereby accelerating structural instability and cycle life deterioration. Additionally, dissolved TM ions act as redox mediators, catalyzing electrolyte decomposition and inducing uncontrolled byproduct deposition at interfaces, which increases interfacial impedance and polarization. Crucially, these multiscale degradation processes exhibit autocatalytic characteristics that synergistically accelerate systemic aging. Therefore, advanced binder systems with TM-chelating functionalities, such as catechol-functionalized polymers or metal–organic framework hybrids, represent a critical pathway to overcome the long-cycle stability limitations of high-nickel cathodes.

Compared to conventional polyvinylidene fluoride (PVDF) binders, functional binders enriched with polar groups effectively suppress TM ion dissolution into electrolytes through chemical chelation mechanisms. Polyacrylic acid (PAA), with its abundant carboxyl groups, has been extensively investigated as a binder for layered oxide cathodes such as $LiNi_xCo_yMn_{1-x-y}O_2$ (NCM) and $LiNi_xCo_yAl_{1-x-y}O_2$ (NCA). Cheng *et al.* developed a multifunctional binder (PAA–PN) *via* chemical crosslinking of sodium phytate (PN) and PAA (Fig. 4a), demonstrating exceptional structural stability for NCM811 under high-voltage cycling (4.6 V cutoff).[80] Studies reveal that PAA–PN induces a dual-layer protection mechanism: an outer dense cathode–electrolyte interphase (CEI) and an inner defect-passivated rock-salt phase (Fig. 4b), synergistically suppressing TM dissolution, electrolyte oxidation, and stress-induced phase fatigue. The three-dimensional crosslinked network and strong surface coordination with NCM811 particles further mitigate grain boundary crack propagation

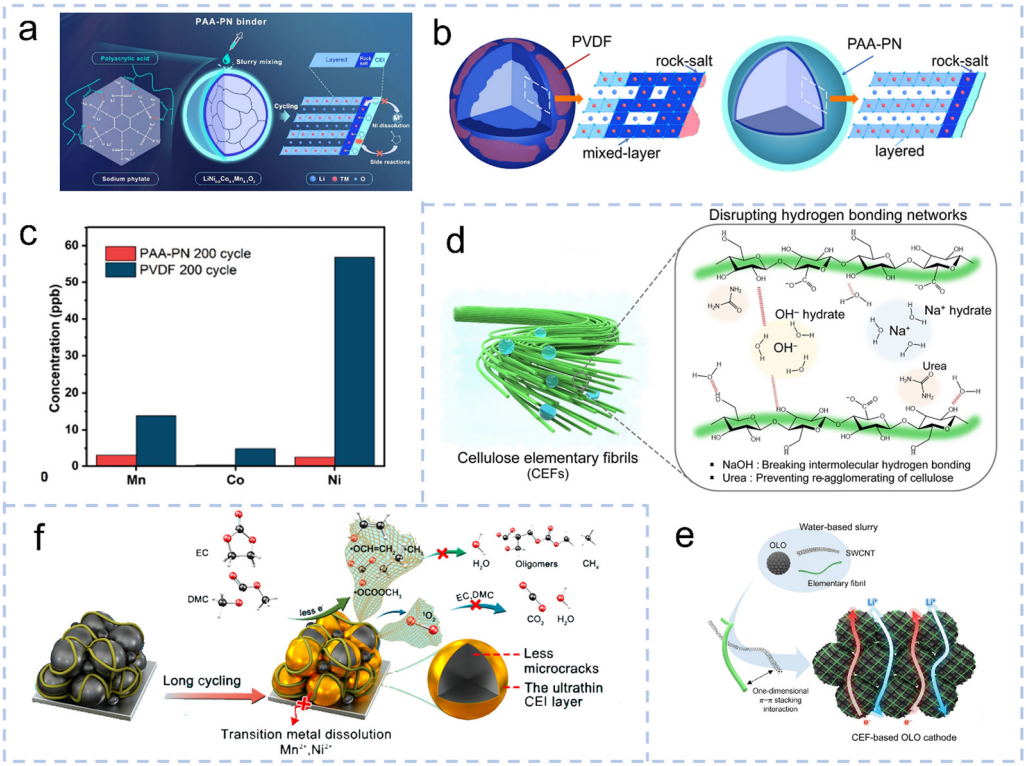

Fig. 4 (a) Schematic illustration of PAA–PN crosslinked binder synthesis and its surface-protective mechanism for NCM811 cathodes under high-voltage/high-temperature conditions. (b) Comparison of transition metal concentrations on cycled lithium foils extracted from NCM811-based cells after 200 cycles using PAA–PN *versus* conventional PVDF binders. (c) Functional mechanism of PAA–PN binder in stabilizing NCM811 surface structures by mitigating rock-salt phase formation under high-voltage operation.[80] Copyright 2025, American Chemical Society. (d) Hierarchical architecture of natural wood-derived cellulose. (e) Ion/electron transport behavior in cellulose elementary fibril (CEF)-based OLO cathodes.[81] Copyright 2025, Springer Nature. (f) Schematic illustration of the working mechanism in LTMOCs with antiaging binder.[82] Copyright 2021, American Chemical Society.

during cycling. Inductively coupled plasma mass spectrometry (ICP-MS) analysis (Fig. 4c) quantified severe interfacial side reactions in PVDF-based systems, showing nickel deposition of 56.95 μg L^{-1} on lithium counter electrodes after 200 cycles. In contrast, the PAA–PN binder reduced Ni deposition to 2.44 μg L^{-1}, confirming its ability to construct homogeneous and stable CEI layers that inhibit TM dissolution, thereby enhancing cathode–electrolyte interfacial stability during prolonged cycling.

To address the poisoning effects of dissolved TM ions on lithium metal anodes, the Sang-Young Lee team developed cellulose-based microfibril sheets (CEFs) derived from natural wood as a deagglomeration binder for high-loading cathodes.[81] The hierarchical disassembly structure of CEFs, featuring micron-scale cellulose units with enhanced surface anionic charge density, not only facilitates uniform integration with conductive carbon but also suppresses electrode–electrolyte interfacial side reactions *via* electrostatic repulsion (Fig. 4d). Leveraging these structural advantages, high-loading lithium-rich manganese-based (OLO) cathodes exhibit highly uniform redox reaction pathways (Fig. 4e). ICP-MS analysis demonstrates that CEFs reduce Ni, Co, and Mn deposition on lithium anodes by >85% compared to PVDF-based systems, effectively mitigating Mn^{2+}-driven SEI overgrowth. This work validates the feasibility of biomass-derived binders in constructing sustainable high-loading electrode architectures. Separately, Manthiram's team achieved concurrent stabilization of phase interfaces and bulk structures in high-nickel layered oxide cathodes through an *in situ* interpenetrating network binder. This binder forms a solid protective film on cathode surfaces *via* 3D interpenetrating networks and strong TM-ion coordination, suppressing electrolyte oxidation. Pouch cells employing this binder retain 82% capacity after 1000 cycles at 4.4 V, with a minimal capacity fade rate of 0.02% per cycle, providing critical insights for interfacial engineering of high-nickel cathodes.

Lattice oxygen evolution represents a critical failure mechanism in high-nickel layered cathodes under high state-of-charge (SOC) conditions, originating from the thermodynamic instability of surface lattice oxygen. During deep delithiation at high voltages, weakly coordinated lattice oxygen (O^{2-}) undergoes oxidation, releasing highly reactive oxygen species (ROS) such as superoxide radicals ($O_2^{-\bullet}$) and singlet oxygen ($^1O_2$). These ROS trigger chain reactions with carbonate-based electrolytes, driving continuous electrolyte decomposition and uncontrolled gas evolution (*e.g.*, CO_2, O_2). More critically, oxygen release induces irreversible layered-to-rock-salt phase transitions (*e.g.*, $5Li_{0.2}NiO_2 \rightarrow LiNiO_2 + 4NiO + 4[O]$), causing active lithium loss and bulk structural collapse, which account for >60% of the capacity fade. This self-accelerating degradation—where ROS-induced electrolyte byproducts exacerbate interfacial reactions, and structural degradation further

promotes oxygen release—leads to exponential performance decline. Thus, suppressing lattice oxygen loss is pivotal for enabling high-voltage operation of Ni-rich cathodes.

To address oxygen-induced degradation, Han's team developed an oxygen-confinement strategy using hindered amine light stabilizers (HALS) integrated into polymer binders. This system creates an antioxidant interface capable of quenching $^1O_2$ *via* energy transfer mechanisms, redirecting oxygen evolution pathways toward thermodynamically stable states. The modified cathodes exhibit exceptional electrochemical stability at 4.7 V and 45 °C, demonstrating concurrent stabilization of bulk structural integrity and cathode–electrolyte interphase (CEI) passivation. In parallel, Cui *et al.* developed a bio-inspired radical-scavenging binder system mimicking natural antioxidant mechanisms.[82] This binder continuously eliminates reactive oxygen species (ROS) through reversible redox reactions while inducing ultrathin and homogeneous CEI layers, thereby mitigating progressive electrolyte degradation (Fig. 4f). Remarkably, the layered transition metal oxide-based cells retain good electrochemical performance even at high temperatures, establishing a novel paradigm for high-temperature/high-voltage lithium-ion battery design.

2.2.2. Superior mechanical properties (mechanical strength, self-healing capability). High-loading cathodes represent a critical strategy for achieving high energy density in lithium-ion batteries. However, drastic volume deformation induced by lithium-ion de/intercalation during cycling amplifies exponentially with increased loading, leading to significant accumulation of diffusion-induced stress (DIS) within the electrode. When DIS exceeds the fracture toughness threshold of the material, it triggers microcrack propagation in cathode particles and delamination of layered structures. Additionally, sustained mechanical stress weakens interfacial bonding between active materials and current collectors, causing electrode-current collector delamination and active material exfoliation. These failures result in fractured conductive networks, surged interfacial impedance, and rapid capacity decay. Therefore, developing polymer binders that integrate high mechanical strength with dynamic adaptability is essential to maintaining structural integrity and electrochemical stability in high-loading cathodes.

The practical application of high-loading transition metal oxide cathodes (TMOCs) is constrained by non-uniform volume expansion/contraction and charge distribution heterogeneity during cycling. Polymer binders with molecularly engineered architectures can provide differentiated mechanical responses: rigid frameworks suppress irreversible TMOC expansion, while flexible/elastic networks dynamically adapt to volume changes and dissipate stress through dynamic bonding. For instance, the cationic semi-interpenetrating polymer network (c-IPN) binder developed by Sang-Young Lee's team (Fig. 5a) effectively suppresses electrode cracking during solvent evaporation while optimizing the dispersion uniformity of active materials/conductive agents *via* surface charge-induced electrostatic double-layer modulation.[83] The c-IPN binder electrostatically anchors electrolyte anions (*e.g.*, PF_6^-) to create localized high-concentration electrolyte environments, while its electrostatic repulsion promotes uniform Li^+ transport, stabilizing the cathode–electrolyte interface. As shown in Fig. 5b, the Li^+ diffusion coefficient (D_{Li^+}) of the c-IPN cathode exceeds that of the control n-IPN cathode across the entire voltage range. These results demonstrate that the c-IPN binder enables unrestricted Li^+ mobility and uniform Li^+ concentration distribution, driven by its electrostatic attraction to PF_6^- and repulsion toward Li^+. Consequently, c-IPN-based cathodes maintain exceptional cycling stability (82% capacity retention after 100 cycles) at areal capacities up to 20 mAh cm^{-2} while fully releasing their theoretical specific capacity (>210 mAh g^{-1}). Furthermore, pouch cells combining c-IPN cathodes with lithium metal anodes achieve energy densities of 376 Wh kg^{-1} and 1043 Wh L^{-1} at 45 °C (Fig. 5c), providing experimental validation for the industrial-scale application of high-loading electrodes.

Self-healing binders leverage dynamic reversible intermolecular interactions (hydrogen bonds, disulfide bonds, and coordination bonds) to enable damage repair in electrode structures, effectively mitigating stress concentration in active particles during high-rate charging/discharging and high-voltage cycling. Their mechanism relies on the dynamic network's ability to reconstitute at mechanical damage sites: strong molecular interactions both suppress crack initiation through energy dissipation and repair microcracks *via* bond reorganization, maintaining mechanical integrity and volumetric stability. However, electrochemical oxidation degradation of highly reactive functional groups (*e.g.*, –S–S–, –COOH) in such binders under high voltages (>4.5 V *vs.* Li^+/Li) remains unresolved, potentially causing irreversible network breakdown and accelerated capacity fade.

To address this trade-off, researchers optimize the balance between oxidation stability and self-healing capability through molecular topology design. Yang *et al.* engineered a polymer binder PVBST with unique viscoelastic behavior by tuning electrolyte-philic and -phobic domains (Fig. 5d).[84] By adjusting the loss modulus to closely match the storage modulus, PVBST achieves ultrahigh damping factors and viscosity–elasticity equilibrium. PVBST exhibits yield behavior at low strains and softening at high strains while maintaining maximum toughness. This rheological profile endows PVBST with three mechanical advantages: (1) high damping across broad frequency ranges to inhibit crack nucleation *via* viscous dissipation; (2) modulus surge post-critical strain to blunt crack propagation through tip passivation; (3) spontaneous micron-scale crack healing *via* reversible dissociation/recombination of dynamic ion pairs. Additionally, its zwitterionic groups immobilize lithium polysulfides while facilitating ion transport. These attributes enable lithium-ion batteries with superior specific capacity and remarkable capacity retention after extended cycling.

Meanwhile, Xiang's team developed a thermoplastic intrinsic self-healing polymer (TISP) binder synthesized from 2,3-butanediol (BDO), 1,3-propanediol (PDO), succinic acid (SuA), sebacic acid (SeA), and itaconic acid (IA).[85] Hydroxyl and ester groups in TISP form hydrogen bonds, ion–dipole interactions, and other bonds with active particles and current collectors, ensuring strong adhesion. Its low glass transition temperature (−60 °C), amorphous structure, and low crosslinking density

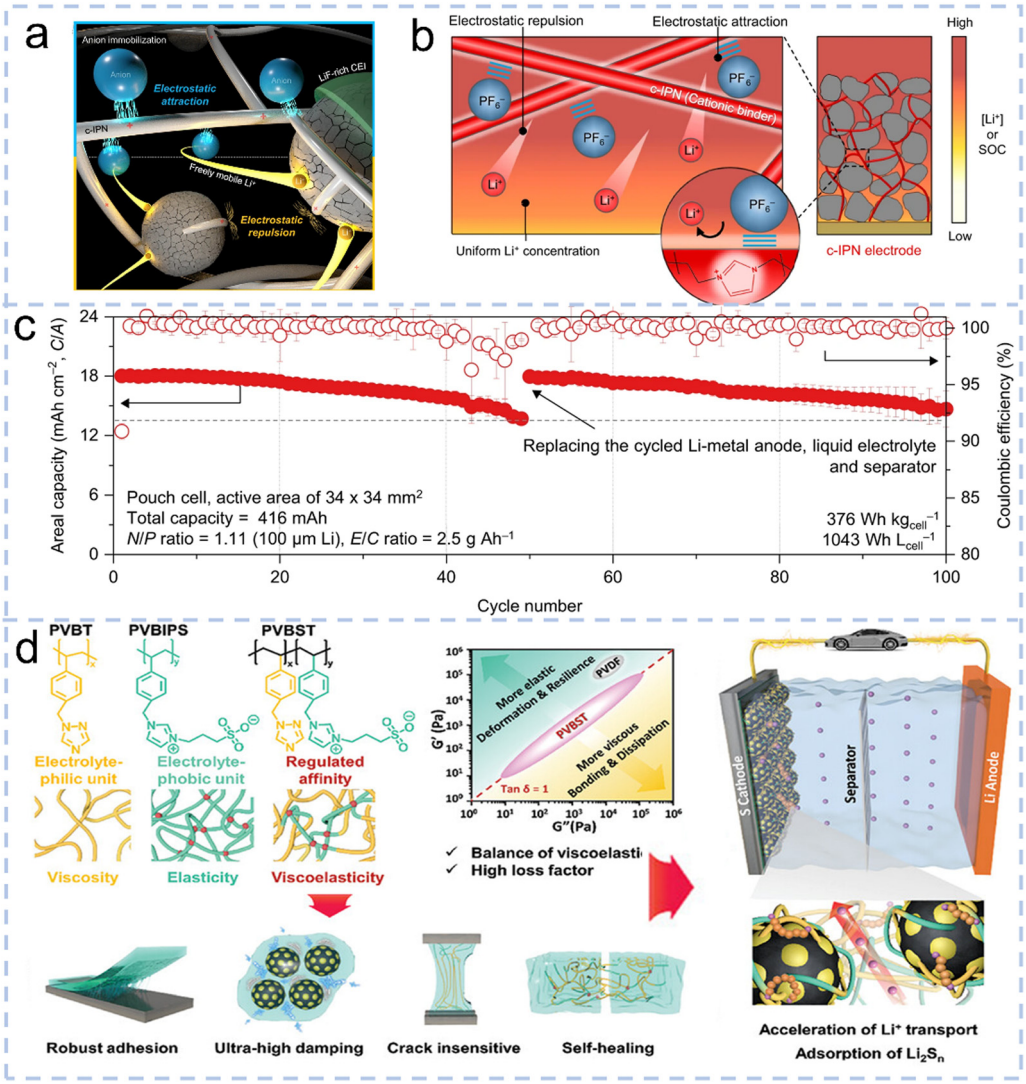

Fig. 5 (a) Schematic illustration showing the superiority of the c-IPN cathode. (b) Schematic illustration showing the role of the c-IPN binder in enabling the prevalence of freely mobile Li^+ with uniform distribution inside the cathode through electrostatic attraction with PF_6^- and electrostatic repulsion with Li^+ in the liquid electrolyte. (c) Pouch cells combining c-IPN cathodes with lithium metal anodes achieve superior energy densities.[83] Copyright 2023, Springer Nature. (d) Schematic illustrating the design of the PVBST binder for Li–S batteries.[84] Copyright 2024, John Wiley and Sons.

enhance polymer chain mobility at 40 °C, facilitating structural recovery and sustained adhesion. With a higher highest occupied molecular orbital (HOMO) level than electrolyte solvents, TISP undergoes preferential oxidation during charging, generating a chemically passivated interphase on cathodes that suppresses side reactions between $LiCoO_2$ and electrolytes under high-voltage conditions. Tests demonstrate that $LiCoO_2$ electrodes with TISP retain 162.4 mAh g^{-1} (86.5% capacity retention) after 349 cycles at 4.5 V. Post-cycling heating (40 °C, 1 h) restores 156.6 mAh g^{-1}, recovering ≈96% of its undamaged capacity, highlighting TISP's critical role in high-voltage systems.

For enhanced safety and electrochemical performance, Fu *et al.* designed a multifunctional binder (FHCP) *via* radical polymerization, integrating self-healing, flame-retardant, conductive, and polar group-rich properties for lithium–sulfur (Li–S) batteries.[86] Dynamic hydrogen and S–S covalent bonds enable FHCP to repair cracks from volume expansion, while polar groups and high conductivity strengthen polysulfide adsorption and charge transfer, mitigating the shuttle effect and accelerating redox kinetics. The binder's flame-retardant properties further improve Li–S battery safety. FHCP-based cells achieve 85% capacity retention after 100 cycles at 0.2 C and a reversible areal capacity of 5.25 mAh cm^{-2} with a sulfur loading of 4.72 mg cm^{-2}, even under reduced electrolyte conditions.

2.2.3. Rapid ionic/electronic transport kinetics (ionic conduction, electronic conduction, mixed ionic/electronic conduction). Inactive components do not participate in electrochemical reactions during battery charging/discharging and thus do not directly contribute to capacity or energy density. However, their mass and spatial distribution critically influence electrode architecture and electrochemical reaction

kinetics. For instance, the quality and dispersion of conductive additives directly determine electrode conductivity, which subsequently affects capacity. Non-uniform distribution or inferior quality of conductive additives may degrade conductivity, leading to reduced capacity. Furthermore, solid-state battery systems incorporate substantial solid ionic conductors ($\sim$10–30% of the composite cathode) *via* blending, casting, or hot pressing to establish continuous Li^+ transport networks within cathodes, inevitably compromising overall energy density.

Most conventional binders like PVDF lack intrinsic conductivity. Conductive binders address this limitation by incorporating conductive fillers to establish three-dimensional conductive networks within electrodes, compensating for the insufficient conductivity of traditional additives (*e.g.*, carbon black). These networks significantly reduce electrode resistance, enhancing rate capability and energy density. Conductive binders are categorized based on their functionality: electronically conductive binders, ionically conductive binders, and mixed ionic/electronic conductive binders.

For example, Li's team synthesized a conductive emulsion binder featuring a dual-continuous architecture with a rigid elastic copolymer core and conjugated polymer shell (Fig. 6a).[87] The elastic copolymer framework not only binds active materials during severe volume fluctuations but also traps lithium polysulfides *via* ester and nitrile functional groups. Simultaneously, the poly(3,4-ethylenedioxythiophene)-based conductive skeleton provides additional charge transport pathways and acts as a redox mediator, accelerating lithium polysulfide conversion kinetics. The immiscible yet electrostatically interactive core–shell polymers form a mesoscale interpenetrating network upon solidification, integrating rigid elastic frameworks with conductive channels. DMSO plasticization promotes mesophase separation between the polymers, while synergistic secondary doping enhances electrical conductivity ($>10^{-2}$ S cm^{-1}) (Fig. 6b). This design enables Li–S batteries with exceptional capacity and cycling stability through elastic confinement, enhanced charge transfer, and accelerated polysulfide conversion. The modular tunability of each component offers a novel design paradigm for multifunctional composite binders adaptable to diverse energy storage systems.

Song *et al.* proposed a novel "bollard-junction" dual-binder system, representing the first polytetrafluoroethylene (PTFE)-free binder for fibrillation-free electrode fabrication (Fig. 6c).[88] Sodium carboxymethyl cellulose grafted with polyacrylic acid (PC) acts as "bollards", forming robust bonds with PTFE "anchors". This system reduces PTFE usage by >70% while enabling high-mass-loading cathodes (up to 90 mg cm^{-2}, 15.6 mAh cm^{-2}) with superior performance. The PAA and CMC components in PC contain abundant polar groups (–OH, –COOH), which enhance ionic conductivity by facilitating Li^+ transfer between adjacent polar sites (Fig. 6d). PC forms strong chemical interactions with oxide layers on NCM particles and fluorine atoms in PTFE, improving interparticle adhesion. Full cells with PC-PTFE cathodes exhibit 84% capacity

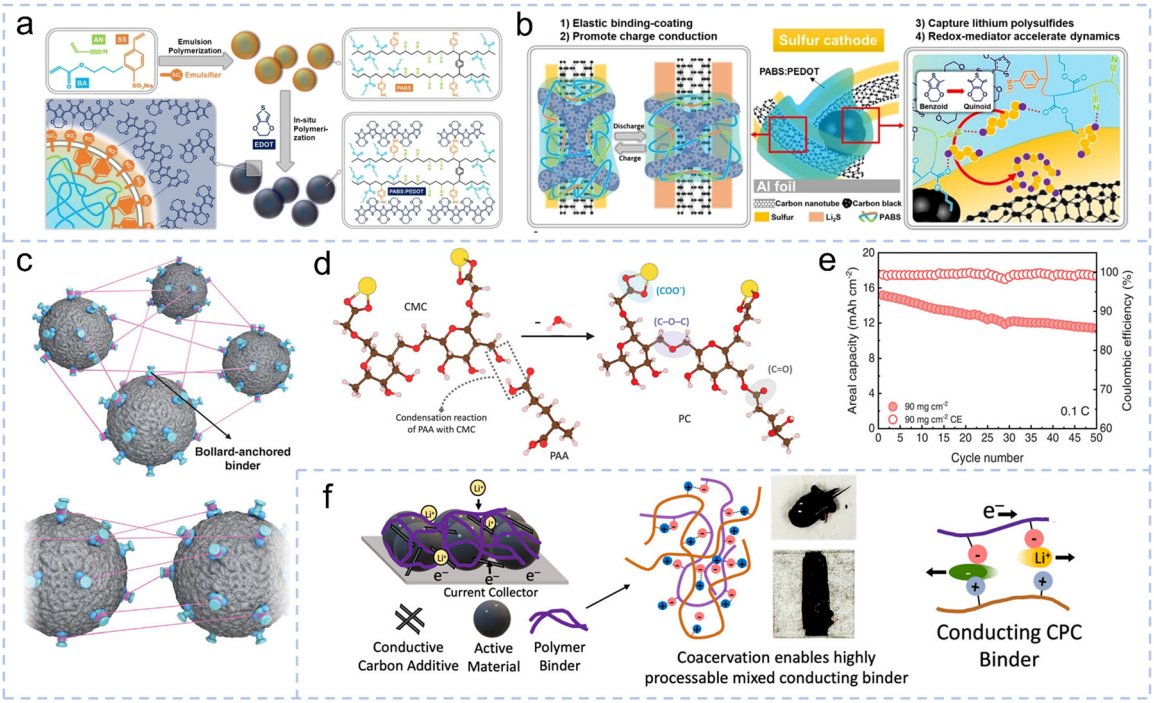

Fig. 6 (a) Schematic illustration of the preparation process and structure of PABS:PEDOT core–shell emulsion. (b) Schematic illustration for the multiple stabilization and enhancement mechanisms of PABS:PEDOT on S/CNT cathode performance.[87] Copyright 2024, John Wiley and Sons. (c) Schematic images of PC-PTFE binder from the dry process in the cathode electrode. (d) Schematic of the PC formation. (e) Cycle performance of each binder at 1/3 C for 25 mg cm^{-2}.[88] Copyright 2025, John Wiley and Sons. (f) Cathode composite composition and interactions, resistive binders create barriers to the transport of both of these charged species.[89] Copyright 2023, the American Chemical Society.

retention after 50 cycles at 0.5C, attributed to enhanced ionic conductivity and high-voltage stability (Fig. 6e). Furthermore, full cells with slurry-cast graphite anodes achieve 86% capacity retention over 100 cycles, outperforming PTFE-only counterparts. The system's improved ionic/mechanical properties make it suitable for high-voltage applications, demonstrating transformative potential for manufacturing durable, high-performance energy storage systems.

Rachel A. Segalman *et al.* developed an electrostatically stabilized blend of oppositely charged conjugated polymers and polyelectrolytes, offering a processable and stable binder with high ionic and electronic conductivity (Fig. 6f).[89] Using $LiFePO_4$ (LFP) cathodes as a model system, the conductive binder demonstrates significant improvements in rate capability and cycling stability. By reducing kinetic overpotential (polarization) and enhancing the apparent lithium diffusion coefficient, the novel binder enables LFP composites to achieve superior rate performance, delivering 65 mAh g^{-1} at 6C---compared to only 2 mAh g^{-1} for PVDF-based composites under identical conditions. The CPC binder's sufficient electronic conductivity ($\sigma \approx 3.1 \times 10^{-3}$ S cm^{-1}) allows carbon-free LFP composite cathodes to deliver a practical discharge capacity of 126 mAh g^{-1} at C/2, whereas PVDF-based composites fail to cycle at this rate without conductive additives. The electrostatically stabilized complex uniquely combines conductivity and stability, as ionic crosslinking prevents binder dissolution, enabling stability over 400 cycles. LFP composite cathodes with CPC binders exhibit exceptional cycling retention, maintaining 93% and 63% capacity after 100 and 400 cycles at 0.5C, respectively, starkly outperforming PVDF-based counterparts (92% at 100 cycles, 6% at 400 cycles). This work highlights the critical role of multifunctional binders in balancing interfacial kinetics and structural integrity for next-generation battery electrodes.

Composite cathodes in solid-state batteries face multifaceted challenges at solid–solid interfaces, including deteriorated physical contact, aggravated electrochemical side reactions, pronounced time-dependent phase separation, and sluggish Li^+/e^- dual-carrier transport kinetics. Constructing composite cathode interfaces with efficient ionic/electronic transport is pivotal for enhancing coulombic efficiency, cycling stability, and energy density. Addressing this, Li's team innovatively designed an electron–ion dual-conductive polymer (DCP) system *via* intermolecular interaction modulation. This system leverages molecular-level co-assembly of lithiated poly(vinyl lithium) (LiPVFM), lithium difluoro(oxalato)borate (LiODFB), and electron-conductive polymers to establish independent Li^+/e^- transport channels.[90] Experimental characterization reveals that strong intermolecular interactions endow DCP with high carrier concentrations: Li^+ conductivity of 2.76×10^{-4} S cm^{-1} and electronic conductivity of 68.9 S cm^{-1}. Simultaneously, rigid-flexible chain synergy ensures mechanical flexibility and interfacial compatibility. Notably, DCP forms uniform, stable coatings on active materials during slurry processing, enabling multifunctional synergy: (1) short-/long-range dual-conductive networks for Li^+/e^-; (2) suppressed electrode/electrolyte side reactions; (3) maintained cathode structural integrity during cycling. High-loading solid-state batteries fabricated *via* this strategy exhibit superior Coulombic efficiency and cycling stability. This study provides an innovative theoretical framework for rational design of multifunctional ion/electron-conductive polymers from a macromolecular perspective, offering critical guidance for developing high-energy-density solid-state energy storage systems.

2.2.4. Superior safety. High-nickel ternary cathode materials, as core components of high-energy lithium-ion batteries, exhibit critical thermal stability challenges. Studies reveal that these materials initiate thermal decomposition at 180–190 °C with significant exothermic effects, substantially increasing thermal runaway risks. Concurrently, gas evolution reactions at the high-nickel cathode/electrolyte interface elevate internal pressure, posing safety hazards. Notably, lattice oxygen evolution triggers a cascade of detrimental effects: structural collapse manifests as rapid capacity and voltage decay, while redox chain reactions may induce parasitic thermal runaway events.

To overcome this issue, through surface modification and component optimization, interfacial side reactions can be suppressed, thereby enhancing the chemical stability of the material. For example, Li's team prepared the amphiphilic copolymers (UMA-F_x) electrolyte by linking hydrophobic C–F side chains with hydrophilic subunits, which could self-assemble on the Ni-rich cathode surface and convert into a stable cathode–electrolyte interphase layer.[91] Thereafter, the oxygen release from the polymer coated cathode was obviously depressed and substituted by Co oxidation ($Co^{3+} \rightarrow Co^{4+}$) at high voltage (>4.2 V), which could suppress irreversible phase transfer and improve cycling stability (Fig. 7a). Moreover, the amphiphilic polymer electrolyte was also stable with a Li anode and had high ion conductivity. Therefore, the pouch cell exhibited outstanding energy density (362.97 Wh kg^{-1}) and durability (cycled 200 times at 4.7 V), which could be stably cycled even at 120 °C without short circuits or explosions.

Hu's team developed a water-based multifunctional binder (PEI-TIC) *via* a rapid epoxy-amine ring-opening reaction (10 min) (Fig. 7b),[92] featuring: (1) a 3D crosslinked network ensuring mechanical stability and adhesion; (2) abundant amino, carboxyl, and isocyanurate groups for polysulfide chemical anchoring and enhanced reaction kinetics; (3) flame-retardant properties validated by TG-FTIR, where thermal decomposition products suppress flame propagation. PEI-TIC-based Li–S batteries achieve an initial discharge capacity of 817.0 mAh g^{-1} at 0.2C and 97.2% capacity retention over 800 cycles (0.035% decay/cycle), maintaining 7.2 mAh cm^{-2} at 7.1 mg cm^{-2} sulfur loading, demonstrating exceptional practicality. Further research reveals a supramolecular β-cyclodextrin polymer (β-CDp) and glycerophosphorylcholine (Cg) crosslinked system (β-CDp-Cg-2AD) with dynamic adaptability.[93] Strong ion–dipole interactions between phosphate/polysulfide anions and Li^+/RNH_3^+ cations enable efficient polysulfide confinement and rapid Li_2S redox kinetics (Fig. 7c). Electrochemical testing shows a specific capacity of 1333 mAh g^{-1} at 0.1C and ultralow decay (0.012% $cycle^{-1}$) over 800 cycles. Remarkably, at 7.36 mg cm^{-2} sulfur loading, 99.0% areal capacity

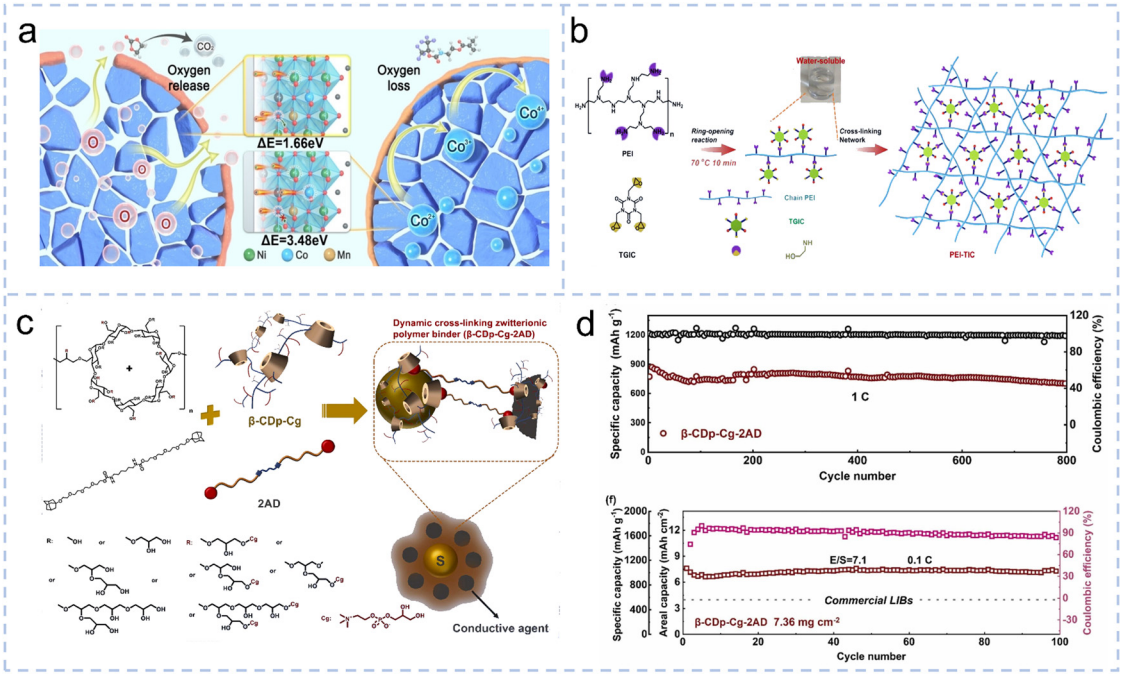

Fig. 7 (a) Schematic diagram of the effect of SNL-UMAF$_6$ and LE on positive electrode oxygen precipitation.[91] Copyright 2024, John Wiley and Sons. (b) Schematic illustration of PEI-TIC binder.[92] Copyright 2023, John Wiley and Sons. (c) Schematic illustration of the β-CDp-Cg-2AD binder. (d) Long cycling stability of the β-CDp-Cg-2AD electrode for 800 cycles and cycling performance of the β-CDp-Cg-2AD electrode with 7.36 mg cm^{-2} S-loaded (*E*/*S* = 7.1).[93] Copyright 2023, Elsevier.

retention (7.28 mAh cm^{-2}) after 100 cycles confirms compatibility with high-loading electrodes (Fig. 7d). TG-FTIR analysis reveals enhanced thermal decomposition temperatures and decomposition products that delay thermal runaway.

2.3. Development and outlook

As a critical functional component in lithium-ion battery (LIB) cathode systems, the structural properties and interfacial behavior of polymer binders directly determine the mechanical integrity, charge transport kinetics, and cycling stability of electrodes. To meet the engineering demands of high-energy-density batteries, researchers have achieved breakthroughs in multifunctional binder development through molecular structure design and functional group modulation. Recent studies focus on constructing smart binder systems with multi-responsive features: (1) enhanced electrochemical compatibility *via* π–π conjugation or ion–dipole interactions; (2) reduced interfacial impedance through conductive networks[94] (*e.g.*, PEDOT: PSS); (3) self-healing capabilities enabled by dynamic reversible bonds (disulfide/hydrogen bonds); (4) improved mechanical strength *via* multiscale structural engineering. These advanced binders not only suppress lattice oxygen evolution and cation disorder in transition metal oxides but also mitigate anisotropic volume strain during deep lithium de/intercalation *via* stress buffering, thereby extending the cycling life of cathodes.

In high-nickel ternary cathode systems, inherent thermal instability remains a critical challenge. Researchers propose synergistic strategies integrating flame-retardant group grafting (*e.g.*, phosphate esters) and self-healing networks to develop high-temperature-resistant binders. These binders repair microcracks *via* reversible covalent bond reorganization while quenching electrolyte combustion chain reactions, delaying thermal runaway initiation under thermal abuse conditions and improving battery safety.

Future advancements will prioritize: (1) biomimetic self-healing binder design using host–guest recognition (*e.g.*, cucurbituril-based supramolecular systems) for room-temperature self-repair; (2) machine learning-guided high-throughput screening of novel biodegradable bio-based binders (*e.g.*, chitosan derivatives); (3) multifunctional nanocomposite systems leveraging interfacial optimization from 2D fillers (MXene/CNT) to enhance lithium-ion transport efficiency.

3. Polymers in high-energy-density anodes

As the primary lithium-ion storage host, the capacity and stability of anode materials fundamentally dictate battery energy density and cycle life. While traditional carbon-based materials exhibit excellent cycling performance, their theoretical capacity (372 mAh g^{-1}) approaches fundamental limits, failing to meet next-generation battery requirements.[95] Silicon-based anodes (theoretical capacity 4200 mAh g^{-1})[96] and lithium metal anodes (3860 mAh g^{-1})[97] are considered ideal candidates to surpass energy density bottlenecks, yet their severe volumetric expansion (Si > 300%, Li metal: infinite) and

interfacial instability critically hinder commercialization.[98] In this context, polymeric materials—through molecular engineering and functional modification—offer innovative solutions for interfacial engineering and bulk-phase stabilization in high-capacity anodes.[98–100] This section systematically examines polymeric material applications in high-energy-density anodes, focusing on binder systems for silicon-based anodes and interfacial stabilizers for lithium metal anodes, while addressing their associated challenges.

3.1. Polymer binders for silicon-based anodes

3.1.1. Interfacial failure mechanisms and binder design principles for silicon-based anodes. Among lithium-ion battery anode materials, silicon-based materials have the greatest potential to replace commercial graphite due to their ultrahigh theoretical capacity ($Li_{22}Si_5$: 4200 mAh g^{-1}, volumetric capacity 9786 mAh cm^{-2}), low operating potential (<0.4 V *vs.* Li/Li^+), and natural abundance.[101] However, rapid capacity degradation remains a critical challenge for silicon anodes, primarily attributed to three failure mechanisms:

(1) Mechanical stress-induced failure:[102] silicon undergoes highly alloying reactions with lithium ions (Li^+) during lithiation/delithiation cycles, accompanied by extreme volumetric expansion/contraction (up to 300%) that generates periodic stress fields and internal stress gradients. In micrometer-scale silicon particles, cycling-induced microcrack propagation and particle pulverization directly disrupt electrical contact pathways between active materials and current collectors. This volume effect-driven mechanical failure mechanism has emerged as a critical constraint on electrode structural integrity.

(2) Interfacial passivation layer failure mechanism:[103] the continuous parasitic reactions between silicon surfaces and organic electrolytes at low potentials drive repetitive reconstruction of the solid electrolyte interphase (SEI) layer under thermodynamically metastable conditions. During silicon particle volume deformation, the dynamic fracture/reformation of the SEI film induces persistent electrolyte decomposition, forming a thick and heterogeneous interfacial passivation layer. This self-accelerating process not only causes irreversible consumption of active lithium but also significantly increases lithium-ion diffusion impedance.

(3) Conductive network failure mechanism:[48] the inherently low electronic conductivity (10^{-5}–10^{-3} S cm^{-1}) and sluggish lithium-ion diffusion coefficient (10^{-14}–10^{-11} cm^2 s^{-1}) of silicon-based materials synergistically exacerbate kinetic limitations in electrode systems. During cycling, three-dimensional volumetric deformation of silicon particles drives topological reconstruction of conductive agent/binder networks, manifested as increased interfacial contact resistance between active materials and conductive carbon phases, heterogeneous porosity distribution, and ultimately structural collapse of the three-dimensional conductive architecture.

To address these failure mechanisms, advanced binder design must fulfill multifunctional requirements: primarily constructing dynamically adaptive interfaces to effectively buffer volumetric stress through molecular chain elasticity; secondarily establishing robust chemical bonding networks (*e.g.*, hydrogen bonds, coordination bonds) to ensure durable adhesion between active materials and current collectors; concurrently optimizing synergistic electron/ion transport by integrating conductive functional groups, thereby enhancing charge transfer kinetics in composite electrodes (Fig. 8).

3.1.2. Design and research advances in silicon anode binders. The fundamental limitations of silicon-based anodes in lithium-ion batteries arise from their severe volumetric expansion effects (up to 300%) during lithium de/intercalation, which trigger electrode structural collapse, dynamic SEI instability, and conductive network failure. As the "molecular framework" governing electrode integrity, polymer binder systems demand coordinated optimization of mechanical robustness, interfacial stability, and charge transport characteristics. Functional engineering of these binders plays a pivotal role in enhancing the electrochemical performance of silicon anodes.

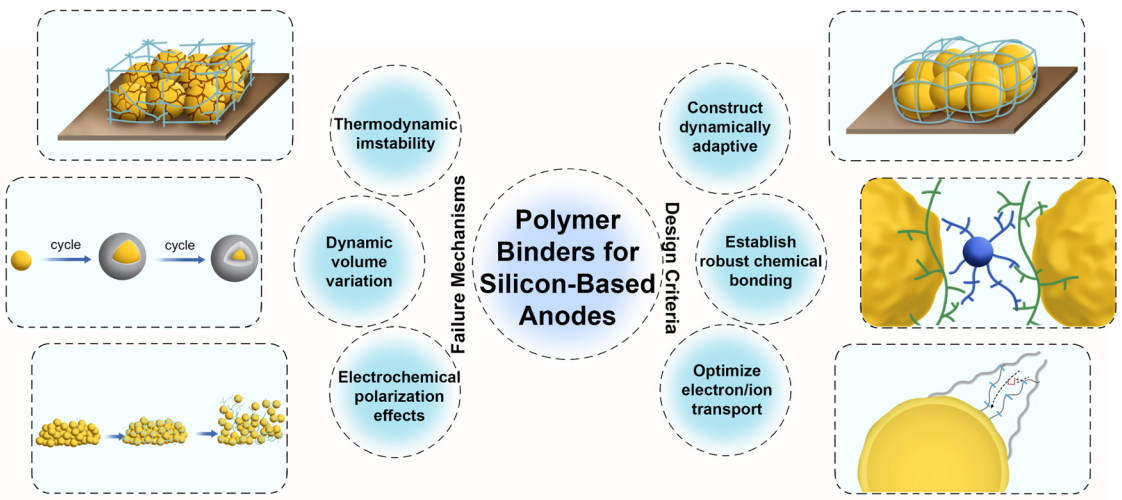

Fig. 8 Interfacial failure mechanisms and binder design principles for silicon-based anodes.

Traditional linear polymer binders (*e.g.*, sodium alginate (SA), carboxymethyl cellulose (CMC), polyacrylic acid (PAA), polyvinyl alcohol (PVA)) leverage abundant polar functional groups (–COOH, –OH) on their molecular chains to form hydrogen bonding interactions with silicon particle surface oxide layers (SiO_x), thereby enhancing interfacial adhesion.[99] However, the extreme volumetric expansion (up to 300%) during silicon lithiation poses severe challenges to the mechanical stability of their linear molecular frameworks. Strategies such as chemical crosslinking (*e.g.*, covalent bond formation) or physical composite approaches (metal ion coordination, small-molecule coupling, polymer blending) enable the construction of three-dimensional network structures within linear polymer matrices. This topological optimization not only significantly improves mechanical strength and strain adaptability but also allows elastic networks to buffer volume-induced stresses *via* stress dissipation mechanisms. To address silicon particle pulverization during cycling, dynamic self-healing binder systems demonstrate unique advantages. These materials achieve *in situ* self-repair of crack interfaces through reversible cleavage-recombination mechanisms involving dynamic covalent bonds (*e.g.*, disulfide, boronic ester) or non-covalent interactions (hydrogen/coordination bonds). Such dynamic adaptability effectively mitigates interfacial failure caused by silicon particle fracturing, thereby preserving electrode structural integrity and electrochemical stability. Notably, while linear polymers remain a research focus due to their polar group richness and modifiability, their inherent linear topology suffers from insufficient tensile modulus and poor creep resistance. Experimental studies confirm that multidimensional structural designs (*e.g.*, hyperbranched architectures, interpenetrating networks) significantly enhance mechanical performance and interfacial adhesion strength, providing critical theoretical guidance and technical pathways for developing high-performance silicon anode binders.

SA and CMC represent two classic linear polysaccharide-based binder materials in silicon anode research. Their molecular chains, rich in carboxyl (–COOH) and hydroxyl (–OH) functional groups, form multiple hydrogen bonds with the oxide layer (SiO_x) on silicon particles, maintaining electrode structural stability through interfacial adhesion.[104] SA (a natural anionic polysaccharide biopolymer extracted from brown algae (*e.g.*, Laminaria, Sargassum)) exhibits high viscosity, exceptional chemical stability, and environmental compatibility. Given its

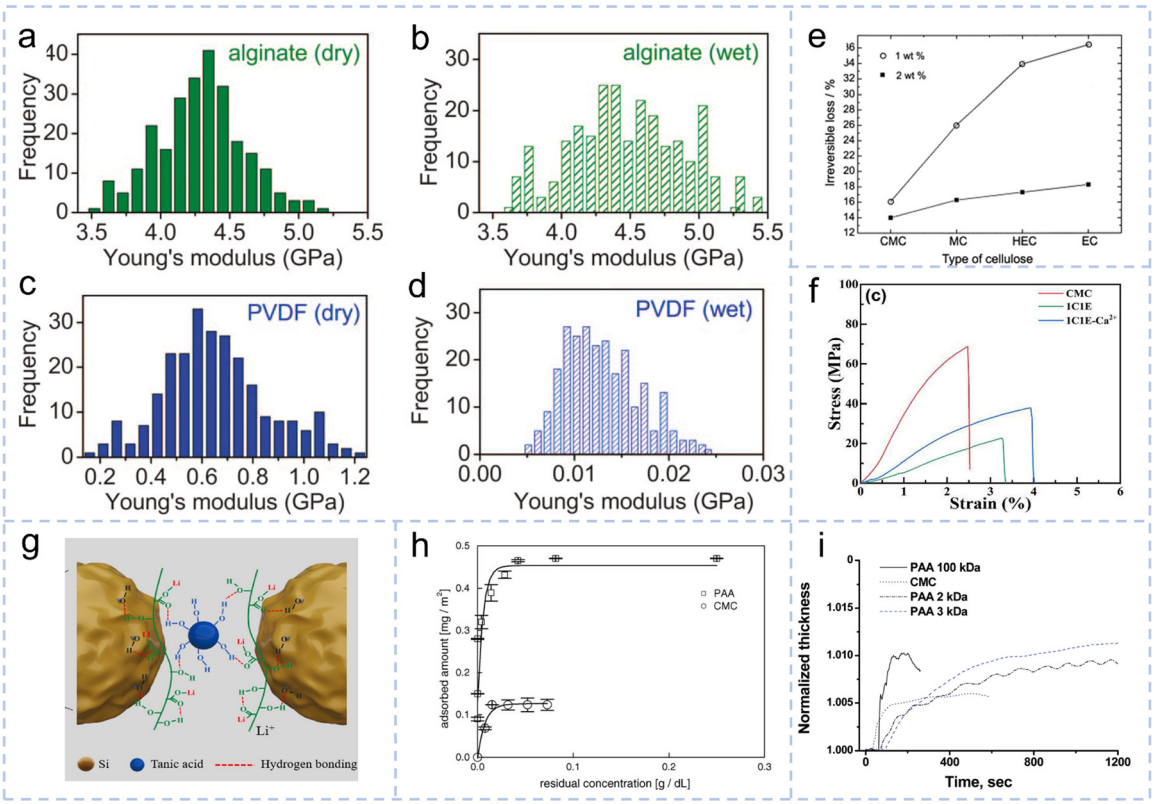

Fig. 9 (a)–(d) Young's modulus comparison of sodium alginate and PVDF in dry *vs.* solvent-swollen electrolyte states.[104] Copyright 2011, the American Association for the Advancement of Science. (e) Dependence of first-cycle irreversible loss on the type of cellulose used as a binding material.[109] Copyright 2002, Elsevier. (f) Stress–strain curves of CMC, 1C1E, and 1C1E-Ca^{2+} binders.[110] Copyright 2022, Elsevier. (g) 3d-crosslinked illustration of the Si electrode based on the LiCMC-TA binder.[111] Copyright 2022, Elsevier. (h) Adsorption isotherms of polyacrylic acid (PAA) and carboxymethyl cellulose (CMC) on graphite in aqueous solutions at 25 °C, with final suspension pH values ranging from 5.2 to 5.6. Error bars represent calculated standard deviations of experimental data.[113] Copyright 2006, Elsevier. (i) Swelling behavior of PAA with varying molecular weights (M_w) and sodium-CMC (Na-CMC) in diethyl carbonate vapor atmospheres.[114] Copyright 2010, the American Chemical Society.

potential for silicon electrode applications, SA's structure–property relationships and modification strategies have been systematically studied. In 2011, Yushin's team pioneered SA as a PVDF alternative, demonstrating its elastic modulus to be 6.7 times higher than PVDF (Fig. 9a–d).[104] This rigidity effectively suppressed particle fracturing caused by anisotropic expansion during initial silicon lithiation. Concurrently, strong hydrogen bonding between Si-OH groups (from silicon hydroxylation) and SA's carboxyl groups significantly enhanced cycling durability. However, SA's intrinsic linear topology restricts interfacial interactions with silicon to single-dimensional bonding, resulting in insufficient adhesion strength and low fracture toughness under extreme volumetric expansion (>300%).[105] Repeated silicon expansion/contraction induces irreversible plastic deformation in SA binder networks, ultimately causing electrode structural collapse. To address this, current research focuses on constructing multidimensional SA-based composite binder systems by integrating functional polymers (*e.g.*, polydopamine),[106] dynamic crosslinkers (*e.g.*, boronic ester compounds),[107] or metal cations (Fe^{3+}, Al^{3+}) to form three-dimensional interpenetrating network architectures.[108] This strategy concurrently enhances the energy dissipation capacity and strain-adaptive characteristics of the binders, offering practical solutions for high-capacity silicon anode commercialization.

CMC, a linear anionic polysaccharide polymer derived from cellulose *via* carboxymethylation, features high-density carboxylate groups ($-COO^-$) that not only confer exceptional water solubility and shear-thinning behavior but also form Si–O–C covalent bonds through dehydration condensation reactions with silicon surface hydroxyl (Si–OH) and silicon oxide (SiO_x) layers, thereby reinforcing electrode structural stability. In 2003, Drofenik's team pioneered CMC application in graphite anode binder systems, where its superior dispersibility and viscoelasticity in aqueous solvents optimized slurry rheology and reduced electrode polarization impedance (Fig. 9e).[109] However, the intrinsic linear topology renders pure CMC films excessively brittle and poorly extensible, failing to accommodate silicon's extreme cyclic volume fluctuations. To overcome this limitation, researchers employ multidimensional structural engineering strategies. For instance, Zhang *et al.* developed a dynamic ionic crosslinked network between ethylenediaminetetraacetic acid disodium (EDTA-2Na) and CMC carboxyl groups, achieving a composite binder fracture strain of 4.0% while maintaining tensile strength above 68 MPa (Fig. 9f).[110] The Tang group engineered a 3D lithiated CMC–tannic acid (LiCMC–TA) composite binder system, where hydrogen bonding between partially lithiated CMC and TA molecules creates a 3D interpenetrating network. This design transforms silicon-binder interfacial contact from discrete point-line interactions to continuous planar engagement, effectively localizing silicon particle expansion stresses and suppressing electrode crack propagation (Fig. 9g).[111]

Polyacrylic acid (PAA), a linear anionic polymer synthesized *via* free radical polymerization of acrylic acid monomers, exhibits exceptional water solubility and chemical versatility due to its hydrophilic carboxyl groups (–COOH). Crucially, the linear chain architecture of PAA enables the construction of three-dimensional network topologies through covalent crosslinking (*e.g.*, amidation reactions) or physical crosslinking (metal ion coordination, hydrogen bonding assemblies), providing an ideal platform for developing high-strength adaptive binder systems.[112] In 2006, Paik's group systematically investigated the influence of PAA on graphite anode slurry rheology and electrode mechanical properties (Fig. 9h).[113] Their findings revealed that electrostatic repulsion between PAA molecular chains significantly enhanced graphite particle suspension stability under low shear rates, while chemical chelation between carboxyl groups and copper current collector oxides substantially improved interfacial adhesion, establishing theoretical foundations for aqueous binder applications in lithium-ion batteries. In 2010, Yushins team pioneered PAA implementation in silicon anodes, demonstrating its low swelling characteristics and high elastic modulus effectively suppressed silicon particle pulverization during lithiation. Dehydration condensation between PAA carboxyl groups and silicon surface hydroxyls (Si–OH) formed robust Si–O–C covalent bonds, enhancing lithium-ion diffusion kinetics and stabilizing SEI layer formation (Fig. 9i).[114] However, excessive hydrogen bonding between PAA chains results in poor flexibility, limiting adaptability to silicon's 300% volumetric expansion. To address this, researchers developed a "rigid-flexible synergy" strategy: constructing dual-network architectures with gradient moduli through topological crosslinking of rigid PAA chains with flexible components (polyethylene glycol, polyurethane). These composite binders localize silicon expansion strains and inhibit crack propagation pathways.[115]

Polyvinyl alcohol (PVA) has been widely adopted in silicon anode binder systems due to its hydroxyl-rich molecular chains forming effective hydrogen bonding interactions with silicon's native oxide layer (SiO_x). However, PVA's inherent low cohesive strength and insufficient interfacial bonding energy lead to active material/current collector delamination under significant cyclic mechanical stresses. Current research focuses on enhancing interfacial stability by integrating PVA as a flexible component into crosslinked polymer networks. For instance, polyacrylic acid (PAA)/PVA composite binders synergistically combine PAA's strong adhesion with PVA's elasticity. Yin *et al.* innovatively designed a dopamine (DA)-modified PAA–DA/PVA composite binder: grafting DA molecules onto PAA chains formed a PAA–DA copolymer that establishes a dynamic hydrogen-bonded network, while thermally initiated covalent crosslinking between PVA and DA created a three-dimensional interpenetrating network (Fig. 10a).[116] This dual-network design synergized stress dissipation (*via* dynamic hydrogen bonds) with structural stability (*via* covalent crosslinks), enabling the Si@PAA–DA/PVA electrode to retain a reversible capacity of 1974.1 mAh g^{-1} after 500 cycles at 4 A g^{-1}. Notably, while functional group crosslinking of linear/branched polymers can enhance mechanical properties through 3D networks, binder design must systematically address chemical compatibility with electrolytes, particularly interfacial side reactions affecting electrode/electrolyte stability.

Self-healing materials, capable of reconstructing microstructures through reversible physical/chemical interactions,

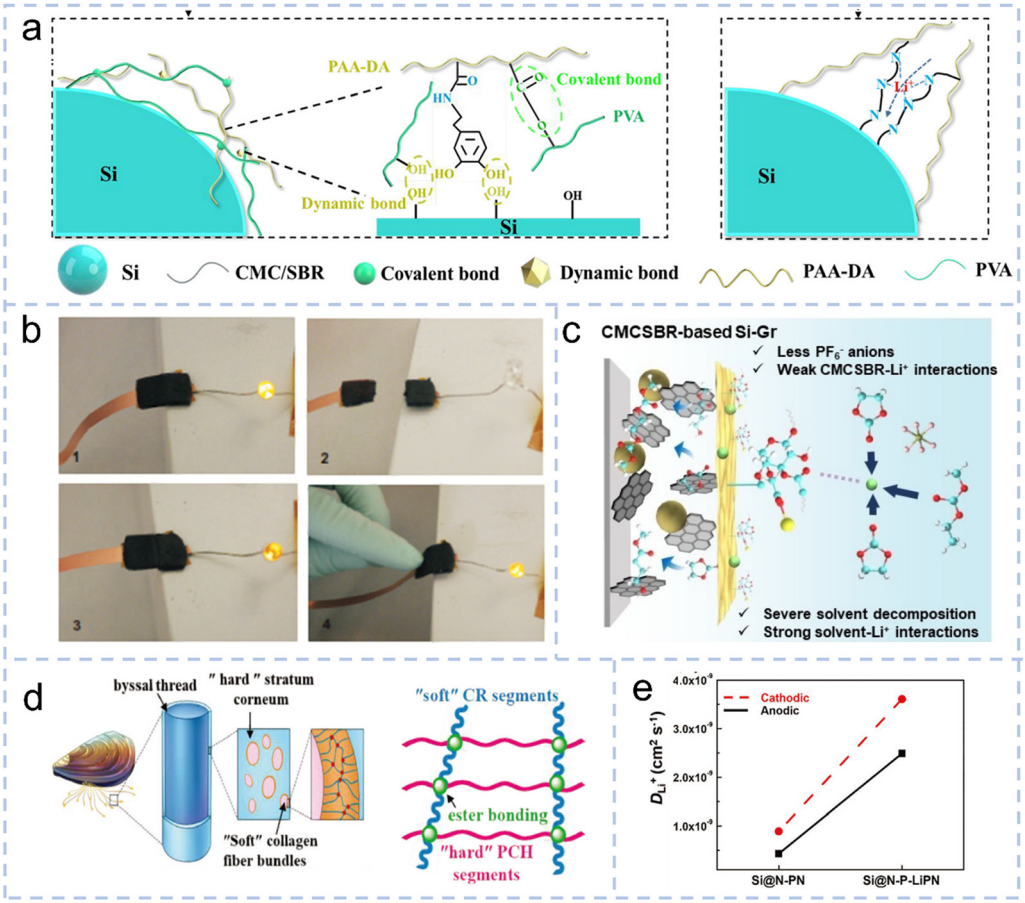

Fig. 10 (a) Schematic illustration of the action mechanism of the CMC/SBR binders in Si electrode during cycling.[116] Copyright 2022, American Chemical Society. (b) Demonstration of the electrical and mechanical self-healing capability of the conductive composite using a battery-powered circuit with the composite SHP as the conductive pathway that connects the LED to the battery.[117] Copyright 2013, Springer Nature. (c) Schematic of the influences of the binder species on Li^+ solvation structures in the binder-electrolyte interphases.[118] Copyright 2024, John Wiley and Sons. (d) Schematic illustration of byssal thread of mussels and the byssal thread-like synergetic soft-hard segment polymer network of the PCH-CR binder.[120] Copyright 2023, John Wiley and Sons. (e) Li^+ coefficient of the Si electrodes using N-P-LiPN and N-PN binders.[123] Copyright 2020, John Wiley and Sons.

demonstrate unique advantages in conductive composites, functional surface engineering, and energy storage/conversion devices. For silicon anode systems, lattice distortion-induced volumetric expansion during deep lithiation/delithiation cycles leads to structural pulverization and interfacial mechanical failure. Self-healing binders based on dynamic bonding mechanisms enable autonomous repair of fractured interfaces *via* dynamic non-covalent interactions (hydrogen bonds, ionic interactions) or electrostatic attraction effects, thereby preserving Ohmic contact among active materials, conductive additives, and current collectors. Notably, the molecular design of such materials often draws inspiration from natural biological self-repair mechanisms. For instance, Cui's group developed a self-healing polymer (SHP) binder leveraging the dynamic associative properties of multiple hydrogen bonds in hyperbranched topological polymers. The reversible breakage-reformation of hydrogen bond networks in its amorphous structure allows spontaneous chain diffusion and rearrangement at crack interfaces, achieving autonomous repair of microscopic defects (Fig. 10b).[117]

The severe volumetric expansion of silicon-based anodes during cycling induces periodic fracture/reconstruction of the solid electrolyte interphase (SEI), driving continuous irreversible consumption of Li^+ and electrolytes. Theoretical studies demonstrate that molecular engineering of functional binders can effectively regulate SEI chemical composition and mechanical stability. Specifically, binder systems containing polar functional groups (–COOH, –OH) establish C–O–Si covalent bonding with silicon surfaces.[118] This interfacial chemical bonding mechanism not only suppresses direct electrolyte-silicon contact but also mitigates SEI overgrowth by reducing interfacial energy. More critically, polar groups modulate Li^+ solvation structures to induce formation of dense SEI layers rich in inorganic components (LiF, Li_2O). The enhanced mechanical flexibility and interfacial adhesion of such SEI layers significantly reduce fracture probability under volumetric strain.

The initial electrochemical cycling of silicon-based anodes involves significant irreversible capacity loss due to the formation of non-active compounds (*e.g.*, Li_2CO_3, LiF) from

lithium-ion and electrolyte reduction.[119] While this passivation layer exhibits electron-insulating and Li^+-selective permeability to prevent direct active material-electrolyte contact, its thermodynamic stability faces severe challenges under dynamic volumetric fluctuations. Repeated mechanical stress induces brittle fracture-regeneration cycles of the SEI layer, accelerating irreversible lithium loss and continuous electrolyte decomposition. Recent advancements reveal that functional binders with tailored ionic groups enable dual modulation: cationic groups alter Li^+ solvation sheath structures *via* coordination, while anionic groups suppress solvent reduction through electrostatic repulsion, synergistically promoting ultrathin SEI layers with high ionic conductivity and mechanical integrity. Current research prioritizes constructing multifunctional smart binder systems. For instance, Manthiram's team developed a zwitterionic binder for silicon-based anodes by grafting and polymerizing zwitterionic moieties onto commercial polysaccharides. This approach establishes a charge-modulated microenvironment that alters the solvation environment at the silicon anode interface, thereby facilitating the formation of a thin, uniform, and mechanically robust SEI (solid electrolyte interphase) layer through tailored interfacial electrochemistry (Fig. 10c).[118] Cui and colleagues created a novel binder, referred to as PCH-CR, drawing inspiration from the structure of mussel byssal threads. This binder features a synergistic combination of hard and soft segments. The hard segment is a hydrophilic copolymer formed from sodium 2-carboxyethylacrylate and *N*-(2-hydroxyethyl)acrylamide, while the soft segment is an oleophilic elastomer, specifically carboxylic styrene butadiene rubber. These components are linked through an *in situ* ester crosslinking reaction. The strategic integration of these distinct segments leads to a significant increase in the topological entropy of the polymer network. Consequently, this design imparts superior mechanical strength and enhanced adhesion to the binder. Such advancements substantially improve the dynamic stability of the solid electrolyte interphase (SEI), effectively suppressing undesirable side reactions at the interface. This study offers crucial theoretical insights for the development of practical, high-capacity silicon anodes (Fig. 10d).[120]

The inherent low electronic conductivity ($\sim 10^{-3}$ S cm^{-1}) and ion migration barriers of silicon-based anodes severely constrain their high-rate performance, causing significant capacity attenuation under dynamic operating conditions. Addressing this challenge, next-generation conductive binder systems synergistically integrate mechanical support and charge transport functions through molecular engineering. For instance, polyaniline derivatives with conjugated π–π structures not only provide strong interfacial adhesion *via* π–π stacking but also establish intrinsic conductive networks through delocalized electrons, enabling continuous electron transport pathways across silicon particles.[118] Crucially, covalent C–O–Si bonding between conductive moieties (*e.g.*, thiophene rings, aniline units) and silicon surface hydroxyls ensures stable conductive pathways during volumetric deformation. Traditional physical blending with conductive additives (*e.g.*, carbon black) struggles to achieve efficient electron percolation due to high interfacial contact resistance. Researchers thus propose *in situ* hybridization of low-dimensional carbons (carbon nanotubes (CNTs), graphene) with functional polymers to construct 3D continuous conductive frameworks.[121] These composite binders achieve tight interfacial contact with silicon particles *via* π–π interactions, exhibiting electron mobility up to 10^2 S cm^{-1}. Concurrently, introducing electron-rich functional groups (ether oxygen (–O–), sulfonic acid (–SO_3H)) optimizes Li^+ solvation/desolvation kinetics by weakening Li^+–solvent binding energy through strong coordination, thereby reducing ion migration activation barriers.[122] Notably, while existing studies predominantly focus on electron transport networks, systematic understanding of binder-intrinsic Li^+ conduction mechanisms remains limited. Lin *et al.*'s N-P-LiPN triple-functional network binder offers an innovative solution (Fig. 10e):[123] molecular-level integration of rigid lithiated polyacrylic acid (P-LiPAA) with flexible lithiated perfluorosulfonic resin (P-LiNF). The –COOLi groups in P-LiPAA form a 3D mechanical framework, while –SO_3Li groups in P-LiNF serve as rapid Li^+ transport channels. Hydrogen-bonded networks in this system synergize stress buffering with ion conduction, achieving exceptional Li^+ migration efficiency and retaining 2021 mAh g^{-1} reversible capacity at an ultrahigh current density of 8.4 A g^{-1}. This rigid/soft dual-phase architecture establishes a critical paradigm for developing smart binders with coupled ionic conductivity and mechanical adaptability.

3.1.3. Development and outlook. The fundamental limitations of silicon-based anodes arise from severe volumetric expansion effects ($\sim$300%) during lithiation/delithiation, triggering multi-mechanistic failure: (1) repetitive silicon particle expansion/contraction induces electrode pulverization and interfacial electrical contact loss; (2) dynamic fracture/regeneration cycles of the SEI accelerate irreversible lithium and electrolyte depletion; (3) sluggish charge transfer kinetics due to silicon's inherently low electronic/ionic conductivity. While conventional linear polymer binders (*e.g.*, CMC, PAA) partially buffer volumetric strain through molecular chain extensibility, their limited mechanical elastic modulus fails to accommodate extreme silicon deformation, and they cannot address rising ion transport impedance caused by SEI thickening.

To address these challenges, current research focuses on multiscale synergistic optimization strategies. At the material design level, three-dimensional crosslinked topological architectures (*e.g.*, epoxy-based crosslinking networks) and supramolecular mechanically interlocked networks (*e.g.*, cucurbituril-based host–guest systems) enhance binder stress dissipation capabilities, while dynamic reversible bonds (disulfide, boronic ester) enable self-healing properties to maintain electrode integrity. At the interface engineering level, nanosilicon/graphene core–shell structures confine volumetric expansion to <150%, and atomic-layer-deposited Al_2O_3 coatings inhibit electrolyte penetration while promoting stable LiF-rich SEI formation. Electrochemical prelithiation (*e.g.*, Li_2S/LiF chemical doping) elevates initial Coulombic efficiency to >90%. Furthermore, *in situ* construction of three-dimensional interpenetrating conductive

networks (*e.g.*, polypyrrole/carbon nanotube composites) enhances bulk electrode conductivity to $\sim 10^2$ S cm^{-1}.

Future breakthroughs require prioritizing: (1) gradient modulus binder systems with spatially arranged rigid-flexible molecular segments for optimized stress distribution; (2) cost-effective scalable fabrication techniques (solution self-assembly, *in situ* polymerization) for industrial compatibility; (3) binder-solid electrolyte interfacial coupling mechanisms for all-solid-state batteries to address the co-optimization challenges of interfacial ion transport kinetics and mechanical compatibility. These innovative strategies will provide critical theoretical and technical foundations for the practical implementation of silicon anodes in high-energy-density energy storage systems.

3.2. Polymer interfacial stabilizers for lithium metal anodes

3.2.1. Failure mechanisms and stabilizer design principles for lithium metal anode interfaces. Lithium metal anodes possess exceptional theoretical capacity (3860 mAh g^{-1}) and the lowest electrochemical potential (−3.04 V *vs.* SHE), yet their practical application is hindered by low Coulombic efficiency (typically <98%), rapid capacity degradation, and safety risks.[124,125] These limitations stem from multifaceted interfacial destabilization mechanisms, as shown in Fig. 11: (1) thermodynamic instability:[48] the high reducibility of lithium induces intense reactions with conventional liquid electrolytes, forming amorphous SEI layers with heterogeneous porous structures. These brittle passivation layers fracture during Li plating/stripping due to inadequate mechanical strength, triggering continuous "SEI rupture-regeneration" cycles that irreversibly deplete active lithium and electrolytes; (2) dynamic volume variation:[126] cyclic volume fluctuations exceeding 200% induce microcracks and stress concentration at the electrode/electrolyte interface, causing heterogeneous Li^+ flux distribution and mossy lithium deposition; (3) electrochemical polarization effects:[127] at high current densities (>3 mA cm^{-2}), diffusion-limited deposition arising from Li^+ concentration gradients initiates dendritic growth, where intensified electric fields at dendrite tips can penetrate separators, inducing internal short circuits.

To address these interfacial failure mechanisms, the development of hierarchically functionalized interfacial stabilizers has emerged as a critical strategy for stabilizing lithium metal anodes. Ideal stabilizers must satisfy three core design criteria: (1) constructing composite SEI layers with high ionic conductivity and Young's modulus through synergistic chemical passivation and mechanical reinforcement;[128] (2) establishing uniform Li^+ transport pathways to eliminate localized current density gradients;[129] (3) maintaining compatibility with existing battery systems without compromising energy density.[130] Current stabilizer systems primarily fall into three categories: (I) organic–inorganic hybrid materials, where inorganic components provide mechanical rigidity while organic phases enhance interfacial flexibility; (II) two-dimensional materials with Li^+-selective transport properties, leveraging nanoconfinement effects to regulate lithium deposition orientation; (III) multifunctional polymer electrolytes (*e.g.*, PEO–LiTFSI composites), where strong ether oxygen-Li^+ coordination enhances lithium-ion transference numbers, suppressing concentration polarization.

Traditional physical blending additives often suffer from phase separation issues that limit their interfacial modification efficacy. Recent advances propose an "*in situ* polymerization-self-assembly" strategy: electrochemically triggered polymerization of acrylate monomers on lithium surfaces forms gradient-modulus polymer layers that simultaneously suppress dendrite penetration and buffer volumetric strain through swelling effects. Bioinspired interfacial designs, such as polydopamine-modified separators, enable dynamic SEI repair *via* reversible redox interactions of amine/phenolic hydroxyl groups. For high-energy-density systems, self-supporting polycarbonate-based electrolyte membranes serve dual roles as ionic conductors and mechanical barriers, extending cycle life while maintaining energy density. Future stabilizer development must prioritize multifunctional integration (ion conduction, stress buffering, and self-healing synergies) and precise regulation of interfacial

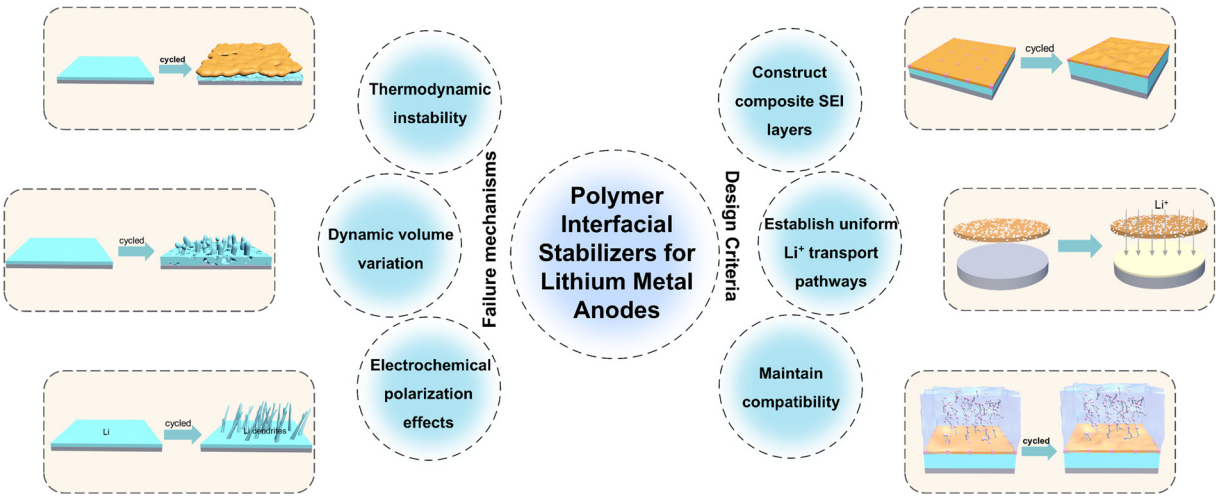

Fig. 11 Polymer interfacial stabilizers for lithium metal anodes.

kinetics (optimizing Li^+ transport barriers *via* Arrhenius equation analysis), coupled with *in situ* characterization to decode dynamic interfacial evolution mechanisms.

3.2.2. Design and research progress of interfacial stabilizers for lithium metal anodes. In commercial lithium-ion battery systems, conventional electrodes operate *via* intercalation/deintercalation mechanisms, where lithium storage relies on reversible ion insertion/extraction within the electrode bulk phase. In contrast, lithium metal anodes function as conversion-type electrodes governed by metal electrocrystallization kinetics: Li^+ undergo electrochemical reduction ($Li - e^- \leftrightarrow Li^+$) at the electrode/electrolyte interface, depositing as metallic lithium on the surface. This interface-dominated deposition behavior inherently promotes lithium dendrite formation, particularly through curvature-driven growth mechanisms that favor dendritic morphologies (Fig. 12). Such irregular deposition structures risk internal short circuits and accelerated capacity decay, making the regulation of lithium deposition dynamics to achieve dense, uniform lithium plating a critical research focus. Achieving controllable lithium deposition necessitates systematic elucidation of key mechanistic factors: nucleation site formation principles, crystallographic growth orientation preferences, and Li^+ concentration gradient characteristics at interfaces. Furthermore, persistent side reactions between highly reactive lithium metal and electrolytes generate a surface SEI layer, a heterogeneous inorganic/organic composite structure that critically determines Coulombic efficiency, reaction reversibility, and cycling stability. The mechanical strength, ionic conductivity, and chemical stability of the SEI are intrinsically linked to its compositional architecture, driving intensive research into engineering adaptive SEI layers through advanced interfacial modification strategies to optimize lithium metal anode performance.[131]

Constructing artificial solid electrolyte interphases (SEI) represents a critical strategy for stabilizing lithium metal anode/electrolyte interfaces. An ideal SEI layer must fulfill dual functions: (1) physically isolating lithium metal from electrolyte contact to suppress parasitic reactions, and (2) combining mechanical toughness with structural adaptability to withstand cyclic volume fluctuations and mitigate dendrite penetration risks. *In situ* construction strategies have gained prominence due to their superior interfacial compatibility.

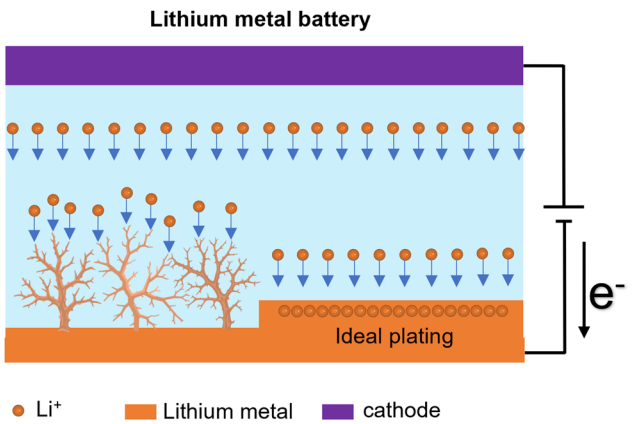

Fig. 12 Real deposition characteristics (left panel) and ideal plating morphology (right panel) for lithium metal battery charging.

Li's team has conducted a large amount of research on this aspect, for example, an artificial SEI layer was coated on a Li anode through *in situ* polymerizing polyester with fluorinated porphyrin, which could accelerate Li^+ desolvation and conductivity of the SEI. Then, the dual-salt eutectic polymer electrolyte tolerate is employed to accelerate Li^+ transfer through optimizing their solvation structure. The matching factor is calculated to evaluate the synergistic effect of σBulk and σSEI on low-temperature Li^+ mobility. Thus, homogenizing the Li^+ flux during Li-plating is achieved by regulating the Li^+ diffusion rate (δ = 1.92), which significantly mitigates overpotential aggravation and suppresses dendrite nucleation. Overall, such regulating factor could provide a theoretical parameter for evaluating the low-temperature tolerability of solid-state lithium batteries (SSBs), which would be useful for improving batteries' durability, safety and flexibility.[132]

Chen *et al.* developed an ultrathin covalent organic framework (COF)-based artificial SEI (denoted a COF-Li) *via in-situ* polycondensation of 1,3,5-tris(4-aminophenyl)benzene (TAPB) and terephthalaldehyde (PDA) on lithium surfaces (Fig. 13a).[133] Structural analysis revealed subnanometer-sized pores enabling ion-sieving effects to regulate Li^+ flux distribution and guide uniform nucleation (Fig. 13b and c). Mechanical testing demonstrated a Young's modulus of 6.8 GPa (Fig. 13d), exceeding the yield strength of lithium dendrites, providing mechanical suppression of dendritic growth. Electrochemical evaluation showed COF-Li symmetric cells achieving exceptional cycling stability over 400 hours at 1 mA cm^{-2} and 1 mAh cm^{-2} (Fig. 13e), attributed to the COF layer's physical blocking of dendrites. Mechanistic studies further identified multifunctional synergies: (1) lithiophilic imine groups in the framework promote $LiPF_6$ dissociation, reducing interfacial ion transport barriers; (2) molecular-scale pores (~0.8 nm) exert steric hindrance on anions (*e.g.*, $PF6^-$), enhancing Li^+ transference number; (3) the rigid porous framework maintains structural integrity during cycling, homogenizing local current density to alleviate polarization. These features collectively enable dense bulk lithium deposition morphology, significantly improving cycling reversibility.

Chen *et al.* developed a reactive block copolymer P(St-MaI) containing both carboxyl groups and crown ether units, which forms an adaptive polymer-based SEI layer *via in situ* polymerization on lithium metal surfaces.[134] This artificial SEI exhibits dynamic topological adaptability, effectively buffering volumetric deformation during cycling while maintaining stable interfacial electrical contact. Mechanistic investigations reveal (Fig. 13f): (1) carboxyl groups regulate lithium-ion solvation structures through coordination effects, reducing desolvation energy barriers; (2) crown ether units enable superior lithium-ion transport capabilities, guiding uniform lithium deposition; (3) rigid benzyl rings in the polymer backbone provide high mechanical modulus (8.2 GPa), suppressing dendrite penetration *via* stress dissipation mechanisms. Consequently, Li||Li symmetric cells with P(St-MaI)@Li composite anodes demonstrate exceptional cycling

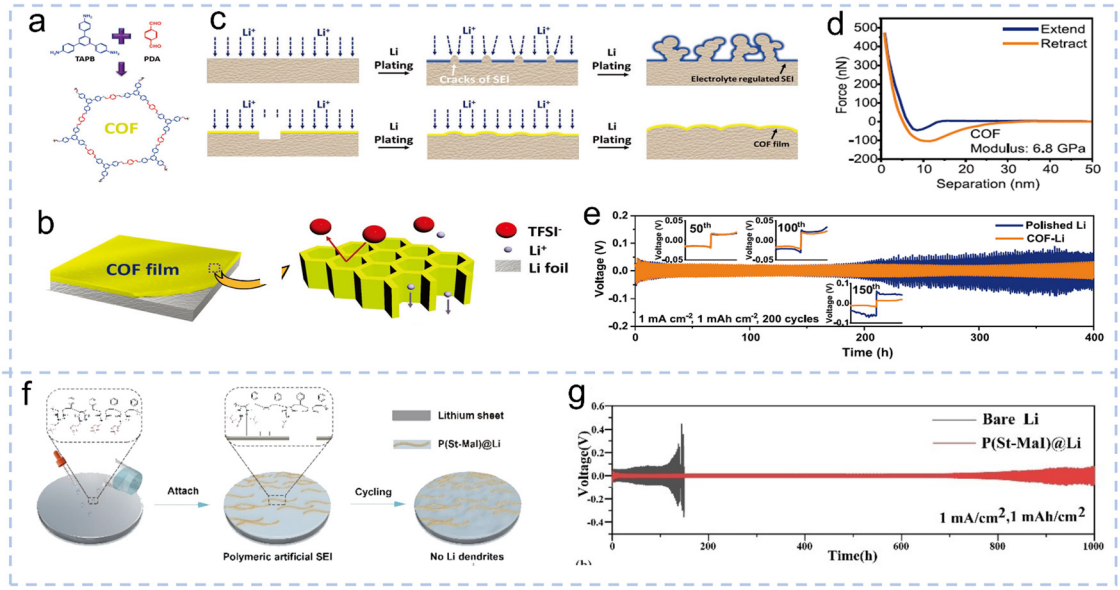

Fig. 13 (a) Schematic illustration of COF synthesis, (b) lithium-ion transport mechanism within the COF film, (c) SEI formation mechanism enabled by the COF film, (d) mechanical robustness of the COF-derived SEI layer, and (e) cycle performance enhancements in batteries employing the COF-SEI structure.[133] Copyright 2019, John Wiley and Sons. (f) Dendrite-free Li deposition morphology of P(St-Mal)@Li during cycling. (g) Cycling stability of P(St-Mal)@Li in Li symmetric cell configurations, demonstrating enhanced interfacial compatibility and electrochemical reversibility.[134] Copyright 2023, John Wiley and Sons.

stability exceeding 900 hours at 1 mA cm^{-2} and 1 mAh cm^{-2} without voltage polarization increase, outperforming unmodified lithium electrodes (Fig. 13g). Full cells (Li||$LiFePO_4$) employing this anode exhibit outstanding long-term cyclability in carbonate-based electrolytes, retaining 96% capacity after 930 cycles at 1C rate. This molecular engineering strategy for precise SEI composition/structure control provides new insights for developing high-stability lithium metal anode interfaces.

Constructing polymorphic polymer SEI layers on lithium metal surfaces effectively isolates electrolyte corrosion and enhances cycling stability. For instance, Xiong *et al.* engineered a supramolecular copolymer (PEO-UPy) protection layer with self-healing properties and strong interfacial adhesion.[135] A 70-nm-thick PEO-UPy coating suppresses dendrite growth under high areal capacity (10 mAh cm^{-2}) (Fig. 14a), enabling symmetric cells to achieve >1000 h cycling at 5 mA cm^{-2} (Fig. 14b). The UPy group's quadruple hydrogen-bonding network forms a stable SEI through *in situ* reactions with lithium, while PEO segments facilitate rapid Li^+ diffusion *via* polar group interactions, ensuring uniform plating/stripping. In composite anode development, Lu *et al.* engineered a poly(melamine-formaldehyde) (PMF)/lithium system that retains 94.7% Coulombic efficiency after 50 cycles at 10 mA cm^{-2}, with voltage plateau stability attributed to PMF's amine and triazine ring functionalities homogenizing Li^+ concentration fields (Fig. 14c).[136] Chen's team implemented an *in situ* polymerization strategy using α-cyanoacrylate to construct an artificial SEI layer, where cyano (–CN) groups react with lithium to form poly(ethyl cyanoacrylate) (PECA), achieving 93% capacity retention after 500 cycles at 2C *via* enhanced ionic conduction and dendrite suppression (Fig. 14d).[137] For optimizing SEI ion transport, Meng *et al.* synthesized a single-ion conductive SEI through copolymerization of lithium bis(trifluoromethanesulfonyl)imide (LiSTFSI) with pentaerythritol tetrakis(3-mercaptopropionate) (PTMP), 1,2-ethanedithiol (EDT), and diethylene glycol divinyl ether (DGDE).[138] This structure effectively suppresses dendrite growth induced by concentration polarization through enhanced lithium-ion transference numbers, enabling symmetric cells to achieve over 1200 hours of cycling stability under high current/capacity conditions (Fig. 14e). Additionally, a poly(diallyldimethylammonium) (PDDA)-bis(trifluoromethanesulfonyl)imide ($TFSI^-$) polycationic layer fabricated *via* solution casting on lithium surfaces by Huang *et al.*, regulates Li^+ deposition orientation through PDDA's electrostatic shielding effect, while the hydrophobic nature of $TFSI^-$ anions enhances interfacial stability. This modified lithium anode demonstrates stable cycling exceeding 700 hours at 1 mA cm^{-2} (Fig. 14f).[98] Crucially, the mechanical properties of polymer SEI layers decisively influence dendrite suppression. Constructing a poly(vinylidene fluoride-*co*-hexafluoropropylene) (PVDF-HFP)/lithium fluoride (LiF) composite interface layer simultaneously maintains high ionic conductivity and enhances mechanical strength, enabling dendrite-free lithium deposition.[139] Similarly, an organic–inorganic composite SEI layer constructed *via in situ* polymerization of poly(ethylene glycol) diacrylate (PEGDA) and lithium difluoro(oxalato)borate (LiDFOB) forms a tightly integrated interface structure with the substrate through lithiation reactions. Its exceptional flexibility and high mechanical strength enable symmetric cells to maintain stable cycling for 700 hours under ultrahigh current density (60 mA cm^{-2}) with overpotential consistently below 5 mV (areal capacity: 1 mAh cm^{-2}).[140] These advancements provide critical theoretical guidance and technical foundations for designing high-safety, long-cycling lithium metal batteries.

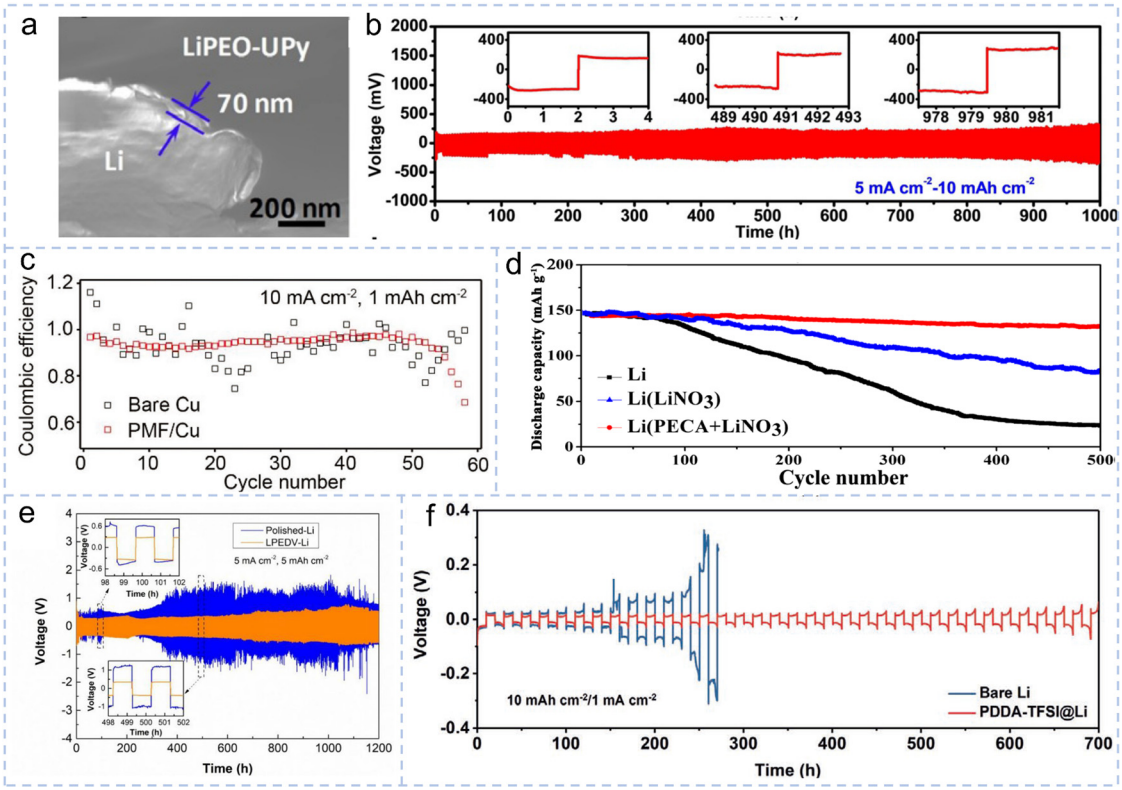

Fig. 14 (a) Cross-section SEM image of the LiPEO–UPy@Li anode. (b) Voltage profiles of bare Li and LiPEO–UPy@Li anodes in a symmetric cell at 5 mA cm^{-2} under a high areal-capacity of 10 mAh cm^{-2}.[135] Copyright 2019, John Wiley and Sons. (c) Lithium Coulombic efficiencies at 10 mA cm^{-2} with a fixed lithiation capacity of 1 mA h cm^{-2}.[136] Copyright 2018, John Wiley and Sons. (d) Cycling performance of Li(PECA + $LiNO_3$) cycled in $LiFePO_4$||Li cells for 500 cycles at 2C (current density: 2.08 mA cm^{-2}).[137] Copyright 2017, American Chemical Society. (e) Galvanostatic cycling test of polished-Li and LPEDV-Li at 5 mA cm^{-2} and 5 mAh cm^{-2}. Insets are detailed voltage profiles.[138] Copyright 2021, American Chemical Society. (f) Cycling performance of Li||Li symmetric cells with or the PDDA–TFSI layer at 10 mAh cm^{-2} and 1 mA cm^{-2}.[98] Copyright 2021, John Wiley and Sons.

Polymer-based electrolytes have emerged as a promising solution for suppressing lithium dendrite growth due to their intrinsic stability, mechanical robustness, and superior interfacial compatibility.[40] First of all, polymer electrolytes (especially solid polymer electrolytes) have a high mechanical modulus (modulus of elasticity). When lithium dendrites begin to grow and attempt to penetrate the electrolyte, sufficient mechanical strength physically prevents the dendrites from piercing through the electrolyte and causing a short circuit. Once again polar groups in the polymer electrolyte (*e.g.*, ether-oxygen bonds in PEO) can coordinate with Li^+ to form homogeneous ion transport channels. This structure promotes uniform distribution of lithium ions on the electrode surface and avoids preferential deposition of lithium due to high localized current density. Secondly, the polymer can form a dense and ion-conducting SEI layer (*e.g.*, containing Li_2O, Li_3N, *etc.*) when it is in contact with lithium metal. This interfacial layer passivates the electrode surface and prevents the continued decomposition of the electrolyte, while regulating the Li^+ deposition behavior, guiding the growth of lithium in a layered rather than dendritic form. Finally, the three-dimensional network structure of the polymer forms a physical barrier layer that restricts the disordered diffusion and aggregation of lithium atoms, forcing lithium ions to be deposited in more regular paths, thereby reducing the probability of dendrite nucleation.[141]

Although polymer electrolytes have advantages in inhibiting lithium dendrites, there are still several key technical shortcomings. However, it should be noted that the actual effect is highly dependent on the polymer composition, molecular weight, cross-linking degree, and interfacial optimization design. Specific modification options for polymer electrolytes will be discussed in section 4.

3.2.3. Development and outlook. The interfacial instability mechanisms of lithium metal anodes primarily stem from the dynamic non-equilibrium evolution of the SEI, severe electrode volume fluctuations during cycling, and uncontrolled dendrite growth. Current polymer-based stabilization strategies (*e.g.*, COF membranes and dynamic self-healing polymers) address these issues by regulating Li^+ flux distribution through ordered microporous structures or enhancing interfacial mechanical strength *via* dynamic hydrogen-bond networks. However, key challenges persist, including limited dynamic self-healing efficiency due to SEI reconstruction kinetics hysteresis and insufficient dendrite suppression at high current densities. Future efforts must focus on constructing composite interfacial engineering systems that integrate dynamic adaptability with high intrinsic ionic conductivity. Examples include designing dual-network polymer electrolytes using dynamic bond crosslinking strategies and developing multiscale interfacial architectures

(*e.g.*, composite gradient structures combining inorganic nanocoatings with flexible polymer matrices) to synergistically optimize mechanical modulus and electrochemical compatibility. Additionally, integrating *in situ* characterization techniques like cryogenic transmission electron microscopy (cryo-TEM) and X-ray diffraction (XRD) can elucidate interfacial phase evolution mechanisms, while machine learning-guided material genomics approaches may predict structure–property relationships among electrolyte components, enabling high-throughput screening and rational design of advanced interfacial stabilizers.

The key to enhancing lithium metal anode interfacial stability lies in establishing dynamic equilibrium at the electrode/electrolyte interface. While current polymer-based stabilizers improve lithium deposition morphology through artificial SEI construction or composite electrolyte design, transformative breakthroughs are still needed in dynamic interfacial regulation mechanisms and multiphysics-coupled synergistic optimization. Future research should prioritize: (1) developing topology-adaptive dynamic bonding material systems (*e.g.*, metal-coordinated polymers); (2) creating multimodal *in situ* analytical platforms for real-time dynamic interrogation of interfacial processes; (3) establishing quantitative structure–property models linking materials, interfaces, and performance. Through coordinated innovation across these technical pathways, the long-term cycling stability bottlenecks of high-areal-capacity lithium metal batteries are expected to be overcome, accelerating their practical deployment in high-specific-energy energy storage systems.

4. Polymers in electrolytes

As the ''lifeblood'' of lithium-ion batteries, electrolytes critically determine battery energy density, safety, and cycle life. While conventional liquid electrolytes exhibit high ionic conductivity (10^{-2}–10^{-3} S cm^{-1}), their flammability and dendrite growth risks limit high-voltage applications.[142] Polymer electrolytes, leveraging inherent solid-state safety, flexible interfacial compatibility, and processability, have emerged as pivotal materials for high-energy-density solid-state batteries.[143] However, challenges persist in low room-temperature ionic conductivity (10^{-7}–10^{-4} S cm^{-1}), narrow electrochemical windows, and insufficient interfacial stability.[144]

Current polymer electrolyte designs primarily encompass four systems: polyethers (*e.g.*, PEO), polyesters (*e.g.*, PMMA), C–F-based polymers (*e.g.*, PVDF), and cyano-group polymers (*e.g.*, PAN).[145] Strategies such as nanofiller compositing (LLZO, MOFs), deep eutectic solvent (DES) plasticization, and cross-linked copolymerization significantly enhance ionic conductivity and mechanical strength. Nevertheless, key challenges remain in electrode–electrolyte interfacial impedance, lithium metal compatibility, and scalable manufacturing. This section systematically reviews multiscale design principles, performance optimization pathways, and technical bottlenecks of polymer electrolytes, providing theoretical foundations for their advancement.

4.1. Traditional polymer electrolytes

Traditional polymer electrolytes, typically composed of polar polymer matrices (*e.g.*, poly(ethylene oxide) (PEO), polyacrylonitrile (PAN)) and lithium salts (*e.g.*, LiTFSI, $LiClO_4$), rely on localized chain segment motion and ion-coordination interactions for ionic transport. Since Wright *et al.*'s pioneering discovery of PEO's ionic conductivity in 1973,[146] their development has evolved through three distinct phases: (1) exploratory phase (1970s–1990s): Focused on elucidating ion transport mechanisms and optimizing fundamental properties of PEO-based systems; (2) technological stagnation (2000s–2010s): Hampered by low room-temperature conductivity ($<10^{-4}$ S cm^{-1}) and interfacial incompatibility, stalling commercialization efforts; (3) revival & innovation (2010s–present): Reignited by solid-state battery demands, traditional polymer electrolytes have resurged through material hybridization and structural engineering. Leveraging flexible molecular architectures, superior interfacial adaptability, and scalable processability, they now demonstrate renewed potential in lithium-ion battery technologies.[147]

PEO holds a prominent position in solid-state electrolyte research due to its unique chain topology and strong lithium salt coordination capability. The polymer features a high density of ether oxygen groups (–CH_2CH_2O–) in its backbone, which facilitate Li^+ dissociation and migration through dynamic reversible weak coordination bonds *via* lone pair electrons. However, PEO-based electrolytes face two critical limitations: (1) restricted chain mobility caused by high crystallinity at room temperature, leading to drastically reduced ionic conductivity (10^{-8}–10^{-6} S cm^{-1} at 25 °C);[148] (2) electrochemical oxidation decomposition of ether oxygen groups at potentials >3.8 V (*vs.* Li^+/Li), limiting compatibility with high-voltage cathode materials (*e.g.*, NCM ternary systems). These intrinsic deficiencies severely restrict their application in practical high-energy-density batteries.[149]

Polyacrylonitrile (PAN)-based polymer electrolytes have garnered significant attention in high-energy-density solid-state lithium batteries due to their superior processability, high ionic conductivity, broad electrochemical window (>5 V), and excellent mechanical properties.[150] PAN-based electrolytes leverage strong coordination between their polar –C$\equiv$N groups and lithium salts to effectively lower dissociation energy barriers, demonstrating exceptional Li^+ dissociation capability. The polymer's high dielectric constant (ε = 36.6) further enhances electrostatic shielding between Li^+ and anions, promoting ion dissociation. However, PAN's rigid molecular chains restrict segmental motion, limiting Li^+ transport and resulting in moderate room-temperature ionic conductivity (10^{-5}–10^{-4} S cm^{-1}).[151] Additionally, its relatively high crystallinity introduces crystalline domains that impede ion migration, further reducing conductivity. Challenges remain in optimizing interfacial side reactions between PAN-based electrolytes and lithium metal anodes.[152]

Poly(methyl methacrylate) (PMMA) electrolytes leverage strong polar groups (*e.g.*, ester functionalities) to achieve broad electrochemical windows, where the electron-withdrawing capacity of carbonyl groups reduces electron cloud density in polymer chains, mitigating oxidation tendencies. Dynamic coordination between ester groups and Li^+ suppresses lithium

salt (LiTFSI) decomposition, thereby minimizing side reactions.[153] However, polyester-based polymer electrolytes still face critical limitations in lithium anode compatibility and high-voltage stability due to interfacial side reactions, unstable SEI layers, inadequate mechanical strength enabling dendrite penetration, poor interfacial contact, and space charge layer effects.

Poly(vinylidene fluoride) (PVDF), featuring strongly polar C–F groups, exhibits exceptional chemical stability, high mechanical strength, broad electrochemical window (>4.6 V), and processability, making it a cornerstone material system for solid-state lithium metal battery research.[154,155] However, challenges persist in its low room-temperature ionic conductivity (typically $<10^{-4}$ S cm^{-1}), restricted chain segment mobility due to high crystallinity, compromised electrode/electrolyte interfacial compatibility, and suboptimal mechanical properties.

Recent advancements address the limitations of low ionic conductivity, insufficient mechanical strength, and interfacial incompatibility through three key approaches: Material design innovations include copolymer synthesis (*e.g.*, PEO–PPO block copolymers) and incorporation of inorganic nanofillers (SiO_2, LLZO) to suppress crystallization while establishing rapid ion transport channels; structural optimization strategies employ crosslinked networks, hyperbranched architectures, or star-shaped topologies to enhance mechanical robustness; interfacial engineering techniques utilize *in situ* polymerization and surface coatings (LiF, Al_2O_3) to improve electrode–electrolyte compatibility.

4.2. Gel polymer electrolytes

Gel polymer electrolytes (GPEs) represent a semi-solid material system bridging liquid electrolytes and all-solid-state polymer electrolytes, comprising a three-dimensionally crosslinked polymer network, plasticizers, and lithium salts.[156] The polymer matrix (*e.g.*, PEO, PVDF, PAN) forms a continuous phase through physical or chemical crosslinking, with pores infiltrated by liquid electrolytes or plasticizers, creating a gel-state architecture that integrates ion transport channels with mechanical support.[157] Ionic conduction primarily occurs *via* liquid-phase transport within the plasticizer, supplemented by dynamic coordination interactions between polar groups (ether oxygen, cyano) in polymer chains and Li^+ to facilitate ionic migration.

GPEs offer distinct advantages: first, their three-dimensional network structure effectively suppresses electrolyte leakage and volatilization, enhancing safety; second, inherent flexibility accommodates electrode volume changes while mitigating dendrite penetration risks; third, room-temperature ionic conductivity (10^{-3}–10^{-2} S cm^{-1}) rivals liquid systems, coupled with a broad electrochemical window (>4.5 V) compatible with high-voltage cathodes. However, inherent limitations constrain practical application: (1) trade-offs between mechanical strength and conductivity (*e.g.*, PEO's high flexibility *vs.* low conductivity, PVDF-HFP's mechanical robustness requiring plasticizer modification); (2) suboptimal interfacial compatibility causing high impedance and side reactions from poor electrode/electrolyte contact;[158] (3) thermal stability disparities (*e.g.*, PMMA's softening at elevated temperatures, PAN's demanding processing conditions). Current research addresses these challenges through multidimensional strategies: segmental/functional group design (*e.g.*, PEO–PPO block copolymers) to reduce crystallinity,[159] inorganic/organic filler hybridization (SiO_2, LLZO)[160] for rapid ion channels, and electrolyte formulation optimization to enhance interfacial contact and mechanical integrity.

4.2.1. Segmental/functional group engineering. Single-component polymer-based gel electrolytes inherently suffer from inadequate lithium salt dissociation, suboptimal ionic conductivity, poor electrode/electrolyte interfacial contact, and insufficient mechanical robustness—fundamental limitations that severely restrict practical performance. In the modification of lithium-ion battery gel electrolyte systems, segmental architecture engineering and functional group integration emerge as critical strategies for performance enhancement. Precise engineering of polymer backbone topology or targeted functional side-chain group incorporation effectively optimizes ion transport kinetics, interfacial compatibility, and mechanical resilience.

The introduction of different chain segments through blending and copolymerization can disrupt the original crystalline structure of the polymer and increase the amorphous region. The migration of ions in the amorphous region is easier, thus increasing the ionic conductivity. The crosslinking of different chain segments to form an interpenetrating network improves the mechanical strength and stability of the electrolyte, while providing richer channels for ion transport. Changing the length and polarity of the chain segments can adjust the flexibility of the chain segments. Flexible chain segments are favorable to the movement of ions, so that the migration of ions in the electrolyte is smoother.

For instance, Zhang *et al.* developed a fluorinated gel polymer electrolyte (F-GPE) system *via in situ* copolymerization of methyl methacrylate (MMA), ethylene glycol dimethacrylate (TEGDMA), and ethoxylated trimethylolpropane triacrylate (ETPTA), constructing an interface layer with dynamic adaptive properties (Fig. 15a).[161] This system reduces Li^+ diffusion barriers, achieving an ionic conductivity of 2.24×10^{-4} S cm^{-1} while significantly enhancing safety. In composite electrolyte design, Dong *et al.* developed a quasi-solid-state composite electrolyte by confining poly(ethylene glycol) dimethyl ether (PEGDME) within a poly(methyl methacrylate) (PMMA) three-dimensional framework, incorporating Li^+-conductive ceramic fillers and lithium salts to establish multiscale ion transport pathways (Fig. 15b).[162] This system demonstrated lithium-ion conductivities of 1.1×10^{-4} S cm^{-1} at 30 °C and 1.0×10^{-3} S cm^{-1} at 80 °C, with an expanded electrochemical stability window to 4.7 V *vs.* Li^+/Li, enabling room-temperature operation and long-term cycling stability in both Li||Li symmetric cells and lithium metal full cells (including $LiFePO_4$ or $LiCoO_2$ cathodes). Ye's group engineered a blended polymer electrolyte (BPE) *via* solution casting to fabricate an ultrathin 8.1 μm film,[163] utilizing a poly(ethylene oxide) (PEO)-PMMA-poly(vinylidene fluoride-*co*-hexafluoropropylene) (PVDF-HFP) matrix synergized with succinonitrile (SN) and fluoroethylene carbonate (FEC) plasticizers to optimize ion transport

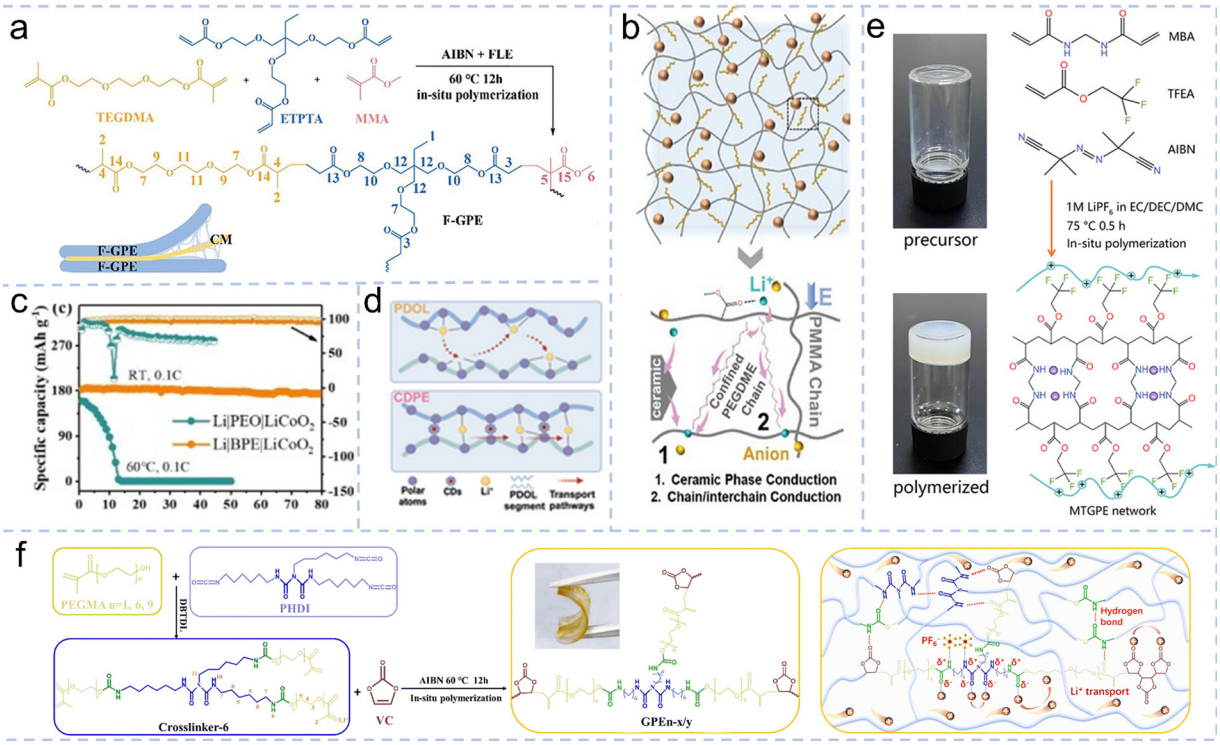

Fig. 15 Design and functional schematics of gel electrolytes modified by various chain segments/functional groups. (a) The structural formulas of TEGDMA, ETPTA and MMA monomers, as well as the possible structural diagrams of F-GPE polymer matrices.[161] Copyright 2023, John Wiley and Sons. (b) Schematic of PEGDME@PMMA-based composite electrolyte with internal Li^+ conduction pathways.[162] Copyright 2024, John Wiley and Sons. (c) Cycling performance of 4.5 V high voltage $LiCoO_2$ batteries with PEO-LiTFS PE and BPE.[163] Copyright 2022, Elsevier. (d) and (f) Schematic illustration of the lithium-ion transport pathways in CDPE, highlighting the role of CDs in enhancing both intra-chain and inter-chain lithium-ion transport within the polymer matrix.[164] Copyright 2025, John Wiley and Sons. (e) Optical images of MTGPE before and after polymerization, as well as schematic diagrams of polymerization.[165] Copyright 2024, John Wiley and Sons. (f) Structural formula of PEGMA (n = 1, 6, 9), PHDI, crosslinker-6, and VC monomers; the acylamino crosslinker synthesis process; the fabrication and possible structural diagram of the polymer skeleton for $GPE_{n-x/y}$.[166] Copyright 2024, the Royal Society of Chemistry.

networks (Fig. 15c). This electrolyte achieved an ionic conductivity of 1.08×10^{-3} S cm^{-1} at 25 °C with a Li^+ transference number of 0.863, demonstrating significantly enhanced capacity retention in 4.5 V $LiCoO_2$||Li cells after 80 cycles compared to conventional PEO-based solid electrolytes. To address the crystallization tendency and limited electrochemical window of traditional poly(1,3-dioxolane) (PDOL)-based electrolytes, Liu *et al.* have successfully developed a carbon-dot-assembled physically crosslinked gel polymer electrolyte (CDPE) *via in situ* polymerization (Fig. 15d).[164] This electrolyte leverages hydrogen-bonding interactions between amino/hydroxyl groups on carbon dot surfaces and PDOL molecular chains to construct a nanoparticle-hybridized crosslinked network. This architecture not only enhances the structural diversity and flexibility of the crosslinked network, creating versatile and adaptive pathways for Li^+ migration, but also significantly enhances ionic conductivity, achieving 3.20 mS cm^{-1} at 30 °C.

The strategic incorporation of specific functional groups into polymer structures significantly enhances electrolyte electrochemical performance. Targeted monomer selection enables precise integration of specialized functional groups to address critical lithium-ion battery requirements, including oxygen-containing groups (carboxyl, carbonyl, hydroxyl), nitrogen-containing groups (amine, cyano), sulfur-containing groups (disulfide, sulfonate), boron/phosphorus-based groups, and unsaturated double bonds from ionic liquids (ILs) for *in situ* polymerized electrolytes *via* radical polymerization. Functional groups with strong polarity can interact with anions or cations in lithium salts, destroying the ion-pair structure of lithium salts, promoting the dissociation of lithium salts, increasing the ion concentration, and improving the ionic conductivity; functional groups can also be used as ''signposts'' or ''channels'' for ion transport, guiding the directional transport of ions in the electrolyte; they can also interact with the functional groups on the surface of the electrode material to enhance the interfacial compatibility between the electrolyte and the electrode, reduce the interfacial impedance, and improve the charging and discharging efficiency of the battery and the cycle stability.

For instance, Jin *et al.* engineered a polymer network integrating $-CF_3$ groups for rapid Li^+ transport channels and secondary amine N–H groups to restrict anion migration (Fig. 15e).[165] This architecture effectively regulates Li^+ primary solvation shells, suppressing solvent decomposition at the anode during charging, while simultaneously promoting stable CEI/SEI formation on electrode surfaces. The resultant gel

polymer electrolyte (GPE) achieves high ionic conductivity (2.6 mS cm^{-1}) and Li^+ transference number (0.67). Guo *et al.* developed a supramolecular GPE network through molecular design featuring permanent chemical crosslinks and reversible hydrogen bonds *via* abundant amide functional groups (Fig. 15f).[166] Combined with optimized polymer soft-segment lengths, this dual-network structure enhances mechanical strength, flexibility, and interfacial adaptability, enabling superior dendrite suppression and cycling stability.

4.2.2. Composite (inorganic/organic filler). To address inherent limitations of single-polymer matrices, such as excessive crystallinity and insufficient mechanical strength, researchers optimize performance by blending inorganic fillers (SiO_2, TiO_2, Al_2O_3 nanoparticles,[167] LLZO, LATP solid electrolytes[168]) or organic fillers (MOFs, COFs porous frameworks) into polymer systems. Inorganic/organic fillers contribute through three primary mechanisms: (1) establishing "ion-electron" dual-conduction networks by reducing matrix crystallinity (fillers disrupt polymer chain ordering to increase amorphous regions) and providing Li^+ transport interfaces; (2) enhancing lithium salt dissociation *via* surface Lewis acid–base interactions to create rapid ion transport channels; (3) physically confining lithium dendrite growth while improving mechanical robustness and electrochemical stability through enhanced electrode/electrolyte interfacial contact.[169] In GPE systems, Li^+ transport pathways involve contributions from both the polymer matrix and liquid electrolyte (LE). Notably, Li^+ in LE is typically solvated by solvent molecules/electrolyte components to form solvation sheaths. During the reductive deposition process at electrode interfaces, solvated Li^+ undergoes desolvation and collaborates with dissociated solvent molecules to form an intermediate phase layer (SEI), whose physicochemical properties critically regulate subsequent lithium deposition behavior. For instance, Hu *et al.* introduced LLZO particles into a LiTFSI/EmimFSI/PMMA ionic liquid system, successfully constructing a high-voltage-tolerant ultraconcentrated ionogel-ceramic composite electrolyte (Fig. 16a).[170] This system demonstrated significantly enhanced cycling stability in both Li||NCM523 and Li||$LiFePO_4$ cells. Wei *et al.* employed the silane coupling agent APTES as a bridging agent to strengthen interfacial compatibility between LLZTO ceramic fillers and a PVEC matrix *via* chemical bonding (Fig. 16b).[171] The synergy of strong chemical bonds and hydrogen bonding not only established multiscale Li^+ transport channels but also enabled assembled $LiCoO_2$-based solid-state lithium batteries (SSLBs) to exhibit superior high-energy-density characteristics. Furthermore, Lv *et al.*'s study incorporating SiO_2 into PETEA-based gel electrolytes demonstrated that SiO_2 not only expands lithium-ion transport channels but also regulates $TFSI^-$ anion migration while increasing the inorganic component in Li^+ solvation structures, thereby promoting the formation of a LiF-rich inorganic interfacial phase.[172] This dual-functional modification mechanism effectively suppresses lithium dendrite growth while optimizing electrolyte/electrode interfacial contact characteristics.

Furthermore, electronically conductive components demonstrate unique advantages in enhancing the electrochemical performance of gel electrolytes. Their mechanism primarily involves polarization effects under electric field induction, driving directional migration of charge carriers (electrons and holes). This field-responsive behavior not only promotes lithium salt dissociation through intensified local electric fields (enhancing Li^+/anion separation) but also significantly improves Li^+ diffusion kinetics. For example, Xiong *et al.* engineered a $La_{0.6}Sr_{0.4}CoO_{3-\delta}$ (LSC)-based functionalized nanofiber framework (Fig. 16c), embedding LSC electronic conductors into a ZnO/Zn_3N_2-modified polyimide (Zn-PI) matrix and combining it with a polyvinyl chloride (PVC)-based electrolyte to form a novel solid-state system.[173] The synergy of high-valence Co and oxygen vacancies in this composite yielded an ionic conductivity of 1.50 mS cm^{-1} at 25 °C and a Li^+ transference number of 0.91, validating the critical role of electron–ion collaborative transport mechanisms in optimizing Li^+ migration pathways.

4.2.3. Electrolyte formulation engineering (additives, ionic liquids, eutectic electrolytes). In recent years, ionic liquid-reinforced gel electrolytes for lithium-ion batteries have attracted significant attention due to their high ionic conductivity, broad electrochemical windows, and exceptional thermal stability. Studies demonstrate that ionic liquids themselves contain a large number of freely movable ions that significantly increase the number of mobile carriers in the system. And there are interactions between these ions and the ions in the lithium salt, which can disrupt the crystalline structure of the lithium salt in the polymer and promote the dissociation of the lithium salt. The ionic liquid can improve the interfacial compatibility between the electrolyte and the electrode and reduce the interfacial impedance. For example, imidazolium-based ionic liquid gel electrolytes exhibit ionic conductivities exceeding 1×10^{-3} S cm^{-1} at room temperature while maintaining superior electrode/electrolyte interfacial compatibility. A notable example is the fluorinated alkyl chain-functionalized imidazolium ionic liquid (F-IL) terminal group gel polymer electrolyte developed by Ali Coskun' group (Fig. 16d).[174] This system achieves concurrent optimization of high ionic conductivity and elevated Li^+ transference numbers through Lewis acidic polymer segments that regulate electrolyte salt solubility. Research reveals that F-IL structural units effectively reduce the binding energy between Li^+ and diol chain segments in the polymer matrix, significantly accelerating Li^+ migration within the three-dimensional gel network. By anchoring anions to ionic liquid functional groups, this design not only suppresses space charge polarization but also amplifies anion coordination with Lewis acidic polymers while weakening cation coordination strength, thereby optimizing charge carrier transport kinetics. However, the electrochemical performance of ionic liquid–polymer composites exhibits significant heterogeneity due to compatibility variations between ionic liquids and polymer matrices. For instance, pyrrolidinium-based ionic liquids, despite their exceptional high-temperature stability, generally demonstrate lower room-temperature ionic conductivity compared to imidazolium-based systems. To reconcile this trade-off, Christopher Li's team engineered a hybrid network based on *N*-methyl-*N*-propylpyrrolidinium bis(fluorosulfonyl)imide (Pyr13FSI), systematically investigating the structure–property

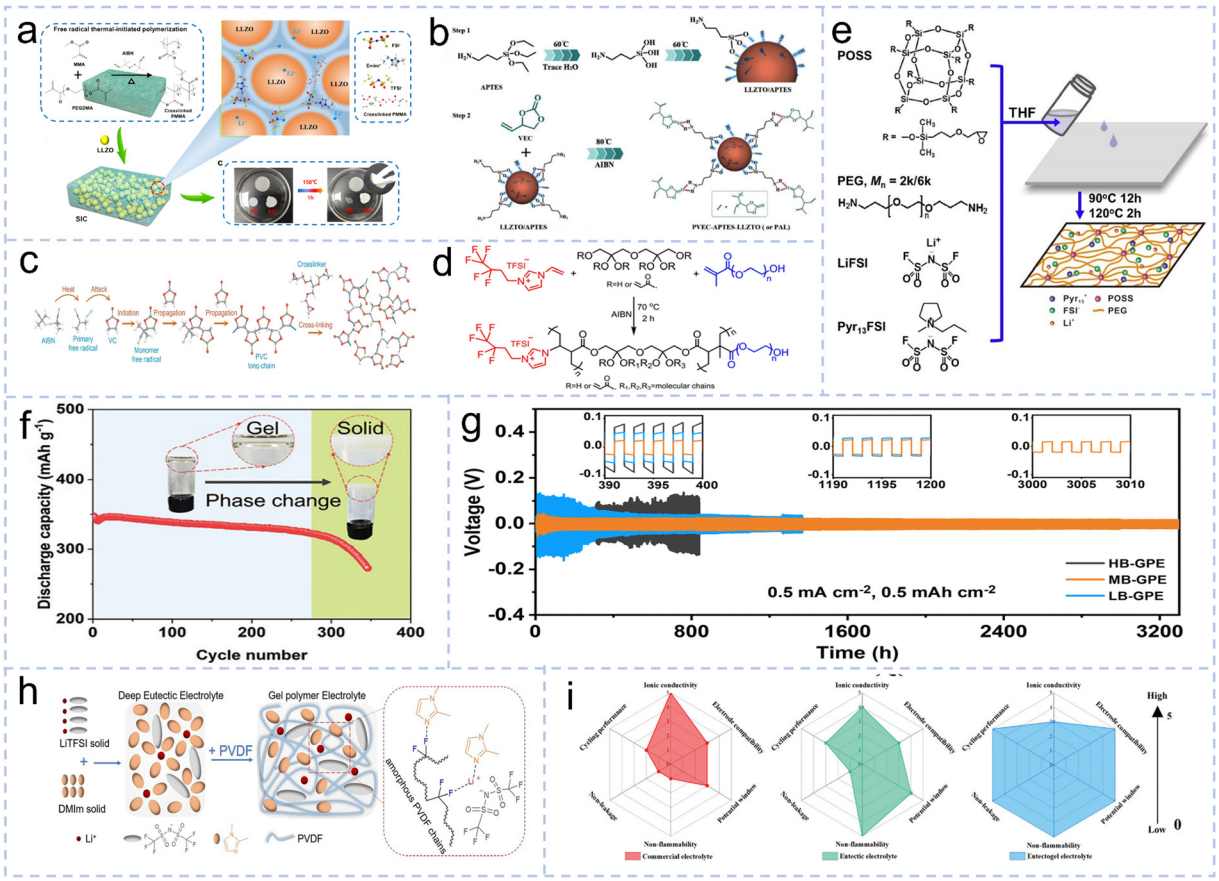

Fig. 16 Design and functional schematics of gel electrolytes modified by composite and electrolyte formulation. (a) Design schematic of SIC electrolyte and comparative thermal resistance analysis between SIC electrolyte and commercial PP separator.[170] Copyright 2022, John Wiley and Sons. (b) Preparation diagram of the composite solid electrolyte PVEC-APTES-LLZTO.[171] Copyright 2023, Elsevier. (c) Schematic diagram of the reaction mechanism of free radical-initiated PVC polymerization.[173] Copyright 2024, John Wiley and Sons. (d) Schematic representation of the synthesis of gel polymer electrolyte containing ionic liquid end groups.[174] Copyright 2021, John Wiley and Sons. (e) Synthetic route of the hybrid network-RTIL GPEs.[175] Copyright 2020, Elsevier. (f) Cycling performance of graphite||Li half cell in GPE (aging two days) at 5C/1C (discharge/charge) and optical images of the initial GPE after aging for 2 days (gel state) and GPE after aging for 30 days (solid state).[177] Copyright 2024, John Wiley and Sons. (g) Cycling performances of Li||Li symmetric cells with HB-GPE, MB-GPE and LB-GPE at 0.5 mA cm^{-2} and 0.5 mA h cm^{-2} [179]. Copyright 2025, the Royal Society of Chemistry. (h) Diagram of the preparation process of DEEs and DEE-based gel polymer electrolytes.[182] Copyright 2022, John Wiley and Sons. (i) Comparison of battery performance with commercial electrolyte, eutectic electrolyte, and eutectogel electrolyte.[183] Copyright 2024, John Wiley and Sons.

relationships between network topology parameters, ionic liquid content, and the mechanical/electrochemical characteristics of gel polymer electrolytes (GPEs) (Fig. 16e).[175] This approach achieved ionic conductivities exceeding 1 mS cm^{-1} under ambient conditions. Current research paradigms are progressively shifting toward multifunctional composite electrolyte systems, emphasizing the synergistic optimization of critical performance metrics—including intrinsic safety (thermal decomposition temperature >300 °C), energy density (>500 Wh kg^{-1}), and cycling stability ($>80\%$ capacity retention over 2000 cycles)—through multiscale structural engineering strategies.

Additives offer systematic solutions for multidimensional optimization of gel electrolytes by regulating solvation structures, interfacial chemistry, and thermal stability.[176] Functioning as SEI-forming agents and cathode protective components, additives play pivotal roles in electrode interface engineering: first, preferentially reducible additives construct dense, stable SEI layers at electrode surfaces, effectively suppressing interfacial side reactions and dendrite growth; second, chelation of transition metal ions and inhibition of electrolyte oxidative decomposition significantly enhance cathode/electrolyte interfacial stability. Recent advances in molecular design and mechanistic understanding of additives have yielded critical breakthroughs. For example, Zheng *et al.* developed a graded polymerization strategy for GPEs, achieving interfacial stabilization through rapid Li^+ transport channels (Fig. 16f).[177] By introducing $LiNO_3$ as a polymerization inhibitor for *in situ* partial polymerization, they successfully fabricated a gel electrolyte with amorphous architecture, achieving a room-temperature ionic conductivity of 5.10 mS cm^{-1} while simultaneously improving Li^+ migration kinetics and graphite anode fast-charging performance. Li's team developed an *in situ* polymerized GPE system based on hexamethylene diisocyanate (HDI), innovatively utilizing fluoroethylene carbonate (FEC) as a fluorine-source additive to construct a LiF-rich gradient SEI

layer on lithium metal surfaces, significantly enhancing SEI homogeneity and mechanical robustness.[178] Benefiting from optimized interfacial mechano-electrochemical properties, the assembled Li||Li symmetric cells achieved over 700 hours of stable cycling. Mu *et al.* engineered a GPE system with Li^+–solvent binding strength gradient through molecular design, where the moderate-binding-strength electrolyte (MB-GPE) enabled precise solvation structure regulation *via* fluorinated solvents (FEC/FEMC).[179] This system combines exceptional ionic conductivity (1.95×10^{-3} S cm^{-1}) with interfacial stability. At a current density of 0.5 mA cm^{-2}, the stable cycling time of the lithium metal anode exceeds 3200 h (Fig. 16g), offering novel insights for designing high-performance gel polymer electrolytes.

Deep eutectic electrolytes (DEEs), formed through intermolecular interactions between a hydrogen bond donor (HBD) and acceptor (HBA), are low-melting mixtures distinguished by low toxicity, cost-effectiveness, and high ionic conductivity.[180] Integrating such systems into gel electrolytes effectively enhances ion transport kinetics, electrode/electrolyte interfacial stability, and environmental adaptability.[181] This is because the ligand in the eutectic electrolyte has a strong coordination effect with the metal ions, which can change the coordination environment of the ions in the eutectic electrolyte, make the lithium salt easier to dissociate, increase the ion concentration, and thus improve the ionic conductivity. The eutectic electrolyte can improve the interfacial contact between the polymer electrolyte and the electrode, so that the ions can be transferred between the electrode and the electrolyte more efficiently, reduce the interfacial impedance, form a stable interface, inhibit the growth of lithium dendrites, and improve the cycle stability and safety of the battery. Eutectic electrolyte usually has higher thermal stability, lower melting point and good fluidity, which can make the electrolyte better adapt to the volume and temperature changes in the charging and discharging process, and improve the safety and lifespan. For instance, Guo *et al.* reported a DMIm-based deep eutectic gel polymer electrolyte (DMIm-DES) that modulates Li^+ transport mechanisms through Li^+–N coordination interactions (Fig. 16h).[182] Research demonstrates that introducing strongly electronegative poly(vinylidene fluoride) (PVDF) polymers can reconstruct Li^+ solvation sheath structures, achieving high Li^+ transference numbers ($t_{Li}{}^+$ = 0.65) and optimized Li/electrolyte interfacial stability. This deep eutectic gel electrolyte exhibits exceptional multiscale performance: flame-retardant properties, high ionic conductivity (1.67 mS cm^{-1} at 30 °C), and elevated oxidation voltage (up to 4.35 V *vs.* Li/Li^+). Li||$LiFePO_4$ batteries employing this electrolyte demonstrate outstanding long-term cycling stability across wide rate ranges. Zhang *et al.* achieved breakthroughs with a eutectic gel electrolyte developed *via* polymer matrix confinement strategies, featuring unique advantages: (1) inducing the formation of LiF/Li_3N-rich inorganic–organic composite solid electrolyte interphases (SEIs) to enable uniform lithium metal deposition; (2) *in situ* construction of cathode electrolyte interphases (CEI) that effectively suppress interfacial side reactions in $LiCoO_2$ (LCO) under high voltages.[183] Consequently, LCO||Li full cells utilizing this electrolyte achieved 72.5% capacity retention after 1500 cycles at a 4.45 V cutoff voltage (mere 0.018% decay per cycle) while maintaining stable operation even at 4.6 V ultrahigh voltage (Fig. 16i). This study provides theoretical guidance for eutectic gel electrolyte design, with its intrinsic safety and interfacial regulation capabilities significantly advancing the practical implementation of high-energy-density lithium metal batteries.

4.2.4. Development and outlook. As the cornerstone material for high-safety, high-energy-density lithium-ion batteries, the future development of composite gel electrolytes will focus on synergistic innovations in multifunctional integration, green sustainability, and intelligent manufacturing technologies, specifically manifested through:

(1) Bioinspired structural engineering and dynamic network regulation. Exemplified by Hou *et al.*'s enamel-inspired multiscale heterogeneous architecture, which integrates amorphous ceramic nanotubes with polymer matrices through rigid inorganic phase-flexible polymer chain synergistic interplay.[184] This design concurrently achieves high room-temperature ionic conductivity (>1 mS cm^{-1}) and dendrite suppression capabilities. The strategy extends into biomimetic gradient interface engineering, where spatially graded ceramic phase distributions enable compatibility with high-voltage cathode materials.

(2) Eco-friendly material systems and sustainable manufacturing. Bio-based polymer electrolytes are gaining prominence due to their lifecycle carbon emission advantages (~40% reduction compared to petroleum-based systems). For instance, Cao's team developed a cellulose/polyacrylic acid composite gel electrolyte, achieving ionic conductivities exceeding 1.0×10^{-3} S cm^{-1} through phosphate ester group covalent grafting.[185] However, cycling stability requires further optimization *via* crosslinking degree adjustment for practical viability. Notably, incorporating degradable fillers (*e.g.*, lignin-derived carbon quantum dots) could further reduce environmental impact, though challenges persist in resolving interfacial compatibility issues with polymer matrices.

(3) Intelligent manufacturing and precision structural control. Advanced fabrication technologies enable novel approaches for electrolyte optimization: (i) microporous gradient architectures *via* 3D printing achieve directional regulation of Li^+ transport pathways, effectively reducing interfacial impedance; (ii) LLZO nanowire arrays constructed through electrospinning significantly enhance solid electrolyte/electrode interface compatibility by minimizing grain boundary resistance. Furthermore, molecular dynamics (MD) simulations integrated with machine learning algorithms (*e.g.*, deep potential models) accelerate the design of novel functional fillers (*e.g.*, MOF-confined Li^+ solvation structures) and polymer matrix matching.

These technological breakthroughs will propel composite gel electrolytes toward practical applications in high-voltage lithium metal batteries (>4.5 V), flexible wearable devices, and extreme-environment energy storage systems. However, industrialization requires critical solutions: (1) uniform nanofiller dispersion control (D90 particle size distribution <100 nm); (2)

enhanced electrode/electrolyte interfacial chemical stability; (3) cost-effective scalable production methodologies.

4.3. Framework electrolytes

Framework electrolytes represent an emerging class of solid-state electrolyte systems constructed from porous framework materials, centered on leveraging crystalline materials with ordered nanochannel architectures as ion transport media. These systems employ highly ordered sub-nanometer pore channel networks to enable directional, rapid lithium-ion conduction, characterized by their unique capacity to maintain rigid solid-state structural integrity at the mesoscale while spatially confining solvent molecules or ionic liquids within periodic nanopores or layered confinement spaces at the molecular scale, thereby creating nano-confined ionic transport microenvironments. This structural duality allows synergistic integration of the mechanical stability inherent to inorganic solid electrolytes with the superior ion transport kinetics of liquid electrolytes. Based on chemical composition and crystalline architecture, framework electrolytes are categorized into three subclasses: metal–organic framework (MOF)-based electrolytes, covalent organic framework (COF)-based electrolytes, and extended systems incorporating novel frameworks such as hydrogen-bonded organic frameworks (HOFs). Organic framework polymer electrolytes achieve high-performance Li^+ transport and lithium dendrite inhibition through the precise design of ligand functional groups. Oxygen-containing ligands (*e.g.*, ether bonds, carboxyl groups) form dynamic coordination interactions with Li^+, lowering the ionic mobility barriers and increasing the ionic conductivity to 10^{-4} S cm^{-1}. The nitrogen-containing ligand (pyridine/imine) selectively anchors the anion, causing the Li^+ mobility number (t_+) to exceed 0.75 and significantly inhibiting interfacial polarization. The fluorinated ligand ($-CF_3$) induces the formation of a LiF-rich SEI layer (LiF percentage $>65\%$), effectively guiding the uniform lithium deposition. Meanwhile, rigid cross-linking ligands (triazine, pyrene) construct a mechanically enhanced skeleton (modulus >5 GPa) to synergistically inhibit dendrite penetration. It is shown that the multifunctional group synergistic strategy can simultaneously optimize the ion transport, interfacial stability and mechanical properties, which provides a new way for the design of high safety solid-state lithium batteries.

4.3.1. MOF-based electrolytes. MOF materials, formed through coordination self-assembly of inorganic metal clusters and multidentate organic ligands, are porous crystalline solids with long-range ordered structures. Their unique structural programmability and topological diversity exhibit significant technological advantages in lithium-ion battery electrolytes.[91] Research indicates that rational selection of metal cluster types (*e.g.*, transition metal clusters, rare-earth metal clusters) and functionalized organic ligands (incorporating polar groups or flexible chain segments) allow precise control over MOF pore dimensions (microporous/mesoporous) and topological connectivity (*e.g.*, cubic, hexagonal symmetries), optimizing Li^+ migration energy barriers and transport pathways.[186] The crystalline frameworks of MOFs incorporate highly ordered nanopore systems combined with ultrahigh specific surface areas (typically 1000–7000 m^2 g^{-1}), enabling precise regulation of Li^+ solvation structures *via* nano-confinement effects to achieve directional ion migration and spatially uniform distribution, thereby markedly enhancing intrinsic ionic conductivity in solid-state electrolytes.[91,187] Notably, the three-dimensional interconnected pore channels of MOFs not only physically adsorb and stabilize large quantities of liquid electrolytes to form robust composite systems but also enable selective Li^+ transport through engineered surface chemistry *via* ligand functionalization modifications (*e.g.*, sulfonic acid groups, crown ethers), effectively suppressing dendrite growth and mitigating interfacial polarization. These characteristics define three primary structure–property relationships in MOF-based electrolyte systems: (1) MOF/polymer composite electrolytes—enhancing mechanical strength through interfacial interactions between MOF nanofillers and polymer matrices; (2) MOF-confined ionic liquid electrolytes—leveraging spatial confinement of ionic liquids within MOF pores to improve thermal stability;[188] (3) MOF host matrix solid electrolytes—directly achieving Li^+ conduction through the intrinsic pore channels of MOF frameworks.

Conventional solid polymer electrolytes typically exhibit coexisting disordered chain segments and high-crystallinity regions, where Li^+ transport must overcome complex chain entanglement resistance and is confined to narrow amorphous diffusion channels, resulting in inefficient migration. The incorporation of MOF materials provides a breakthrough strategy: their highly ordered 3D pore channels establish directional high-speed pathways for Li^+ transport, significantly shortening migration distances and reducing activation energy. For instance, Fan's team developed an asymmetric electrolyte architecture by integrating MOF layers (*e.g.*, ZIF-8) into polymer matrices. The ordered microporous network not only optimizes Li^+ transport pathways but elevates ionic conductivity to practical levels (*e.g.*, $\sim$1.02 mS cm^{-1}). Concurrently, open metal sites (OMS) within MOFs selectively coordinate with lithium salt anions, weakening ion-pair association effects and enhancing Li^+ transference numbers (*e.g.*, reaching 0.68 in asymmetric MOF-based electrolytes (Fig. 17a)).[189] The rigid framework of MOFs effectively suppresses polymer chain recrystallization, establishing a stable continuous transport network of amorphous phases while homogenizing lithium-ion flux through physical barrier effects to inhibit dendrite growth. Studies demonstrate that MOF-modified electrolytes enable stable lithium deposition/stripping over 1300 hours in Li||Li symmetric cells, with dense and smooth lithium metal deposition morphology, significantly enhancing interfacial compatibility. Notably, the customizable chemical microenvironment of MOFs (*e.g.*, surface functionalization) synergizes with polymer matrices to expand electrochemical windows to 4.9 V and improve thermal stability, enabling full-cell compatibility with high-voltage cathodes like $LiNi_{0.5}Co_{0.2}Mn_{0.3}O_2$. These systems achieve 95.6% capacity retention after 100 cycles at a rate of 0.5C. Such attributes endow MOF–polymer composite electrolytes with unparalleled advantages in ionic conductivity, interfacial stability, and safety compared to conventional systems. Furthermore, Wook's team have proposed a strategy incorporating multiple components

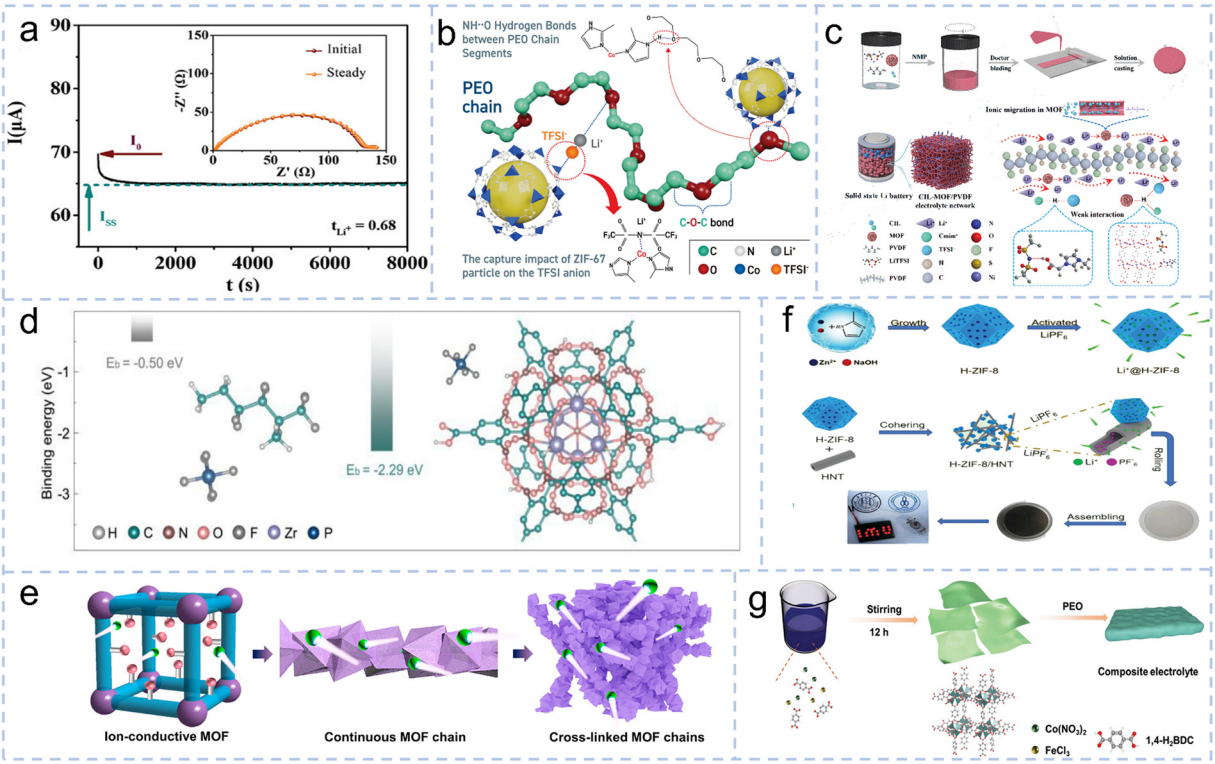

Fig. 17 Design schematics and performance of MOF-based electrolytes. (a) Current variation with time during polarization of Li/SPE2-PI-ZIF8/Li symmetrical cells at room temperature.[189] Copyright 2020, John Wiley and Sons. (b) Illustration for interactions of ZIF-67 particles with LiTFSI and PEO chain in the electrolyte matrix.[190] Copyright 2020, John Wiley and Sons. (c) Synthesis of CIL-MOF/PVDF solid polymer electrolyte and structural schematic of a solid-state battery.[144] Copyright 2025, John Wiley and Sons. (d) Binding energies of PF_6^- on PVDF-HFP and UIO-66-NH_2.[191] Copyright 2024, John Wiley and Sons. (e) Bottom-up synthesis of cross-linked MOF chains on BC skeleton.[192] Copyright 2021, the American Chemical Society. (f) Fabrication process of hierarchical porous composite H-ZIF-8/HNT SSE.[193] Copyright 2023, John Wiley and Sons. (g) Schematic diagram of the process for preparing MOFs and composite electrolyte membranes.[194] Copyright 2023, John Wiley and Sons.

(including zeolitic imidazolate framework (ZIF-67) as filler and ionic liquid electrolyte (ILE) as plasticizer) into a PEO/LiTFSI matrix (Fig. 17b).[190] Through manufacturing process optimization, they developed an ultrathin integrated electrolyte (PEO/LiTFSI-ILE-ZIF-67, PLiZ) with 32 μm thickness, achieving high ionic conductivity (1.19×10^{-4} S cm^{-1} at 25 °C), broad electrochemical stability (5.66 V), and elevated lithium-ion transference number (0.8).

Metal–organic framework-confined ionic liquid (ILs@MOFs) electrolytes, as an emerging solid-state system for lithium-ion batteries, have become a focal point in high-safety, high-energy-density energy storage research due to their unique structure–property synergy. Compared to conventional liquid electrolytes and single-phase solid systems, this composite architecture integrates the functional design of ionic liquids with the structural confinement of MOFs, demonstrating superior performance in ion transport kinetics, interfacial compatibility, and thermal stability. The performance enhancement mechanisms stem from: (1) MOF lattice confinement effects—ordered nanochannels engineer topology-optimized Li^+ transport pathways while surface functional groups (*e.g.*, carboxyl, sulfonic acid) reduce migration activation energy *via* Li^+ coordination; (2) ionic liquid interfacial modulation—ILs form molecular-scale wetting layers at MOF/polymer interfaces, reconstructing electric double-layer structures through weak anion-metal cluster interactions (hydrogen bonding, π–π stacking), thereby lowering interfacial diffusion barriers and boosting room-temperature ionic conductivity; (3) dynamic dissociation promotion—weak interactions between carboxyl-functionalized ionic liquids (CILs) and MOF frameworks reduce lithium salt dissociation energy. As exemplified by Ni *et al.*'s weakly coordinated MOF-IL composite electrolyte (Fig. 17c), its unique Li^+ transport network achieves a broad electrochemical window of 4.82 V. In $LiFePO_4$||Li full-cell tests, the system retains 98.9% capacity retention (96.2 mAh g^{-1}) after 500 cycles at a rate of 6C.[144] This performance superiority arises from the synergistic interplay between MOF pore-channel-optimized Li^+ pathways and IL-mediated interfacial charge distribution regulation. Chen *et al.* proposed an *in situ* MOF-based preparation strategy to successfully fabricate gel polymer electrolytes (MOF@Polymer) with uniform microdomain structures.[191] The incorporation of UIO-66-NH_2 enhances Li^+ migration by weakening chemical interactions and facilitating the dissociation of Li salt (Fig. 17d). This innovative design significantly enhances ionic conductivity, mechanical strength, and interfacial stability of the electrolyte, offering a novel approach to addressing microdomain uniformity challenges in SSLMBs.

MOF-dominated electrolyte systems demonstrate exceptional advantages in lithium-ion batteries, particularly in

single-ion-conductive architectures. Leveraging the programmable molecular structures of MOFs, this approach immobilizes anions *via* covalently anchored functional groups to generate abundant free Li^+ that migrate along porous channels, typically achieving high ion transference numbers. Huang *et al.* developed a sulfonic acid-functionalized MOF (Zr-BPDC-2SO_3H), where high-density –SO_3H groups endow the material with superior ionic conductivity and single-ion conduction capability. By integrating MOF nanoparticles into a 1D continuous array on nanocellulose networks, they formed a 3D crosslinked network with continuous ion transport channels (Fig. 17e).[192] This ordered MOF architecture eliminates long-range interfacial resistance through interparticle rapid ion transfer pathways, achieving enhanced lithium-ion conductivity (7.88×10^{-4} S cm^{-1}), transference number (0.88), and reduced interfacial impedance (74 Ω). In hierarchical porous structure design, Liu *et al.* engineered ZIF-8-derived materials (HZIF-8/HNT) with meso-microporous architectures on halloysite nanotube (HNT) surfaces *via* topological defect modulation (Fig. 17f).[193] The functionalized H-ZIF-8/HNT electrolyte exhibits markedly improved electrochemical performance, including high ionic conductivity (7.74×10^{-3} S cm^{-1}), superior single-ion permeation (t_{Li^+} = 0.84), and excellent interfacial compatibility. Zou *et al.* developed a high-performance composite electrolyte through molecular engineering of functionalized two-dimensional (2D) MOF nanosheets, where electron-donating substituents in the 2D-MOF effectively restricted ClO_4^- anion migration while enhancing the mechanical properties of PEO and elevating the ion transference number (from 0.36 to 0.64) (Fig. 17g).[194]

4.3.2. COF-based electrolytes. Covalent organic frameworks (COFs), an emerging class of solid-state electrolyte materials, demonstrate transformative potential in solid-state battery applications through their unique topological architectures and exceptional physicochemical properties.[195,196] COFs are crystalline porous materials formed *via* ordered assembly of organic building blocks through dynamic covalent bonds, where periodically aligned nanochannels and ultrahigh specific surface areas provide ideal pathways and interfaces for ion transport. Compared to MOFs, COFs exhibit superior thermal stability and chemical inertness due to their rigid covalent-bonded frameworks. Current research focuses on two-dimensional layered COF systems, where strong π–π stacking interactions create highly ordered lamellar stacking structures. This long-range ordering enables anisotropic alignment under mechanical stress, establishing continuous ion transport channels that facilitate rapid directional cation migration. COF-based solid-state electrolyte systems are broadly categorized into two classes: intrinsic COF-dominant electrolytes and composite electrolytes integrating COFs as functional fillers within polymer matrices.[197]

COF-based host electrolytes significantly enhance interfacial stability, ion transport kinetics, and cycling durability in lithium-ion batteries through precise pore engineering strategies, including pore size modulation and surface functionalization. Their densely crosslinked covalent frameworks confer exceptional structural rigidity, while abundant modifiable sites (*e.g.*, lithium carboxylate groups, amine ligands) serve as molecular design platforms for chemical functionalization. Incorporating lithiophilic groups (sulfonic acid, crown ether units) into COF skeletons enables strong Li^+-polar group coordination, promoting lithium salt dissociation and reducing migration activation energy.

For instance, Li's team successfully designed and synthesized a novel single-ion conducting nitrogen hybrid conjugated skeleton (NCS) as all solid electrolyte, whose backbone consisted of triazine and piperazine rings (Fig. 18a).[195] A loose bonding between the triazine rings and cations would lower the energy barrier during ion transfer, and electrostatic forces with piperazine rings could "anchor" anions to increase the selectivity during ion transfer. Thus, the NCS electrolyte exhibits excellent room temperature lithium-ion conductivity up to 1.49 mS·cm^{-1} and high transference number of 0.84 without employing any solvent.

Cao *et al.* innovatively designed urea-linked COF-531 (Fig. 18b).[198] where dynamic reversible urea-bond networks balance the low reactivity of melamine units while forming ordered ion channels rich in nitrogen coordination sites. This architecture enables efficient Li^+ transport and uniform deposition by lowering Li^+ desolvation energy barriers. Additionally, zwitterionic COF (Zwitt-COF) forms hexagonal close-packed ion channels through spatial separation of cationic/anionic domains, exhibiting a room-temperature ionic conductivity of 1.65×10^{-4} S cm^{-1} and 99% capacity retention in all-solid-state batteries after 100 cycles[199] (Fig. 18c). Theoretical simulations confirm that COFs' periodic mesoporous structures reduce Li^+ migration resistance *via* quantum confinement effects.

COF–polymer composite systems demonstrate breakthrough advancements in ion transport, interfacial stabilization, and dendrite suppression through multiscale structural synergy. COF surface functional groups (*e.g.*, amino, sulfonic acid) regulate Li^+ solvation sheath structures *via* Lewis acid–base interactions, reducing free solvent molecule activity. For instance, Chen *et al*. developed a COF-modified gel electrolyte (HGPE/TaPa-2) that reconstructs Li^+–solvent coordination environments to induce LiF-rich SEI formation (Fig. 18d),[200] enabling Li$FePO_4$||Li cells to achieve 75% capacity retention after 1000 cycles at 0.5C. The innovation lies in the interpenetrating network formed by topological entanglement between COF rigid frameworks and polymer flexible chains, maintaining mechanical integrity while enabling adaptive electrode interface contact. Shi *et al.* synthesized a sulfonated COF (Tp$PaSO_3Li$) as a filler in PVDF-based solid polymer electrolytes (PVDF-Tp$PaSO_3Li$) (Fig. 18e).[201] Li||Li symmetric cells demonstrated exceptional cycling stability (2500 hours at 60 °C (0.1 mA cm^{-2}) and 700 h at room temperature) effectively suppressing dendrite growth. These enhancements originate from COFs' ordered pore channels minimizing ion transport stochasticity, while polymer matrices (*e.g.*, PEO) improve electrolyte flexibility, compensating for pure COFs' rigidity limitations.

4.3.3. HOF-based electrolytes. Hydrogen-bonded organic frameworks (HOFs), formed through hydrogen-bond-driven self-assembly of organic molecular units (primarily C, H, O, N),

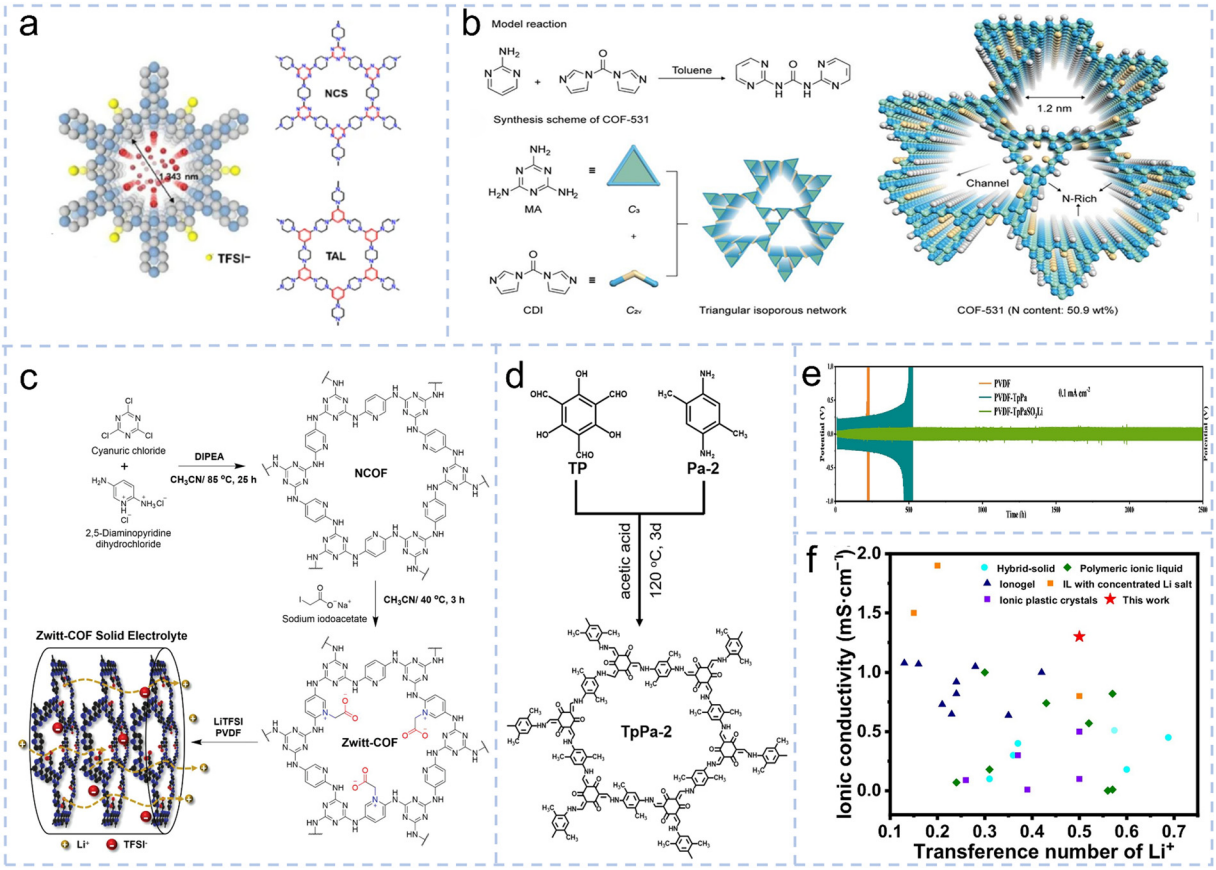

Fig. 18 Design schematics and performance of COF/HOF-based electrolytes. (a) The top views of the AA-stacking model of NCS-Li.[195] Copyright 2022, Springer Nature. (b) Synthetic route for urea-linked COF-531.[198] Copyright 2025, John Wiley and Sons. (c) Schematic illustration for the synthesis of a zwitterionic covalent organic framework (Zwitt-COF) solid electrolyte.[199] Copyright 2023, John Wiley and Sons. (d) Conceptual diagram of TpPa-2 synthesis.[200] Copyright 2022, Elsevier. (e) Cycling performance of Li symmetric cells with PVDF, PVDF-TpPa, and PVDF-TpPaSO$_3$ electrolytes.[201] Copyright 2025, Elsevier (f) HT-HOF-IL CQSE was prepared by confining ILE into the pore of the HOF lamellar framework.[203] Copyright 2025, SciOpen.

exhibit mild synthesis conditions and superior environmental compatibility. While initially explored for gas adsorption, separation, and sensing applications, HOFs are emerging as promising candidates for lithium-ion battery electrolytes. Leveraging the dynamic reversibility of hydrogen bonds and molecular design flexibility, HOFs enable precise structural customization by modulating organic precursors' functional groups and spatial configurations to meet diverse electrolyte performance requirements. Compared to COFs and MOFs, HOFs' relatively weaker hydrogen-bond networks offer unique advantages through their dynamic responsiveness, allowing "adaptive adjustment" of ion transport pathways. Current research focuses on 3D interpenetrated HOF architectures, where continuous hydrogen-bond channels and highly open pore systems facilitate solvent- or ion-induced optimization of pore surface chemical microenvironments, thereby promoting long-range ordered lithium-ion migration. These distinctive attributes are drawing increasing attention for solid-state electrolyte design.

The dynamic reorganization of hydrogen bonds represents the core of HOF distinction from COFs and MOFs. During charge/discharge cycles, volumetric changes in electrode materials induce mechanical stresses at the electrolyte-electrode interface. HOFs' hydrogen-bond networks enable "self-adaptive adjustment" through dynamic bond breaking and reformation, effectively mitigating interfacial stresses and preventing crack formation, thereby enhancing interfacial stability. With specific surface areas ranging from 500 to 2000 $m^2 g^{-1}$, the interconnected hierarchical pores of HOF not only provide rapid Li^+ diffusion pathways but also suppress electrolyte decomposition side reactions *via* confinement effects. Their open framework architecture offers a unique platform for functionalization: post-synthetic modification strategies (*e.g.*, *in situ* synthesis or surface grafting) enable targeted introduction of functional groups (crown ethers, PEG chains, sulfonic acids) into pore surfaces or organic monomers, allowing precise regulation of ion transport behavior. For example, Xu *et al.* engineered a novel HOF-based solid-state electrolyte (HOF-DAT) leveraging multisite hydrogen bonds and stable π–π stacking interactions.[202] The abundant C═O groups of framework act as ion-hopping sites, while its flexible hydrogen-bond architecture enables rapid Li^+ conductivity (2.2×10^{-4} S cm^{-1}), high Li^+ transference number (0.88), and a broad electrochemical window (5.05 V). This directional design capability stems from hydrogen bonds' dynamic reversibility, permitting solvent/ion-

induced optimization of pore surface microenvironments to enhance Li^+ transport efficiency.

Furthermore, the dynamic hydrogen-bond networks of HOFs facilitate seamless integration with functional materials (MXenes, MOFs, ionic liquids) to create synergistic ion transport systems, transcending the limitations of individual components. For instance, Wang *et al.* developed a hydrogen-bonded organic framework/ionic liquid quasi-solid electrolyte (HT-HOF-IL CQSE), where weak HOF hydrogen bonding and ILE-HOF framework interactions enable uniform ILE distribution within the HOF matrix (Fig. 18f).[203] The HOF framework effectively restricts IL migration, mitigating ion aggregation while anchoring ILs as additional Li^+ hopping sites to enhance low-temperature conductivity. The HT-HOF-IL CQSE achieves remarkable ionic conductivities of 5.8×10^{-4} S cm^{-1} at -20 °C and 5.7×10^{-5} S cm^{-1} at -60 °C, coupled with a high Li^+ transference number (0.69). This exemplifies how HOFs' open frameworks and dynamic hydrogen-bond features serve as ideal platforms for functionalization and composite design, enabling collaborative optimization of ion transport efficiency, interfacial stability, and environmental adaptability through precise functional group integration or multidimensional material engineering.

HOF materials, leveraging their eco-friendly synthesis pathways, dynamic structural responsiveness, and interfacial compatibility, offer novel approaches for developing high-performance lithium-ion battery electrolytes. While challenges persist in hydrogen-bond stability (particularly under high-voltage/high-temperature conditions) and scalable manufacturing processes, the convergence of supramolecular chemistry and battery technology positions HOF-based electrolytes for breakthroughs in flexible electronics and safety-critical solid-state batteries. Future research should prioritize hydrogen-bond network reinforcement strategies (*e.g.*, π–π stacking-assisted stabilization) to accelerate practical implementation, alongside advanced processing techniques to balance structural integrity with ionic transport efficiency across operational extremes.

4.3.4. Development and outlook. Framework electrolytes, as novel porous materials, demonstrate unique advantages in solid-state systems through designable topological architectures, ultrahigh specific surface areas, and functionalization potential. MOF-based electrolytes achieve room-temperature ionic conductivities ($\sim 10^{-3}$ S cm^{-1}) *via* ionic liquid confinement (*e.g.*, IL@MOF) or polymer hybridization (*e.g.*, PEO/MOF), yet their chemical stability remains constrained by coordination bond strength, making them prone to structural collapse under high humidity or acidic conditions. COF-based systems exhibit exceptional thermal stability (>400 °C) from robust covalent frameworks, where 3D COF designs further optimize ion transport channels, though challenges persist in synthesis complexity and flammability of lightweight components. HOFs leverage dynamic hydrogen-bond networks for self-healing capability and environmental adaptability, yet insufficient mechanical strength and solvent sensitivity currently limit practical implementation.

Future research should prioritize: (1) multiscale pore engineering and dynamic function modulation: enhancing ion transport efficiency *via* topological optimization (*e.g.*, MOF/COF heterojunctions) and developing photo-/thermal-responsive frameworks for real-time performance regulation; (2) interface optimization and environmental resilience: employing *in situ* growth techniques (*e.g.*, graphene coatings) to reduce interfacial impedance while improving extreme-condition stability through fluorination or hydrophobic group modifications; (3) multiframework integration and cross-domain applications: exploring synergistic effects in MOF/COF/HOF ternary systems, such as catalytic MOF-COF hybrids (CMOFs) combining MOF catalytic sites with COF stability, to expand applications in photo/electrocatalytic energy conversion; (4) sustainable synthesis and standardized evaluation: advancing hydrothermal or solvent-free processes to reduce production costs and establishing *in situ* characterization methods (*e.g.*, synchrotron X-ray scattering) for real-time ion transport monitoring.

Framework electrolyte research is transitioning from material design to device integration, yet requires deeper interdisciplinary collaboration to establish a ''structure–performance–application'' integrated design paradigm, accelerating their scalable deployment in high-safety, high-energy-density energy storage systems.

5. Conclusions and perspectives

Polymers have emerged as pivotal materials driving advancements in high-energy lithium-ion battery technologies, leveraging their designable architectures, mechanical flexibility, and multifunctional adaptability. As core components in electrolytes, binders, and composite electrodes, polymers demonstrate exceptional performance in high-energy-density and safety-critical battery systems. In electrolyte engineering, solid/gel polymer electrolytes significantly enhance safety by suppressing lithium dendrite growth and improving interfacial compatibility. For electrode materials, conductive polymers (*e.g.*, polypyrrole, polyaniline) and functional binders (*e.g.*, polyacrylic acid, carboxymethyl cellulose) address cycling stability challenges in high-capacity silicon anodes and sulfur cathodes by mitigating volume expansion and parasitic reactions. Furthermore, polymer-based composites (*e.g.*, sulfur-polymer hybrid cathodes) offer innovative pathways to transcend the energy density limitations of conventional electrode materials.

Despite their immense potential, polymer applications face multidimensional challenges in structural stability, ion transport efficiency, processing techniques, and system integration. Critical issues such as oxidative degradation of high-voltage cathode binders, insufficient dynamic self-healing capabilities in silicon anode binders, and the intrinsic room-temperature ionic conductivity limitations of polymer electrolytes severely constrain further performance enhancements. Additionally, technical complexities escalate with scale-up requirements, including coating uniformity control, cost-performance trade-offs, and environmental sustainability demands, necessitating

coordinated innovations in material science and manufacturing engineering.

Future research directions should prioritize the following objectives:

(1) Innovative polymer architecture design: developing polymer architectures that concurrently achieve high chemical/mechanical stability and rapid ion transport capabilities. For instance, molecular engineering strategies—such as tuning backbone rigidity (*e.g.*, aromatic polymers) or side-chain functionalization with ion-transporting moieties—can balance structural integrity and ionic conductivity.

(2) Interfacial optimization and multiscale synergy: addressing high interfacial impedance at electrode–electrolyte interfaces by designing multifunctional interphases (*e.g.*, polymer–inorganic hybrid coatings) to enhance compatibility and suppress side reactions. Concurrently, exploring synergistic mechanisms between polymers and high-capacity electrode materials (*e.g.*, lithium metal, silicon-based anodes) will enable the construction of stable three-dimensional composite architectures for long-term cycling performance.

(3) Advanced processing and system integration: transcending conventional polymer processing limitations through emerging techniques like 3D printing and electrospinning to fabricate highly uniform thin films or flexible electrodes, while driving scalable production of novel architectures such as all-solid-state and flexible batteries.

(4) Interdisciplinary innovation: integrating computational materials science (*e.g.*, machine learning-guided polymer screening), *in situ* characterization (XRD/TEM), and sustainable chemistry principles to accelerate rational polymer design and lifecycle assessment.

(5) Industrial production: for most of the polymer lithium-ion batteries in the laboratory pilot stage, their cost compared to liquid batteries is still not comparable, but along with technological breakthroughs as well as the realization of large-scale production, their cost is expected to be rapidly reduced. In the future, while researching and developing new high-capacity, long-life materials to enhance battery performance, the amount of materials used should be reduced, thereby reducing costs. In the production process, the introduction of automation and intelligent production equipment can significantly improve production efficiency and reduce labor costs and losses in the production process.

(6) Recycling industry: currently there is limited awareness of the recyclability of polymer batteries compared to the recycling process of conventional lithium-ion batteries, so the development of multi-product, multi-process process routes is essential, such as integrating industrial steps such as shredding, batch processing, dry and wet processing, reconditioning and re-synthesizing after pre-sorting the polymer batteries to achieve a collegiate and safe recycling process with a high recycling rate.

The convergence of materials science and battery technologies positions polymer-based high-energy lithium-ion batteries for breakthroughs in energy density (>500 Wh kg^{-1}), intrinsic safety (*via* solid-state architectures), and cycling endurance (>2000 cycles). However, commercialization demands concerted academic-industrial efforts to address the ''last-mile'' challenges from lab to market. Beyond revolutionizing lithium-ion batteries, polymer materials have transformative potential for next-generation energy storage systems like sodium-ion and lithium-sulfur batteries through innovative interfacial engineering and multifunctional composite solutions.

Author contributions

Y Du: analyzing, discussing, writing, reviewing and editing. S Deng: conceptualization, discussing and checking. Y Zhu, J Jiang and G Yang: analyzing, discussing and writing. M Wu: reviewing and checking. Z Li: conceptualization, discussing, reviewing and checking.

Conflicts of interest

There are no conflicts to declare.

Data availability

No primary research results, software or code have been included and no new data was generated or analyzed as part of this review.

Acknowledgements

We are grateful for the support of the following funds, projects and laboratories: the National Key R&D Program of China (2023YFE0203600), the National Natural Science Foundation of China (22409215), project 2025HWYQ-037 supported by Shandong Provincial Natural Science Fund for Excellent Young Scientists Fund Program (Overseas), Taishan Scholar Project (tsqn202312113), China University of Petroleum (East China) Independent Innovation Research Program Project (25CX06008A), and the Shandong Key Laboratory of Advanced Electrochemical Energy Storage Technologies.

References

1 S. Chu, Y. Cui and N. Liu, *Nat. Mater.*, 2017, **16**, 16–22.
2 J. B. Goodenough and K.-S. Park, *J. Am. Chem. Soc.*, 2013, **135**, 1167–1176.
3 W. Li, E. M. Erickson and A. Manthiram, *Nat. Energy*, 2020, **5**, 26–34.
4 R. Schmuch, R. Wagner, G. Hörpel, T. Placke and M. Winter, *Nat. Energy*, 2018, **3**, 267–278.
5 F. Zheng, M. Kotobuki, S. Song, M. O. Lai and L. Lu, *J. Power Sources*, 2018, **389**, 198–213.
6 Y. Nishi, *J. Power Sources*, 2001, **100**, 101–106.
7 S. Yan, C.-H. Yim, V. Pankov, M. Bauer, E. Baranova, A. Weck, A. Merati and Y. Abu-Lebdeh, *Batteries*, 2021, **7**, 75.

8 D. Aurbach, Y. Talyosef, B. Markovsky, E. Markevich, E. Zinigrad, L. Asraf, J. S. Gnanaraj and H.-J. Kim, *Electrochim. Acta*, 2004, **50**, 247–254.
9 J. Janek and W. G. Zeier, *Nat. Energy*, 2023, **8**, 230–240.
10 A. Manthiram, *Nat. Commun.*, 2020, **11**, 1550.
11 X. Feng, M. Ouyang, X. Liu, L. Lu, Y. Xia and X. He, *Energy Storage Mater.*, 2018, **10**, 246–267.
12 X. Lai, Q. Chen, X. Tang, Y. Zhou, F. Gao, Y. Guo, R. Bhagat and Y. Zheng, *eTransportation*, 2022, **12**, 100169.
13 J. Liu, Y. Zhang, J. Zhou, Z. Wang, P. Zhu, Y. Cao, Y. Zheng, X. Zhou, C. Yan and T. Qian, *Adv. Funct. Mater.*, 2023, **33**, 2302055.
14 W. Dou, M. Zheng, W. Zhang, T. Liu, F. Wang, G. Wan, Y. Liu and X. Tao, *Adv. Funct. Mater.*, 2023, **33**, 2305161.
15 W. Liu, P. Oh, X. Liu, S. Myeong, W. Cho and J. Cho, *Adv. Energy Mater.*, 2015, **5**, 1500274.
16 B. Xiao, J. Liu, Q. Sun, B. Wang, M. N. Banis, D. Zhao, Z. Wang, R. Li, X. Cui, T.-K. Sham and X. Sun, *Adv. Sci.*, 2015, **2**, 1500022.
17 L. Sun, Y. Liu, L. Wang and Z. Jin, *Adv. Funct. Mater.*, 2024, **34**, 2403032.
18 C. A. Angell, C. Liu and E. Sanchez, *Nature*, 1993, **362**, 137–139.
19 Y. Liu, D. Lin, Y. Li, G. Chen, A. Pei, O. Nix, Y. Li and Y. Cui, *Nat. Commun.*, 2018, **9**, 3656.
20 J. Liu, Z. Bao, Y. Cui, E. J. Dufek, J. B. Goodenough, P. Khalifah, Q. Li, B. Y. Liaw, P. Liu, A. Manthiram, Y. S. Meng, V. R. Subramanian, M. F. Toney, V. V. Viswanathan, M. S. Whittingham, J. Xiao, W. Xu, J. Yang, X.-Q. Yang and J.-G. Zhang, *Nat. Energy*, 2019, **4**, 180–186.
21 H. Niu, N. Zhang, Y. Lu, Z. Zhang, M. Li, J. Liu, N. Zhang, W. Song, Y. Zhao and Z. Miao, *J. Energy Storage*, 2024, **88**, 111666.
22 J. Xu, J. Zhang, T. P. Pollard, Q. Li, S. Tan, S. Hou, H. Wan, F. Chen, H. He, E. Hu, K. Xu, X.-Q. Yang, O. Borodin and C. Wang, *Nature*, 2023, **614**, 694–700.
23 Y. Zheng, D. Wang, S. Kaushik, S. Zhang, T. Wada, J. Hwang, K. Matsumoto and R. Hagiwara, *EnergyChem*, 2022, **4**, 100075.
24 Z. Zhang, Y. Qu, Y. Li, Y. Song, X. Wang, D. Ren, H. Huo, L. Wang, Y. Xia and X. He, *Energy Storage Mater.*, 2024, **73**, 103802.
25 D.-H. Guan, X.-X. Wang, L.-N. Song, C.-L. Miao, J.-Y. Li, X.-Y. Yuan, X.-Y. Ma and J.-J. Xu, *Angew. Chem., Int. Ed.*, 2024, **63**, e202317949.
26 P. M. Attia, E. Moch and P. K. Herring, *Nat. Commun.*, 2025, **16**, 611.
27 T. Zeng, Z. Jiao, X. Gao, M. Yang, X. Wang, W. Zhao, W. Tang, M. Chu, Z. He, J. Li, Z. Huang, G. Chen, Z. Chen, R. Wang, L. Wang, J. Zhang, L. He, Y. Pu and Y. Xiao, *Angew. Chem., Int. Ed.*, 2025, **64**, e202501777.
28 X. Zhu, X. Xie, J. Lin, Y. Liu, G. Gao, Y. Yang, Y. Zhang, W. Xiong, Y. Jiang, Q. Li and D.-L. Peng, *Nano Energy*, 2025, **134**, 110588.
29 Z. Zhuo, K. Dai, R. Qiao, R. Wang, J. Wu, Y. Liu, J. Peng, L. Chen, Y.-D. Chuang, F. Pan, Z.-X. Shen, G. Liu, H. Li, T. P. Devereaux and W. Yang, *Joule*, 2021, **5**, 975–997.
30 R. Yan, Z. Zhao, R. Zhu, M. Wu, X. Liu, M. Adeli, B. Yin, C. Cheng and S. Li, *Angew. Chem., Int. Ed.*, 2024, **63**, e202404019.
31 L. Ji, D. Yang, J. Xue, M. Jia, T. Wu, Q. Zhuang, Y. Zhang, J. Liu and Y. Zhang, *Adv. Energy Mater.*, 2025, **15**, 2404738.
32 R. Yu, Y. Pan, Y. Jiang, L. Zhou, D. Zhao, G. Van Tendeloo, J. Wu and L. Mai, *Adv. Mater.*, 2023, **35**, 2306504.
33 Z. Liu, Y. Wang, G. Liu, X. Yue, Z. Shi, Y. Tan, J. Zhao, Y. Lei, X. Yan and Z. Liang, *J. Am. Chem. Soc.*, 2024, **146**, 34491–34500.
34 Y. Wang, G. Liu, H. Qiao, J. Tan, S. Li, M. Ye and J. Shen, *J. Am. Chem. Soc.*, 2025, **147**, 15344–15356.
35 H.-M. Hau, T. Mishra, C. Ophus, T.-Y. Huang, K. Bustilo, Y. Sun, X. Yang, T. Holstun, X. Zhao, S. Wang, Y. Ha, G.-H. Lee, C. Song, J. Turner, J. Bai, L. Ma, K. Chen, F. Wang, W. Yang, B. D. McCloskey, Z. Cai and G. Ceder, *Nat. Nanotechnol.*, 2024, **19**, 1831–1839.
36 J. Luo, Q. Huang, D. Shi, Y. Qiu, X. Zheng, S. Yang, B. Li, J. Weng, M. Wu, Z. Liu, Y. Yu and C. Yang, *Adv. Funct. Mater.*, 2024, **34**, 2403021.
37 J. Chen, D. Zhang, L. Zhu, M. Liu, T. Zheng, J. Xu, J. Li, F. Wang, Y. Wang, X. Dong and Y. Xia, *Nat. Commun.*, 2024, **15**, 3217.
38 X. Liu, A. Mariani, T. Diemant, M. E. Di Pietro, X. Dong, A. Mele and S. Passerini, *Adv. Mater.*, 2024, **36**, 2309062.
39 R. Shi, S. Jiao, Z. Yang, Z. Bo, J. Jiao and Y. Zhao, *ACS Nano*, 2025, **19**, 8462–8508.
40 X. Lu, Y. Wang, X. Xu, B. Yan, T. Wu and L. Lu, *Adv. Energy Mater.*, 2023, **13**, 2301746.
41 Z. Huang, H. Lyu, L. C. Greenburg, Y. Cui and Z. Bao, *Nat. Energy*, 2025, **10**, 811–823.
42 T. Yang, X. Xu, S. Chen, Y. Yang, F. Li, W. Fan, Y. Wu, J. Zhao, J. Liu and Y. Huo, *Angew. Chem., Int. Ed.*, 2025, **64**, e202420973.
43 C. Liu, X. Huang, X. Yu, Z. Wang, Y. Shen, S. Yuan and Y. Wang, *Angew. Chem., Int. Ed.*, 2025, **64**, e202415915.
44 D. Zhang, Y. Liu, D. Li, S. Li, Q. Xiong, Z. Huang, S. Wang, H. Hong, J. Zhu, H. Lv and C. Zhi, *Energy Environ. Sci.*, 2025, **18**, 227–235.
45 Q. He, J. Ning, H. Chen, Z. Jiang, J. Wang, D. Chen, C. Zhao, Z. Liu, I. F. Perepichka, H. Meng and W. Huang, *Chem. Soc. Rev.*, 2024, **53**, 7091–7157.
46 Y. Chen, S. Liu, S. Cheng, S. Gao, J. Chai, Q. Jiang, Z. Liu, X. Liu, J. Liu, M. Xie and W. Dai, *ACS Appl. Energy Mater.*, 2022, **5**, 3072–3080.
47 J. Ahn, H.-G. Im, Y. Lee, D. Lee, H. Jang, Y. Oh, K. Chung, T. Park, M.-K. Um, J. W. Yi, J. Kim, D. J. Kang and J.-K. Yoo, *Energy Storage Mater.*, 2022, **49**, 58–66.
48 S. Dong, L. Wang, X. Huang, J. Liang and X. He, *Adv. Funct. Mater.*, 2024, **34**, 2404192.
49 Y. S. Meng, V. Srinivasan and K. Xu, *Science*, 2022, **378**, eabq3750.
50 Y. Lyu, X. Wu, K. Wang, Z. Feng, T. Cheng, Y. Liu, M. Wang, R. Chen, L. Xu, J. Zhou, Y. Lu and B. Guo, *Adv. Energy Mater.*, 2021, **11**, 2000982.
51 W. Tang, L. Liu, Y. Zhu, H. Sun, Y. Wu and K. Zhu, *Energy Environ. Sci.*, 2012, **5**, 6909–6913.

52 W.-J. Zhang, *J. Power Sources*, 2011, **196**, 2962–2970.
53 H. Zhang and J. Zhang, *eTransportation*, 2021, **7**, 100105.
54 W.-J. Kong, C.-Z. Zhao, S. Sun, L. Shen, X.-Y. Huang, P. Xu, Y. Lu, W.-Z. Huang, J.-Q. Huang and Q. Zhang, *Adv. Mater.*, 2024, **36**, 2310738.
55 Q. Jiang, M. Li, J. Li, J. Wang, G. Zhang, J. Wang, J. Zuo, G. Cao, R. Duan, Y. Hao, M. Li, Z. Yang, H. Yang, M. Bai, X. Song, Y. Xi, W. Li, X. Sun and X. Li, *Adv. Mater.*, 2025, **37**, 2417620.
56 Z. Li, J. Fu, S. Zheng, D. Li and X. Guo, *Small*, 2022, **18**, 2200891.
57 H. Liu, S. Wang, W. Kong, Y. Liu and H. Wang, *Angew. Chem., Int. Ed.*, 2025, **64**, e202507579.
58 T. Liu, J. Liu, L. Li, L. Yu, J. Diao, T. Zhou, S. Li, A. Dai, W. Zhao, S. Xu, Y. Ren, L. Wang, T. Wu, R. Qi, Y. Xiao, J. Zheng, W. Cha, R. Harder, I. Robinson, J. Wen, J. Lu, F. Pan and K. Amine, *Nature*, 2022, **606**, 305–312.
59 N.-Y. Park, S.-M. Han, J.-H. Ryu, M.-C. Kim, J.-I. Yoon, J.-H. Kim, G.-T. Park, J. E. Frerichs, C. Erk and Y.-K. Sun, *ACS Energy Lett.*, 2024, **9**, 3595–3604.
60 J. Yang, X. Liang, H.-H. Ryu, C. S. Yoon and Y.-K. Sun, *Energy Storage Mater.*, 2023, **63**, 102969.
61 M. Zheng, X. Zhu, H. Zheng, Z. Bo and J. Lu, *Nat. Energy*, 2025, **10**, 789–792.
62 G. Ji, J. Wang, Z. Liang, K. Jia, J. Ma, Z. Zhuang, G. Zhou and H.-M. Cheng, *Nat. Commun.*, 2023, **14**, 584.
63 L. Deng, J.-K. Liu, Z. Wang, J.-X. Lin, Y.-X. Liu, G.-Y. Bai, K.-G. Zheng, Y. Zhou, S.-G. Sun and J.-T. Li, *Adv. Energy Mater.*, 2024, **14**, 2401514.
64 X. Zhong, J. Han, L. Chen, W. Liu, F. Jiao, H. Zhu and W. Qin, *Appl. Surf. Sci.*, 2021, **553**, 149564.
65 N.-Y. Park, H.-U. Lee, T.-Y. Yu, I.-S. Lee, H. Kim, S.-M. Park, H.-G. Jung, Y.-C. Jung and Y.-K. Sun, *Nat. Energy*, 2025, **10**, 479–489.
66 L. Bai, Y. Xu, Y. Liu, D. Zhang, S. Zhang, W. Yang, Z. Chang and H. Zhou, *Nat. Commun.*, 2025, **16**, 3484.
67 G.-Y. Bai, W.-J. Sun, Y. Zhou and J.-T. Li, *J. Energy Storage*, 2024, **97**, 112816.
68 C. Wang, Y. Ni, C. Zhu, Y. Li, Z. Yan, Y. Lu and J. Chen, *Angew. Chem., Int. Ed.*, 2025, **64**, e202423992.
69 F. Xia, W. Zeng, H. Peng, H. Wang, C. Sun, J. Zou and J. Wu, *J. Mater. Sci. Technol.*, 2023, **154**, 189–201.
70 H. Wang, Q. Shi, J. Dong, M. Wang, Y. Lu, Y. Liu, J. Liu, N. Li, Q. Huang, Y. Su, F. Wu and L. Chen, *Adv. Funct. Mater.*, 2025, **35**, 2422806.
71 L. Wang, A. Dai, W. Xu, S. Lee, W. Cha, R. Harder, T. Liu, Y. Ren, G. Yin, P. Zuo, J. Wang, J. Lu and J. Wang, *J. Am. Chem. Soc.*, 2020, **142**, 14966–14973.
72 F. Zou and A. Manthiram, *Adv. Energy Mater.*, 2020, **10**, 2002508.
73 L. Wang, T. Liu, A. Dai, V. De Andrade, Y. Ren, W. Xu, S. Lee, Q. Zhang, L. Gu, S. Wang, T. Wu, H. Jin and J. Lu, *Nat. Commun.*, 2021, **12**, 5370.
74 L. Wang, T. Liu, T. Wu and J. Lu, *Nature*, 2022, **611**, 61–67.
75 Z. Fu, H. L. Feng, X. D. Xiang, M. M. Rao, W. Wu, J. C. Luo, T. T. Chen, Q. P. Hu, A. B. Feng and W. S. Li, *J. Power Sources*, 2014, **261**, 170–174.
76 L. Wei, H. Wu, S. Liu, Y. Zhou and X. Guo, *Small*, 2024, **20**, 2312059.
77 F. Zhang, S. Lou, S. Li, Z. Yu, Q. Liu, A. Dai, C. Cao, M. F. Toney, M. Ge, X. Xiao, W.-K. Lee, Y. Yao, J. Deng, T. Liu, Y. Tang, G. Yin, J. Lu, D. Su and J. Wang, *Nat. Commun.*, 2020, **11**, 3050.
78 Y.-H. Zhang, S. Zhang, N. Hu, Y. Liu, J. Ma, P. Han, Z. Hu, X. Wang and G. Cui, *Chem. Soc. Rev.*, 2024, **53**, 3302–3326.
79 Y. Huang, Y. Dong, Y. Yang, T. Liu, M. Yoon, S. Li, B. Wang, E. Y. Zheng, J. Lee, Y. Sun, Y. Han, J. Ciston, C. Ophus, C. Song, A. Penn, Y. Liao, H. Ji, T. Shi, M. Liao, Z. Cheng, J. Xiang, Y. Peng, L. Ma, X. Xiao, W. H. Kan, H. Chen, W. Yin, L. Guo, W.-R. Liu, R. Murugananthan, C.-C. Yang, Y. Zhu, Q. Li and J. Li, *Nat. Energy*, 2024, **9**, 1497–1505.
80 H. Wang, F. Zhang, N. Qin, Z. Wang, Y. Wang, Z. Wang, C. Zeng, H. Li, Q. Liu, Y. Li, Z. Lu, D. Luo and H. Cheng, *ACS Energy Lett.*, 2025, **10**, 136–144.
81 Y.-K. Hong, J.-H. Kim, N.-Y. Kim, K.-S. Oh, H.-I. Kim, S. Ryu, Y. Ko, J.-Y. Kim, K.-H. Lee and S.-Y. Lee, *Nano-Micro Lett.*, 2025, **17**, 112.
82 P. Mu, H. Zhang, H. Jiang, T. Dong, S. Zhang, C. Wang, J. Li, Y. Ma, S. Dong and G. Cui, *J. Am. Chem. Soc.*, 2021, **143**, 18041–18051.
83 J.-H. Kim, K. M. Lee, J. W. Kim, S. H. Kweon, H.-S. Moon, T. Yim, S. K. Kwak and S.-Y. Lee, *Nat. Commun.*, 2023, **14**, 5721.
84 M. Si, X. Jian, Y. Xie, J. Zhou, W. Jian, J. Lin, Y. Luo, J. Hu, Y. J. Wang, D. Zhang, T. Wang, Y. Liu, Z. L. Wu, S. Y. Zheng and J. Yang, *Adv. Energy Mater.*, 2024, **14**, 2303991.
85 X. Peng, X. Chen, C. Tang, S. Weng, X. Hu and Y. Xiang, *ACS Appl. Mater. Interfaces*, 2023, **15**, 21517–21525.
86 M. Liu, P. Chen, X. Pan, S. Pan, X. Zhang, Y. Zhou, M. Bi, J. Sun, S. Yang, A. L. Vasiliev, P. J. Kulesza, X. Ouyang, J. Xu, X. Wang, J. Zhu and Y. Fu, *Adv. Funct. Mater.*, 2022, **32**, 2205031.
87 W. Wang, L. Hua, Y. Zhang, G. Wang and C. Li, *Angew. Chem., Int. Ed.*, 2024, **63**, e202405920.
88 J. Kang, H. Eom, S. Jang, D. Yoo, H. Lee, M. Kim, M. L. Seol, J. W. Han, I. Nam and H. Song, *Adv. Mater.*, 2025, **37**, 2416872.
89 G. T. Pace, M. L. Le, R. J. Clément and R. A. Segalman, *ACS Energy Lett.*, 2023, **8**, 2781–2788.
90 H. Li, F. Lian, N. Meng, C. Xiong, N. Wu, B. Xu and Y. Li, *Adv. Funct. Mater.*, 2021, **31**, 2008487.
91 J. Chen, Y. Lin, Q. Li, H. Ren, L. Zhang, Y. Sun, S. Zhang, X. Shang, W. Zhou, M. Wu and Z. Li, *Angew. Chem., Int. Ed.*, 2024, **63**, e202407024.
92 T. Zhang, B. Li, Z. Song, W. Jiang, S. Liu, R. Mao, X. Jian and F. Hu, *Energy Environ. Mater.*, 2024, **7**, e12572.
93 T. Zhang, R. Mao, W. Jiang, B. Li, Z. Song, S. Liu, X. Jian and F. Hu, *Nano Energy*, 2023, **114**, 108603.
94 L. V. Kayser and D. J. Lipomi, *Adv. Mater.*, 2019, **31**, 1806133.
95 W. Liu, X. Zhang, Y. Xu, C. Li, K. Wang, X. Sun, F. Su, C.-M. Chen, F. Liu, Z.-S. Wu and Y. Ma, *Batteries Supercaps*, 2021, **4**, 407–428.

96 X. Chen, B. Wang, Y. Ye, J. Liang and J. Kong, *Energy Environ. Mater.*, 2025, **8**, e12838.
97 D. Lin, Y. Liu and Y. Cui, *Nat. Nanotechnol.*, 2017, **12**, 194–206.
98 J. Wu, Z. Rao, X. Liu, Y. Shen, C. Fang, L. Yuan, Z. Li, W. Zhang, X. Xie and Y. Huang, *Adv. Mater.*, 2021, **33**, 2007428.
99 L. Deng, Y. Zheng, X. Zheng, T. Or, Q. Ma, L. Qian, Y. Deng, A. Yu, J. Li and Z. Chen, *Adv. Energy Mater.*, 2022, **12**, 2200850.
100 Q. Qu, Y. Zhu, X. Gao and Y. Wu, *Adv. Energy Mater.*, 2012, **2**, 950–955.
101 J. Li, Y. Cai, H. Wu, Z. Yu, X. Yan, Q. Zhang, T. Z. Gao, K. Liu, X. Jia and Z. Bao, *Adv. Energy Mater.*, 2021, **11**, 2003239.
102 Y. Yang, S. Wu, Y. Zhang, C. Liu, X. Wei, D. Luo and Z. Lin, *Chem. Eng. J.*, 2021, **406**, 126807.
103 Z. Hu, R. Zhao, J. Yang, C. Wu and Y. Bai, *Energy Storage Mater.*, 2023, **59**, 102776.
104 I. Kovalenko, B. Zdyrko, A. Magasinski, B. Hertzberg, Z. Milicev, R. Burtovyy, I. Luzinov and G. Yushin, *Science*, 2011, **334**, 75–79.
105 H. Liu, J. Cai, P. Zhou, L. Li, Z. Ma, X. Zhao and J. Nan, *Chem. Eng. J.*, 2023, **475**, 146284.
106 Z. Li, Z. Liang, Z. Ma, P. Qu and Y. Zhang, *J. Alloys Compd.*, 2024, **971**, 172738.
107 J. Li, X. Hu, H. Zhao, Y. Ren and X. Huang, *Langmuir*, 2022, **38**, 402–410.
108 S.-J. Zhang, Y.-P. Deng, Q.-H. Wu, Y. Zhou, J.-T. Li, Z.-Y. Wu, Z.-W. Yin, Y.-Q. Lu, C.-H. Shen, L. Huang and S.-G. Sun, *ChemElectroChem*, 2018, **5**, 1321–1329.
109 J. Drofenik, M. Gaberscek, R. Dominko, F. W. Poulsen, M. Mogensen, S. Pejovnik and J. Jamnik, *Electrochim. Acta*, 2003, **48**, 883–889.
110 S. Zhang, X. Xu, J. Tu, F. Chen, J. Xie, T. Zhu and X. Zhao, *Mater. Today Sustainability*, 2022, **19**, 100178.
111 B. Tang, S. He, Y. Deng, Y. Shan, H. Qin, H. Noor and X. Hou, *J. Power Sources*, 2023, **556**, 232237.
112 W. Yi, T. Zhao, D. Li, Q. Yuan, Z. Zhao, B. Chen and N. Dang, *Chem. – Eur. J.*, 2025, **31**, e202500321.
113 J.-H. Lee, U. Paik, V. A. Hackley and Y.-M. Choi, *J. Power Sources*, 2006, **161**, 612–616.
114 A. Magasinski, B. Zdyrko, I. Kovalenko, B. Hertzberg, R. Burtovyy, C. F. Huebner, T. F. Fuller, I. Luzinov and G. Yushin, *ACS Appl. Mater. Interfaces*, 2010, **2**, 3004–3010.
115 Z. Liu, C. Fang, X. He, Y. Zhao, H. Xu, J. Lei and G. Liu, *ACS Appl. Mater. Interfaces*, 2021, **13**, 46518–46525.
116 X. Wan, C. Kang, T. Mu, J. Zhu, P. Zuo, C. Du and G. Yin, *ACS Energy Lett.*, 2022, **7**, 3572–3580.
117 C. Wang, H. Wu, Z. Chen, M. T. McDowell, Y. Cui and Z. Bao, *Nat. Chem.*, 2013, **5**, 1042–1048.
118 B. Jin, A. Dolocan, C. Liu, Z. Cui and A. Manthiram, *Angew. Chem., Int. Ed.*, 2024, **63**, e202408021.
119 S. Pan, J. Han, Y. Wang, Z. Li, F. Chen, Y. Guo, Z. Han, K. Xiao, Z. Yu, M. Yu, S. Wu, D.-W. Wang and Q.-H. Yang, *Adv. Mater.*, 2022, **34**, 2203617.
120 C. Gao, H. Zhang, P. Mu, R. Wu, X. Zhang, X. Chen, C. Sun, Q. Wang and G. Cui, *Adv. Energy Mater.*, 2023, **13**, 2302411.
121 X. Fan, Z. Wang, T. Cai, Y. Yang, H. Wu, S. Cao, Z. Yang and W. Zhang, *Carbon*, 2021, **182**, 749–757.
122 G. Wu, Y. Gao, Z. Weng, Z. Zheng, W. Fan, A. Pan, N. Zhang, X. Liu, R. Ma and G. Chen, *Carbon Neutralization*, 2024, **3**, 857–872.
123 Z. Li, Y. Zhang, T. Liu, X. Gao, S. Li, M. Ling, C. Liang, J. Zheng and Z. Lin, *Adv. Energy Mater.*, 2020, **10**, 1903110.
124 H. Yuan, X. Ding, T. Liu, J. Nai, Y. Wang, Y. Liu, C. Liu and X. Tao, *Mater. Today*, 2022, **53**, 173–196.
125 Q. Zhou, X. Xiong, J. Peng, W. Wu, W. Fan, H. Yang, T. Wang, Y. Ma, F. Wang and Y. Wu, *Energy Environ. Mater.*, 2025, **8**, e12831.
126 S.-e Sheng, L. Sheng, L. Wang, N. Piao and X. He, *J. Power Sources*, 2020, **476**, 228749.
127 J. Park, S. Ha, J. Y. Jung, J.-H. Hyun, S.-H. Yu, H.-K. Lim, N. D. Kim and Y. S. Yun, *Adv. Sci.*, 2022, **9**, 2104145.
128 H. Wu, H. Jia, C. Wang, J.-G. Zhang and W. Xu, *Adv. Energy Mater.*, 2021, **11**, 2003092.
129 X. Xu, X. Jiao, O. O. Kapitanova, J. Wang, V. S. Volkov, Y. Liu and S. Xiong, *Adv. Energy Mater.*, 2022, **12**, 2200244.
130 X. Shen, H. Liu, X.-B. Cheng, C. Yan and J.-Q. Huang, *Energy Storage Mater.*, 2018, **12**, 161–175.
131 X. Xiong, W. Yan, Y. Zhu, L. Liu, L. Fu, Y. Chen, N. Yu, Y. Wu, B. Wang and R. Xiao, *Adv. Energy Mater.*, 2022, **12**, 2103112.
132 W. Ren, X. Shang, Y. Lin, H. Ren, L. Zhang, H. Su, Q. Li, L. Zhi, M. Wu and Z. Li, *Adv. Energy Mater.*, 2025, **15**, 2405284.
133 D. Chen, S. Huang, L. Zhong, S. Wang, M. Xiao, D. Han and Y. Meng, *Adv. Funct. Mater.*, 2020, **30**, 1907717.
134 T. Naren, G.-C. Kuang, R. Jiang, P. Qing, H. Yang, J. Lin, Y. Chen, W. Wei, X. Ji and L. Chen, *Angew. Chem., Int. Ed.*, 2023, **62**, e202305287.
135 G. Wang, C. Chen, Y. Chen, X. Kang, C. Yang, F. Wang, Y. Liu and X. Xiong, *Angew. Chem., Int. Ed.*, 2019, **59**, 2055–2060.
136 L. Fan, H. L. Zhuang, W. Zhang, Y. Fu, Z. Liao and Y. Lu, *Adv. Energy Mater.*, 2018, **8**, 1703360.
137 Z. Hu, S. Zhang, S. Dong, W. Li, H. Li, G. Cui and L. Chen, *Chem. Mater.*, 2017, **29**, 4682–4689.
138 J. Zhang, Y. Zhong, S. Wang, D. Han, M. Xiao, L. Sun and Y. Meng, *ACS Appl. Energy Mater.*, 2021, **4**, 862–869.
139 R. Xu, X.-Q. Zhang, X.-B. Cheng, H.-J. Peng, C.-Z. Zhao, C. Yan and J.-Q. Huang, *Adv. Funct. Mater.*, 2018, **28**, 1705838.
140 W. Cao, J. Lu, K. Zhou, G. Sun, J. Zheng, Z. Geng and H. Li, *Nano Energy*, 2022, **95**, 106983.
141 G. Xi, M. Xiao, S. Wang, D. Han, Y. Li and Y. Meng, *Adv. Funct. Mater.*, 2021, **31**, 2007598.
142 Y.-K. Liu, C.-Z. Zhao, J. Du, X.-Q. Zhang, A.-B. Chen and Q. Zhang, *Small*, 2023, **19**, 2205315.
143 J. Luo, M. Yang, D. Wang, J. Zhang, K. Song, G. Tang, Z. Xie, X. Guo, Y. Shi and W. Chen, *Angew. Chem., Int. Ed.*, 2023, **62**, e202315076.

144 M. Gao, D. Zhou, B. Wen, S. Zhu and J. Ni, *Adv. Funct. Mater.*, 2025, **35**, 2500727.
145 Z. Zhao, W. Liang, S. Su, X. Jiang, Y. Bando, B. Zhang, Z. Ma and X. Wang, *Next Mater.*, 2025, **7**, 100364.
146 D. E. Fenton, J. M. Parker and P. V. Wright, *Polymer*, 1973, **14**, 589.
147 S. Xu, K. Zhang, R. Xu, P. Tang, H.-M. Cheng, Z. Sun and F. Li, *Energy Storage Mater.*, 2025, **74**, 103941.
148 L. Liu, T. Wang, L. Sun, T. Song, H. Yan, C. Li, D. Mu, J. Zheng and Y. Dai, *Energy Environ. Mater.*, 2024, **7**, e12580.
149 J. Shen, Z. Lei and C. Wang, *Chem. Eng. J.*, 2022, **447**, 137503.
150 Z. Zhang, T. Zhao, S. Huang, S. Wang, D. Han, H. Guo, M. Xiao and Y. Meng, *Adv. Energy Mater.*, 2025, **15**, 2403678.
151 Z. Zhang, M. Zhang, J. Wu, X. Hu, B. Fu, X. Zhang, B. Luo, K. Khan, Z. Fang, Z. Xu and M. Wu, *Small*, 2024, **20**, 2304234.
152 Z. Fang, M. Zhang, Z. Zhang, J. Li, H. Peng, J. Wu, H. Zhou, Z. Xu and M. Wu, *Adv. Sci.*, 2024, **11**, 2411421.
153 F. Liu, J. Wang, W. Chen, M. Yuan, Q. Wang, R. Ke, G. Zhang, J. Chang, C. Wang, Y. Deng, J. Wang and M. Shao, *Adv. Mater.*, 2024, **36**, 2409838.
154 Y. Zhu, S. Xiao, Y. Shi, Y. Yang, Y. Hou and Y. Wu, *Adv. Energy Mater.*, 2014, **4**, 1300647.
155 X. Xiong and Y. Wang, *Chem. Eng. J.*, 2024, **488**, 151130.
156 C. Lu, H. Jiang, X. Cheng, J. He, Y. Long, Y. Chang, X. Gong, K. Zhang, J. Li, Z. Zhu, J. Wu, J. Wang, Y. Zheng, X. Shi, L. Ye, M. Liao, X. Sun, B. Wang, P. Chen, Y. Wang and H. Peng, *Nature*, 2024, **629**, 86–91.
157 Y. Zhu, F. Wang, L. Liu, S. Xiao, Z. Chang and Y. Wu, *Energy Environ. Sci.*, 2013, **6**, 618–624.
158 M. S. Choi, S. G. Kang, J. Choi, J. Ko and J. H. Park, *Angew. Chem., Int. Ed.*, 2025, **64**, e202424568.
159 Z. Lin, X. Guo, Y. Yang, M. Tang, Q. Wei and H. Yu, *J. Energy Chem.*, 2021, **52**, 67–74.
160 M. J. Counihan, J. Lee, P. Mirmira, P. Barai, M. E. Burns, C. V. Amanchukwu, V. Srinivasan, Y. Zhang and S. Tepavcevic, *Energy Mater.*, 2025, **5**, 500032.
161 Q. Sun, S. Wang, Y. Ma, D. Song, H. Zhang, X. Shi, N. Zhang and L. Zhang, *Adv. Mater.*, 2023, **35**, 2300998.
162 R.-A. Tong, Y. Huang, C. Feng, Y. Dong and C.-A. Wang, *Adv. Funct. Mater.*, 2024, **34**, 2315777.
163 X. Ye, J. Liang, J. Hu, D. Wu, Y. Li, X. Ouyang, Q. Zhang, X. Ren and J. Liu, *Chem. Eng. J.*, 2023, **455**, 140846.
164 X. Liu, L. Sun, F. Zhai, T. Wu, P. Wang, H. Du, Y. Xu and X. Wang, *Adv. Energy Mater.*, 2025, **15**, 2405433.
165 X. Miao, J. Hong, S. Huang, C. Huang, Y. Liu, M. Liu, Q. Zhang and H. Jin, *Adv. Funct. Mater.*, 2025, **35**, 2411751.
166 J. Zheng, L. Duan, H. Ma, Q. An, Q. Liu, Y. Sun, G. Zhao, H. Tang, Y. Li, S. Wang, Q. Xu, L. Wang and H. Guo, *Energy Environ. Sci.*, 2024, **17**, 6739–6754.
167 C. Ma, J. Zhang, M. Xu, Q. Xia, J. Liu, S. Zhao, L. Chen, A. Pan, D. G. Ivey and W. Wei, *J. Power Sources*, 2016, **317**, 103–111.
168 Y. Guo, E. Zhao, W. Su, Z. Liu and J. Li, *Chem. Eng. J.*, 2025, **511**, 162127.
169 Y. Xu, X. Xiong, J. Peng, Q. Zhou, W. Wu, W. Gao, Y. Peng, T. Wang, F. Wang and Y. Wu, *J. Mater. Chem. A*, 2024, **12**, 26848–26856.
170 Y. Zhai, W. Hou, M. Tao, Z. Wang, Z. Chen, Z. Zeng, X. Liang, P. Paoprasert, Y. Yang, N. Hu and S. Song, *Adv. Mater.*, 2022, **34**, 2205560.
171 L. Wu, Y. Wang, M. Tang, Y. Liang, Z. Lin, P. Ding, Z. Zhang, B. Wang, S. Liu, L. Li, X. Guo, X. Yin and H. Yu, *Energy Storage Mater.*, 2023, **58**, 40–47.
172 C. Guo, K. Du, R. Tao, Y. Guo, S. Yao, J. Wang, D. Wang, J. Liang and S.-Y. Lu, *Adv. Funct. Mater.*, 2023, **33**, 2301111.
173 Y. Jin, R. Lin, Y. Li, X. Zhang, S. Tan, Y. Shuai and Y. Xiong, *Angew. Chem., Int. Ed.*, 2024, **63**, e202403661.
174 T. Zhou, Y. Zhao, J. W. Choi and A. Coskun, *Angew. Chem., Int. Ed.*, 2021, **60**, 22791–22796.
175 X. Li, Y. Zheng and C. Y. Li, *Energy Storage Mater.*, 2020, **29**, 273–280.
176 M. Martinez-Ibañez, E. Sanchez-Diez, L. Qiao, Y. Zhang, X. Judez, A. Santiago, I. Aldalur, J. Carrasco, H. Zhu, M. Forsyth, M. Armand and H. Zhang, *Adv. Funct. Mater.*, 2020, **30**, 2000455.
177 X. Liu, L. Guo, Z. Zhang, J. Wang, H. Lin, G. Li, X. Ou, D. Wang and W. Zheng, *Adv. Funct. Mater.*, 2025, **35**, 2408525.
178 Q. Hao, J. Yan, Y. Gao, F. Chen, X. Chen, Y. Qi and N. Li, *ACS Appl. Mater. Interfaces*, 2024, **16**, 44689–44696.
179 S. Zhang, Z. Li, Y. Zhang, X. Wang, P. Dong, S. Lei, W. Zeng, J. Wang, X. Liao, X. Chen, D. Li and S. Mu, *Energy Environ. Sci.*, 2025, **18**, 3807–3816.
180 X. Hou, T. P. Pollard, X. He, L. Du, X. Ju, W. Zhao, M. Li, J. Wang, E. Paillard, H. Lin, J. Sun, K. Xu, O. Borodin, M. Winter and J. Li, *Adv. Energy Mater.*, 2022, **12**, 2200401.
181 P. Dong, X. Zhang, K. S. Han, Y. Cha and M.-K. Song, *J. Energy Chem.*, 2022, **70**, 363–372.
182 X. Pei, Y. Li, T. Ou, X. Liang, Y. Yang, E. Jia, Y. Tan and S. Guo, *Angew. Chem., Int. Ed.*, 2022, **61**, e202205075.
183 W. Wu, D. Li, C. Gao, H. Wu, Y. Bo, J. Zhang, L. Ci and J. Zhang, *Adv. Sci.*, 2024, **11**, 2310136.
184 J. Hou, W. Sun, Q. Yuan, L. Ding, Y. Wan, Z. Xiao, T. Zhu, X. Lei, J. Lin, R. Cheacharoen, Y. Zhou, S. Wang, F. Manshaii, J. Xie, W. Li and J. Zhao, *Angew. Chem., Int. Ed.*, 2025, **64**, e202421427.
185 J. Li, Z. Hu, S. Zhang, H. Zhang, S. Guo, G. Zhong, Y. Qiao, Z. Peng, Y. Li, S. Chen, G. Chen and A.-M. Cao, *Nat. Sustain.*, 2024, **7**, 1481–1491.
186 S. Li, Y. Chen, X. Leng, M. Yang, W. U. Arifeen and T. J. Ko, *Chem. Eng. J.*, 2024, **500**, 157209.
187 T. Hou and W. Xu, *J. Energy Chem.*, 2023, **81**, 313–320.
188 M. Farina, B. B. Duff, C. Tealdi, A. Pugliese, F. Blanc and E. Quartarone, *ACS Appl. Mater. Interfaces*, 2021, **13**, 53986–53995.
189 G. Wang, P. He and L.-Z. Fan, *Adv. Funct. Mater.*, 2021, **31**, 2007198.
190 M. C. Nguyen, H. L. Nguyen, T. P. M. Duong, S.-H. Kim, J.-Y. Kim, J.-H. Bae, H.-K. Kim, S. N. Lim and W. Ahn, *Adv. Funct. Mater.*, 2024, **34**, 2406987.

191 Y. Feng, Y. Fan, L. Zhao, J. Yu, Y. Liao, T. Zhang, R. Zhang, H. Zhu, X. Sun, Z. Hu, K. Zhang and J. Chen, *Angew. Chem., Int. Ed.*, 2025, **64**, e202417105.
192 Q. Zeng, J. Wang, X. Li, Y. Ouyang, W. He, D. Li, S. Guo, Y. Xiao, H. Deng, W. Gong, Q. Zhang and S. Huang, *ACS Energy Lett.*, 2021, **6**, 2434–2441.
193 F. Tao, X. Wang, S. Jin, L. Tian, Z. Liu, X. Kang and Z. Liu, *Adv. Mater.*, 2023, **35**, 2300687.
194 L. Xu, X. Xiao, H. Tu, F. Zhu, J. Wang, H. Liu, W. Huang, W. Deng, H. Hou, T. Liu, X. Ji, K. Amine and G. Zou, *Adv. Mater.*, 2023, **35**, 2303193.
195 Z. Cheng, L. Lu, S. Zhang, H. Liu, T. Xing, Y. Lin, H. Ren, Z. Li, L. Zhi and M. Wu, *Nano Res.*, 2023, **16**, 528–535.
196 W. Yan, X. Gao, J.-L. Yang, X. Xiong, S. Xia, W. Huang, Y. Chen, L. Fu, Y. Zhu and Y. Wu, *Small*, 2022, **18**, 2106679.
197 X. Liu, S. Wang, S. Liu, C. Liu, X. Li, J. Wu, D. Li, S. Xu, C. Liu and W.-Y. Lai, *Sci. China: Chem.*, 2024, **67**, 1647–1652.
198 C. Zhang, Z. Luo, K. Chen, C. Yan, L. Yi, C. Gong, Y. Cao and F.-S. Ke, *Angew. Chem., Int. Ed.*, 2025, **64**, e202500314.
199 T. W. Kang, J.-H. Lee, J. Lee, J. H. Park, J.-H. Shin, J.-M. Ju, H. Lee, S. U. Lee and J.-H. Kim, *Adv. Mater.*, 2023, **35**, 2301308.
200 Z. Lin, Y. Wang, Y. Li, Y. Liu, S. Zhong, M. Xie, F. Yan, Z. Zhang, J. Peng, J. Li, A. Wang, X. Chen, M. Zhai, H. Zhang and J. Qiu, *Energy Storage Mater.*, 2022, **53**, 917–926.
201 C. Zhang, Z. Jiang, P. Guo, J. Song and C. Shi, *Chem. Eng. J.*, 2025, **503**, 158146.
202 Y. Wang, L.-N. Song, X.-X. Wang, Y.-F. Wang and J.-J. Xu, *Angew. Chem., Int. Ed.*, 2024, **63**, e202401910.
203 J. Zhang, Y. Wu, C. Wang, Y. Liu, Z. Yang, S. Zhou, W. Li, W. Wu and J. Wang, *Nano Res.*, 2025, **18**, 94906993.

